

Roller Compaction of Theophylline

Inauguraldissertation

zur

Erlangung der Würde eines Doktors der Philosophie

vorgelegt der

Philosophisch - Naturwissenschaftlichen Fakultät

der Universität Basel

von

Ervina Hadzovic

aus Bosnien und Herzegowina

Basel, 2008

Genehmigt von der Philosophisch-Naturwissenschaftlichen Fakultät
auf Antrag von

Prof. Dr. H. Leuenberger,
Dr. G. Betz
und
PD Dr. P. Van Hoogevest

Basel, den 22. April 2008

Professor Dr. H-P Hauri
Dekan

To my family

Acknowledgements

I would like to express my deep gratitude to my supervisor Prof. Dr. Hans Leuenberger for his guidance and support during this study.

I would like to thank to PD Dr. Peter van Hoogevest who accepted assuming the co-reference of this work.

I am sincerely grateful to Msc. Seherzada Hadzidedic for giving me the opportunity to perform this thesis and her trust and encouragement during this work.

I deeply thanks to Dr. Gabriele Betz for her support, understanding and unlimited optimism which made this work much easier for me.

Many thanks to Dr. Silvia Kocova El-Arini for nice scientific collaboration.

Thanks to Fitzpatrick Company for their kind offer of the machine to me and help during these three years.

Special thanks to my friends and colleagues from Industrial Pharmacy Lab: Selma Sehic, Maja Pasic, Krisanin Chansanroj, Imjak Jeon, Murad Ruman, Sameh Abdel - Hamid, Hiroshi Yamaguchi, Etienne Krausbauer, Vincenzo Balzano, Mohanned Saeed , Maxim Puchkov and Hidetoshi Myojyo for creating extraordinary pleasant and inspiring working atmosphere and help which they unselfish offered during this work.

I am ever grateful to my husband Mirnes, my mother Pasa, my sister Samra and her family for their love, support and encouragement during this study

| | |
|--|------|
| Abbreviations | VIII |
| 1. Summary..... | IX |
| 2. Theoretical Section | 1 |
| 2.1. Introduction | 1 |
| 2.2. Tablet Dosage Form | 1 |
| 2.2.1. Particle-Bonding Mechanisms..... | 1 |
| 2.3. Methods of Granulation..... | 3 |
| 2.3.1. Wet Granulation | 3 |
| 2.3.2. Dry Granulation | 4 |
| 2.3.2.1. Mechanisms of Roll Compaction..... | 6 |
| 2.3.2.2. Model of Roll Compaction Process | 7 |
| 2.3.2.3. Equipment..... | 9 |
| 2.3.2.4. Process Parameters | 11 |
| 2.3.3. Milling | 12 |
| 2.3.3.1. Classification of Mills | 13 |
| 2.3.3.3. Process Parameters | 14 |
| 2.4. Tablets | 15 |
| 2.4.1. Compression Bonding Mechanisms..... | 17 |
| 2.4.2. Properties of Tableting Materials | 18 |
| 2.4.3. Mechanical Properties of Tablets..... | 18 |
| 2.4.3.1. Heckel Equation..... | 19 |
| 2.4.3.2. Modified Heckel Equation..... | 21 |
| 2.4.3.3. Leuenberger Equation | 22 |
| 2.4.4. Factors Affecting Compactibility of Ppowders..... | 23 |
| 2.5. Tablet Press | 24 |
| 2.5.1. Principles of Eccentric Tablet Machine | 24 |
| 2.5.2. Principles of Rotary Tablet Machine | 25 |
| 2.5.3. Compaction Simulator..... | 25 |
| 2.6. Theophylline..... | 27 |
| 2.7. Polymorphism | 29 |
| 3. Objectives | 32 |
| 4. Materials and Methods | 33 |
| 4.1. Powder Characterization..... | 33 |

| | |
|--|----|
| 4.1.1. Scanning Electron Microscopy (SEM) | 33 |
| 4.1.2. Density..... | 33 |
| 4.1.3. Moisture Content | 34 |
| 4.1.4. Particle Size Distribution | 34 |
| 4.1.5. Specific Surface Area..... | 35 |
| 4.1.6. Solubility | 36 |
| 4.1.7. Contact Angle..... | 36 |
| 4.1.7. X – Ray Diffractometry | 37 |
| 4.1.8. Differential Scanning Calorimetry (DSC) | 37 |
| 4.2. Preparation of the Binary Mixtures | 38 |
| 4.2.1. Characterization of the Powder Binary Mixtures..... | 38 |
| 4.3. Roller Compaction | 38 |
| 4.4. Compacts Characterization..... | 39 |
| 4.4.1. Differential Scanning Calorimetry (DSC) | 39 |
| 4.4.2. Porosity of Compacts | 40 |
| 4.5. Granules Characterization | 41 |
| 4.5.1. Scanning Electron Microscopy (SEM) | 41 |
| 4.5.2. Particle Size Distribution | 41 |
| 4.5.3. X–Ray Diffractometry | 41 |
| 4.5.4. Differential Scanning Calorimetry (DSC) | 41 |
| 4.6. Tablet Production..... | 42 |
| 4.7. Tablet Characterization..... | 43 |
| 4.7.1. Differential Scanning Calorimetry (DSC) | 43 |
| 4.7.2. Compression Behavior Analysis | 43 |
| 4.7.2.1. Heckel and Modified Heckel Equation..... | 43 |
| 4.7.2.2. Measurement of Radial Tensile Strength | 44 |
| 4.7.3. Disintegration Time | 45 |
| 4.7.4. Dissolution Rate | 45 |
| 4.7.5. Statistical Analysis..... | 46 |
| 5. Results and Discussion | 47 |
| 5.1. Powder Characterization..... | 47 |
| 5.1.1. Scanning Electron Microscopy..... | 47 |
| 5.1.2. Density..... | 48 |
| 5.1.3. Moisture content..... | 50 |

| | |
|--|-----|
| 5.1.4. Particle Size Distribution and Specific Surface Area | 51 |
| 5.1.5. Solubility | 52 |
| 5.1.6. Contact Angle | 53 |
| 5.1.7. X-Ray Diffractometry | 53 |
| 5.1.8. Differential Scanning Calorimetry (DSC) | 54 |
| 5.2. Characterization of the Powder Binary Mixtures | 54 |
| 5.2.1. Density and Flowability..... | 54 |
| 5.3. Compact Characterization | 56 |
| 5.3.1. Differential Scanning Calorimetry (DSC) | 57 |
| 5.3.2. Compact Porosity | 57 |
| 5.4. Granule Characterization | 58 |
| 5.4.1. Scanning Electron Microscopy | 58 |
| 5.4.2. Density and Flowability..... | 60 |
| 5.4.3. Particle Size Distribution | 62 |
| 5.4.4. X - Ray Diffractometry | 63 |
| 5.4.4. Differential Scanning Calorimetry (DSC) | 66 |
| 5.5. Tablet Characterization..... | 67 |
| 5.5.1. Differential Scanning Calorimetry (DSC) | 67 |
| 5.5.2. Heckel and Modified Heckel Analysis | 71 |
| 5.5.3. Tensile Strength | 87 |
| 5.5.4. Leuenberger Equation - Compressibility and Compactibility | 97 |
| 5.5.5. Disintegration time..... | 107 |
| 5.5.5. Dissolution Rate | 112 |
| 6. Conclusions | 122 |
| 7. Appendix..... | 126 |

Abbreviations

| | |
|--------|--|
| ANOVA: | Analysis of Variance |
| BET: | Equation of Brunauer, Emmet and Teller |
| DSC: | Differential Scanning Calorimetry |
| HFS: | Horizontal Feed Screw |
| MCC: | Microcrystalline cellulose |
| THAFP: | Theophylline Anhydrate Fine Powder |
| THAP: | Theophylline Anhydrate Powder |
| THMO: | Theophylline Monohydrate |
| RH: | Relative humidity |
| rpm: | round per minute |
| s.d.: | standard deviation |
| SEM: | Scanning Electron Microscopy |
| USP: | United States Pharmacopoeia |
| VFS: | Vertical Feed Screw |
| w/w % | percentage by weight |

1. Summary

Direct compaction requires a very good flowability and compressibility of the materials. Those parameters become even more critical if the formulation contains large amount of active substance. To overcome these problems, several alternatives have been used. Roller compaction is a very attractive technology in the pharmaceutical industry. It is a fast and efficient way of producing granules, especially suitable for moisture sensitive materials.

The intention of this work was to understand the effect of roller compaction on the tablet properties.

In the literature it is often shown that after roller compaction a material tend to loose mechanical strength. This phenomenon is affected by deformation behavior of the materials exposed to roller compaction. Plastic deformable materials are particularly sensitive because of the limiting binding potential which may be consumed in the first compression step by increasing particle size and decreasing specific surface area. However, materials which undergo fragmentation under pressure showed less or even no loss of tableability after roller compaction. The loosing of mechanical strength is called loss of reworkability or loss of tableability. To diminish or even eliminate loss of reworkability the crucial moment is the development of a correct and robust formulation. If excipients with adequate properties, regarding an active material, are chosen it is possible to hold mechanical strength of the tablets. Another problem that could take place during roller compaction is disruption of crystal lattice and changing of polymorphic form of the material. Polymorphic transformation may occur as a result of applied pressure during roller compaction or even due to double compaction after tableting. Due to the fact that Theophylline exists as two polymorphic forms of anhydrate and as monohydrate, it was used as a model drug. Two grade of Theophylline anhydrate: Theophylline anhydrate powder (THAP) and Theophylline anhydrate fine powder (THAFP) were employed in order to check if there is difference in compactibility and tablet properties produced from the same material with different particle size distribution. There is the risk that during the compaction cycle hydrate loses water and transforms to anhydrate, therefore Theophylline monohydrate (THMO) was compacted. Microcrystalline cellulose (MCC) was chosen as a material to combine with THAP, THAFP and THMO because it is

widely used pharmaceutical excipient and its mechanical properties are well understood.

Due to the importance of active material and excipientes properties on the process parameters of roller compaction the materials were characterized in detail. Differential scanning calorimetry (DSC) and X-Ray analysis confirmed that roller compaction, milling and tableting did not influence polymorphic / pseudopolymorphic forms of THAP, THAFP and THMO. It is well known that various materials have a different behavior under compression pressure. In order to see effect of roller compaction on compressibility and compactibility of the materials after roller compaction various mathematical equation were applied. The most used equations for checking the compressibility of a material are Heckel and modified Heckel equation. Compactibility of the materials with and without roller compaction was determined by measuring the tensile strength of the tablets produced from the granules and the original materials. Leuenberger equation, which connects compressibility and compactibility parameters and this equation, was also applied in this study.

According to the equations which are responsible for compressibility measuring, THAP, THAFP, THMO and MCC belong to the same group and showed plastic behavior when they were exposed to pressure. However, when tensile strength of tablets produced by direct compaction and roller compaction was measured, differences in behavior were occurred. Tensile strength of MCC tablets after roller compaction was extremely decreased, while THAP, THAFP and THMO tablets showed slightly decreased tensile strength. The phenomenon of loosing tableting properties during roller compaction is characteristic for plastic materials and since the tablets produced from THAP, THAFP and THMO showed almost the same tensile strength after roller compaction led to the conclusion that these materials showed significantly less plastic behavior than MCC. Tablets composed of the mixture of 10% Theophylline and 90% MCC showed the best compressibility and compactibility properties.

In order to check the influence of roller compaction on disintegration and dissolution rate, tablets with the same properties were produced from the original materials and granules produced by roller compaction at pressure of 20 and 30 bars. Tablets of THAP, THAFP and THMO produced by direct compaction and roller compaction showed very slow disintegration because these materials do not show any

disintegrant properties and tablets were more dissolvable. Adding MCC to the tablets formulation extremely improved disintegration, especially if tablets were produced by roller compaction. During the dissolution process anhydrate underwent transformation to monohydrate. However, during the dissolution process THAP and THAFP were transformed to monohydrate and showed slightly higher dissolution rate than THMO. This could be explained by different particles shape and surface area of THMO and hydrate which was obtained from initially anhydrate surface. Due to the faster disintegration rate of the tablets produced by roller compaction, dissolution rate of these tablets was higher as well. As it was demonstrated that roller compaction improves disintegration time and dissolution rate of the tablets it could be proposed as a method of choice for immediate release tablets.

2. Theoretical Section

2.1. Introduction

Since in recent years the concern about environmental effects was increased, there is a high interest for methodologies which are environmentally friendly ¹. Due to the fact that roller compaction is a technology where no organic solvent are used it became widely accepted in pharmaceutical technology. Although, it has been used since more than 50 years, it has recently drawing increasing attention.

Roller compaction is conceptually a very simple process: the feed powder is passed between two counter - rotating rolls where the flow being induced by the friction acting at the surface of the rolls ². Even though, it looks very simple at the first sight compaction in a roll press is a complex process and not yet fully understood. A lot of parameters are involved in the process and a lack of understanding of the compaction mechanisms can lead to undesirable results.

2.2. Tablet Dosage Form

The tablet is the most commonly used dosage form for pharmaceutical preparations. For manufacturing of tablets certain qualities of the powder are required: low segregation tendency, good flowability and compactibility ³. Therefore, granulation becomes an integral part of pharmaceutical processes that attempts to improve powder characteristics.

Granulation is any process of size enlargement, whereby small particles are gathered together into larger permanent agglomerates in which the original particles can still be identified. Pharmaceutical granules typically have a size range between 0.1 and 2.0 mm.

2.2.1. Particle-bonding Mechanisms

To form granules, bonds must be formed between powder particles so that they adhere to each other and further these bonds must be sufficiently strong to prevent breakdown of the granules into individual particles powder in subsequent handling

operations⁴. The magnitude of these forces is determined by the size of the particles, the structure of the granules, the moisture content, and the surface tension of the liquid.

There are five primary bonding mechanisms for agglomeration between particles^{4,5}.

1. Adhesion and cohesion forces in immobile films

The availability of sufficient moisture in a powder to form a very thin, immobile layer can contribute to the bonding of fine particles by effectively decreasing the distance between particles and increasing the interparticle contact area. In dry granulation the pressure used will increase the contact area between the absorption layers and decrease the interparticle distance, and this will contribute to the final granule strength.

2. Interfacial forces in mobile liquid films

When the liquid level on the surface increases beyond that in a thin film, mobile liquid forms bridges wherein capillary pressure and interfacial forces create strong bonds. Although, wet bridges are temporary structures in wet granulation, because the moist granules will be dried, these bonds precede the formation of solid bridges.

3. Solid bridges

These can be formed by diffusion of molecules from one particle to another through partial melting at points of contact where high pressure is developed, crystallization of dissolved substances, hardening of binders and solidification of melted components.

4. Attractive force between solid particles

If the particles approach each other closely enough, forces at surfaces (van der Waals forces, electrostatic forces or magnetic type interactions) can interact to bond particles. During dry granulation magnitude of van der Waals forces increases as the distance between particles decreases. This is achieved by using pressure to bring particles together.

5. Mechanical interlocking

The term is used to describe the hooking onto and twisting together of fibrous or irregular particles in a compact. Smooth spherical particles will have little tendency to interlocking.

2.3. Methods of Granulation

Granulation methods can be divided into two main categories:

- Wet granulation
- Dry granulation

2.3.1. Wet Granulation

Wet granulation is a method which utilizes some form of liquid to bind the primary particles together. All components involved in the wet granulation process form a three phase system made of the disperse solid (powder or powder blend), the granulation liquid and the air ⁶. The general method for doing wet granulation is shown in the flow sheet in figure 2.1. The granulation liquid usually contains solvent, which must be volatile so that it can be removed by drying, and adhesive (binding agent). Typical liquids include water, ethanol, isopropanol, in combination or alone. The most useable liquid is water for ecological and economical reason. Its disadvantages are that it can adversely affect drug stability leading to hydrolysis of product, and it requires a longer drying time than the organic solvent ⁴.

Different operations and processes are involved in wet granulation process. The most important ones, which can affect the tablets of the resulting granulation, are: (see figure 2.1) ⁷.

- Preparation of the powder mixture with screening and mixing
- Spraying with solution to the appropriate wetness
- Drying the solid - liquid mixture
- Milling the dry granulate to proper particle size

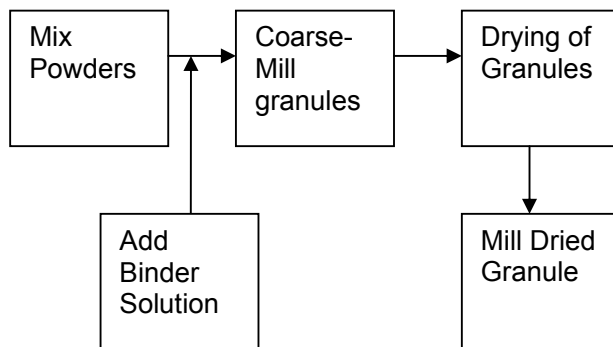


Figure 2.1.: Flow sheet for granule production ⁷

2.3.2. Dry Granulation

As all granulates in this work were made by a dry granulation, a special accent is given to this process.

Dry granulation is a method where no moisture and heat is used to process powders into granules. Although, dry granulation has been used in pharmaceutical industry since more than 50 years, it has recently drawn increasing attention ⁷.

There are two types of dry granulation: slugging – where a powder is compressed into large tablets or slugs, and roller compaction - process in which uniformly mixed powders are compressed between two counter rotating rolls to form a compact (ribbons) (see figure 2.2). In both cases these intermediate products, slugs and ribbons, are broken using suitable milling technique to produce granular material, which is then sieved to separate desired particle size.

In the pharmaceutical industry, dry granulation process in the 1950s – 1970s favored a slugging. Slugging involves the use of circulating dies to produce a large compact, often 25 mm or larger in diameter, for granulation. In this process, round, flat – faced punches should be used in order to avoid trapped an air within the slug, which may be trapped with concave punches. To get better feeding and high production rate the maximum diameter should be used ⁸. Slugging tends to be more limiting in terms of uniformity and capacity than roller compaction system.

The advances of roller compaction over slugging are: greater production capacity, more control over operating parameters, simpler and continuous processing.

The bonding mechanisms which occur during dry granulation process are described as a mixture of van der Waals forces, mechanical interlocking, and recombination of bonds established between created surfaces and solid bridges, which are created as a result of partial melting and solidification during compression.

Formation of granule bond usually occurs in the following order ⁸:

1. Particle rearrangement – when powder is filled in void space air begins to leave the powder blend's interstitial spaces and particles move closer. Spherical particles will tend to move less than particles of the other shape because of their packing.
2. Particle deformation – as compression force is increased particle fragmentation occurs. This deformation increases the point of contact between particles where bonding occurs and is described as plastic deformation.
3. Particle fragmentation – the next bonding stage which occurs at increased force level.
4. Particle bonding – with created of particle deformation and fragmentation particle bonding occurs. In general, it is accepted that bonding take place at molecular level, and that is due to the effect of van der Waals forces.

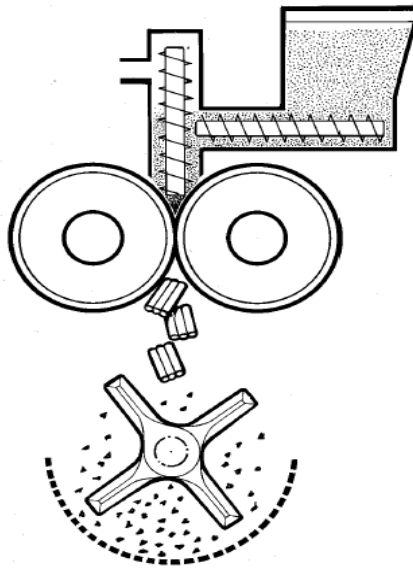


Figure 2.2.: A typical roll compaction process (Fitzpatrick Company) ⁹

2.3.2.1. Mechanisms of Roll Compaction

The principle of compaction is based on equipment design and operating parameters that influence the starting material in a manner to produce an optimum compact ¹⁰.

The space between two rolls, where different mechanisms occurs, is generally divided in three regions (see figures 2.3) ¹¹:

1. Slip region (feeding zone) – this zone is characterized with particles slipping at the roll surface and at the same time rearrangement and de-aeration can occur. The effectiveness of the slip region is related to wall friction and interparticle friction of the feed ¹⁰. The speed of the material is lower than the peripheral speed of the rolls.

2. Nip region (compaction zone) – in the nip region, the material is trapped between two rolls and is moving at the same speed as the roll surface. This forces the material through the region of the maximum pressure where the particles deform plastically and/or break. The limit between feeding and compaction zones is the nip angle α . This angle is directly affected by the roll diameter and established in a line through the rolls' centers to a point on both roll where the powder starts to move at the same speed as the roll (see figure 2.3). To achieve acceptable compaction, the nip angle should be sufficiently large. It is about 12° and material characteristics, as particle size and density, can have influence on this value.

3. Extrusion region (release zone) – when the roll gap starts to increase, the compacted ribbon exhibits relaxation as it is released from the rolls.

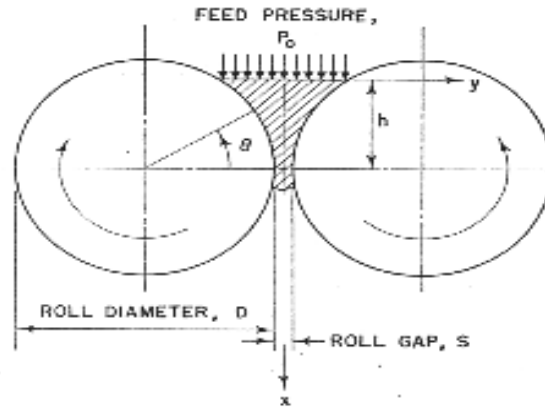


Fig. 1 Roll press

Figure 2.3.: Schematic diagram of the roll compaction process ¹²

Equation 1 is developed for the linear variation of compact thickness at a specific roll diameter ⁸.

$$e_1 = D \left(\frac{d_0}{d_1 - d_0} \right) (1 - \cos \alpha) \quad (1)$$

Where e_1 is compact thickness, D is roll diameter, d_0 is material density at angle α and d_1 is compact density.

According to equation 1 it can be concluded that if the same compact thickness is required with different roller diameters, the density of the compacts would be greater with the larger diameter rollers.

2.3.2.2. Model of Roll Compaction Process

Theoretical analysis of the operation of roll-type pressing machines has first been proposed by Johanson in 1965. It was based on understanding the behavior of the material within roll press which involves the interaction between the particles of the material itself as well as the interaction between the material and roll surface. According to Johanson ¹² roller compaction involves the continuous shear deformation of the material into a solid mass. The material is assumed to be isotropic, frictional, cohesive and compressible.

Two zones are considered in this approach ¹³:

- $\alpha < \theta < \theta_h$: slip zones, the rolls moves faster than the powder
- $\theta = \alpha$: the powder sticks to the rolls $V_{\text{powder}} = V_{\text{roll}}$
- $0 < \theta < \alpha$: densification takes place

To determine the nip angle two equations are considered, as it is shown in Figure 2.4. Determination of the pressure distribution above the nip region was based on the continuous plane-strain deformation and assuming the slip along the roll surface in the slip region, pressure gradient ($d\sigma/dx$) is given by the following equation 2.

$$\frac{d\sigma}{dx} = \frac{4(\pi/2 - \theta - \nu)\tan \delta}{\frac{D}{2}[1 + S/D - \cos \theta][\cot(A - \mu) - \cot(A + \mu)]} \quad (2)$$

Where θ is the angular position of the surface of a roll, such that $\theta = 0$ corresponds to the minimum gap, ν acute angle, δ angle of internal friction, μ friction coefficient, and parameter A is given by:

$$A = \frac{\theta + \nu + (\pi/2)}{2}$$

A typical $d\sigma/dx$ function is shown by the solid line in Figure 2.4.

In the nip region no slip occurs along the rolls surface and all material trapped between the rolls at the position of nip angle must be compressed into a compact with a thickness equal to the roll gap. In this case, where slip does not occur, pressure gradient ($d\sigma/dx$) is given by equation 3.

$$\frac{d\sigma}{dx} = \frac{K\sigma_0(2\cos\theta - 1 - S/D)\tan\theta}{\frac{D}{2}[d/D + (1 + S/D - \cos\theta)\cos\theta]} \quad (3)$$

This function is illustrated by the dashed line in Figure 2.4.

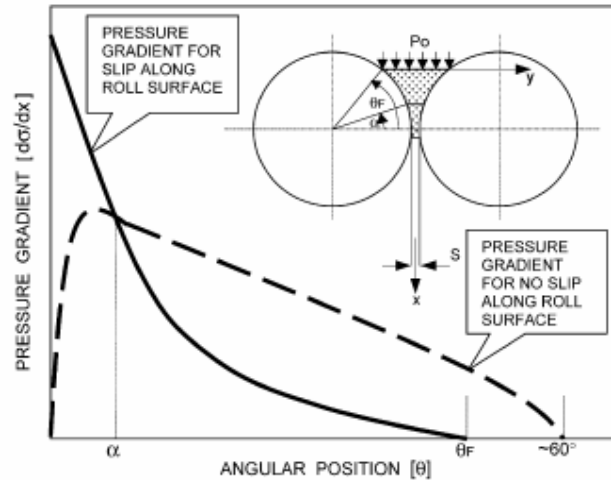


Figure 2.4.: Vertical pressure gradient vs. angular position in roll bite (comparison of different methods) ¹⁴

According to Johanson ¹² at the nip angle α (equation 4) the pressure gradient in the slip and nip regions are equal

$$\left(\frac{d\sigma}{dx}\right)_{slip} = \left(\frac{d\sigma}{dx}\right)_{nip} \quad (4)$$

The intersection point of two curves (see figure 2.4.) gives the angles of nip α .

In general, the nip angle strongly depends on the material compressibility factor K , material flow properties, angle of internal friction, angle of wall friction. Dependence on the roll diameter and roll gap is almost negligible, especially when dimensionless roll gap S/D is less than 1 ^{10,12,13}.

2.3.2.3. Equipment

The successful roll compaction of a powder depends on the matching powder properties, especially its compressibility and flowability, and to both the design and operating conditions of the compactor ¹³. In the pharmaceutical field only a few producer of roll compactors are established. Although the general layout of the machines looks alike, there are some features that differ from compactor to compactor. These lead to a type classification:

- Roll assembly: rolls can be mounted in a horizontal, inclined and vertical position (see figure 2.5)².

Horizontal position of rolls is a characteristic for Fitzpatrick Company, Bepex, Komarek (A), inclined for Gerteis (B) and Vertical for Alexanderwerk (C)¹¹.

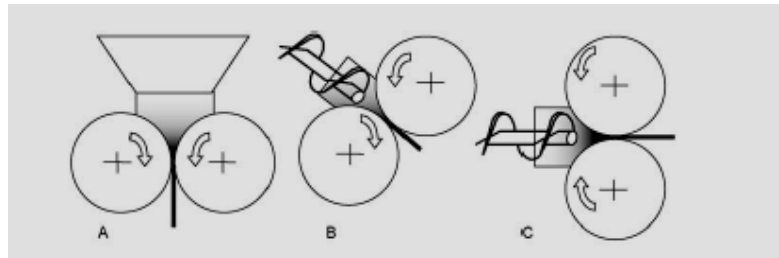


Figure 2.5.: Configuration of roll compactor ²

The position of the rolls is mainly a manner of design and therefore it only plays minor role. However, the vertical assembly might induce that the nip angles in upper and lower roll differ. This can happen because the direction of force by friction and force of gravity is completely different for the two rolls. If nip angle is quite small the powder might stay in place, showing an increase in temperature, giving reason for concerning a thermal degradation of the material. When vertically assembled rolls are used differences in nip angles should be taken in to account ².

- Fixed vs. movable rolls: according to gap system two type of roller compactors exist.

One in which the distance between the rolls is constant during the process of powder densification and one in which this distance can be changed ². In the first case gap size cannot be varied during the process of compaction. Ribbons which are produced have the same geometrical dimensions, but porosity can be changed with the fluctuating mass flow ¹¹. Compactors with variable gap system have one fixed and one moveable roll. The consolidating force on the material between two rolls is supplied by hydraulic units. This unit acts upon the floating roll which can move horizontally depending on feeding rate and applied pressure ⁹.

- Roll surface: Roll surface has an effect on the efficiency and production rate in the powder compaction. According to powder properties different roll surface can be used: smooth, knurled and pocket design (see figure 2.6).

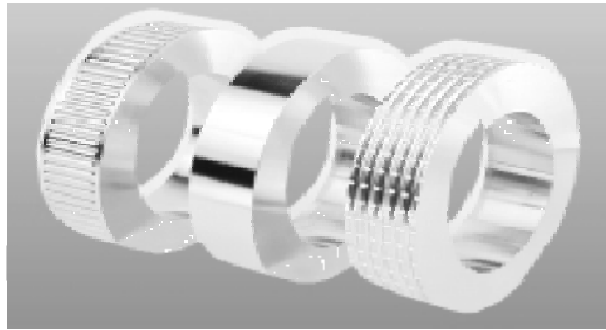


Figure 2.6.: Various roll surfaces for compaction⁹

- Feeding system: three different ways of feeding material into to the compactor exist, gravity transport, single screw feeder and double screw feeder (see figure 2.7). It must achieve a uniform and continuous flow of material in order to fill the nip between the rolls correctly and sufficiently, so that the formed compacts are not heterogeneous². When powder is dense and free flowing gravity feeder can be used, but for most powders, which are lightweight and do not fly freely single or double screw feeder is required. During feeding, vacuum deaeration can be applied to remove air from a powder with low bulk density^{9,15}.

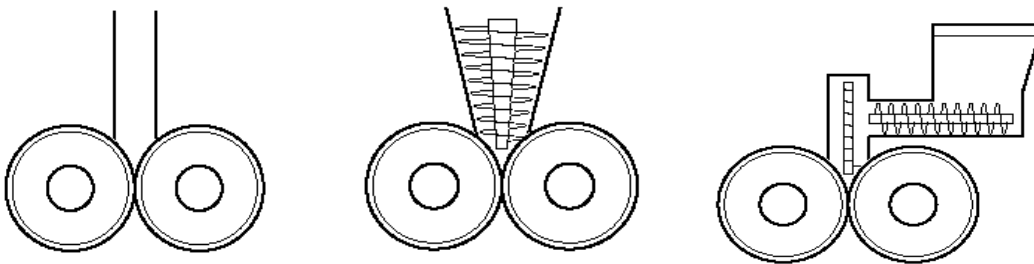


Figure 2.7.: Different feeding system: a) gravity feeder, b) single screw feeder, c) double screw feeder¹⁶

2.3.2.4. Process Parameters

Compaction in a roll press is more complicated than it looks at the first sight. Efficiency of roller compaction is based on the equipment design and operating parameters. The main process variables which can affect compaction are:

- Compaction pressure: if pressure is too low there is no compaction, but in the same time if it is too high over compaction will occur.

- Speed of feeding screw (vertical vs. horizontal): speed of vertical and horizontal screw should be optimized otherwise feeding is not continuous and compaction is not homogeneous.
- Roll speed affects the compaction by determining the dwell time that material should spend in the nip region which has an impact on the ability of the product to deaerate prior to passing between two rolls.

Roll gap is the distance between the rolls at their closest point. This is the critical parameter of compaction and one that needs to be stabilized by the process parameters mentioned above. It is in a function of pressure applied to the rolls and the amount of material that is passed between them ⁹.

Table 2.1.: Advantages and disadvantages of roller compaction

| Advantages | Disadvantages |
|--|----------------------------------|
| - Binder-less agglomeration | - Weakening or disruption of the |
| - Suitable for heat and moisture sensitive material (no liquid and drying) | crystal lattice |
| - Use less equipment and time (cheap) | - Production of fines |
| - Continuous process | - Loss of reworkability |

Since granulating solvent is not used during dry granulation, solution or solution-mediated phase transformations are eliminated, thus the probability of phase transitions with this granulation unit operation is reduced. However, the applied mechanical stresses during processing may lead to phase transformation via the solid-state or melt mechanisms ¹⁷.

2.3.3. Milling

The final product of the roller compaction – ribbons, must be subsequently broken to the required particle size. In general, the milling or size reduction is the mechanical process of reducing of the size of particles or aggregates. To initiate reduction of particle size external forces should be applied ¹⁸.

The milling is affected by a variety of factors and has a direct influence on the quality of the final product. The selection of equipment which should be used for this process is determined by the properties of feed material and specification of the product.

2.3.3.1. Classification of Mills

The most convenient classification of size reduction equipment is according to the way in which forces are applied; impact, shear attrition and shear-compression ¹⁹.

Table 2.2.: Characteristic of Different Types of Mill ¹⁹

| Mechanism of Acting | Example | Particle size |
|---------------------|--------------------------|------------------|
| Impact | Hammer mill | Medium to fine |
| Shear | Extruder and hand screen | Coarse |
| Attrition | Oscillating granulator | Coarse to medium |
| Shear-compression | Comil | Medium to coarse |

The type of mill can affect the shape of the granules and throughput, and shape of the granules affect the flow properties.

An impact mill produces sharp and irregular granule where flowability sometimes may be a problem, whereas granules produced by attrition mill are more spherical.

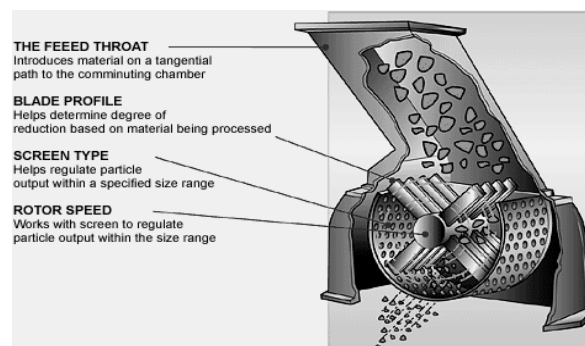


Figure 2.8.: Hammer mill - the principle of operation ²⁰

2.3.3.3. Process Parameters

Besides the type and design of mill, the most important factors which can affect the quality of particles are: feed rate, screen size and rotor speed.

- Feed rate controls amount of material that enter to the mill and can control overfeeding or underfeeding. Although, either phenomenon should be avoided, overfeeding is relatively more harmful. When amount of material which is fed is bigger than amount which is discharged it stays in the milling chamber and it leads to greater size reduction, over loads the motor and reduced capacity of the mill ¹⁹. In general, the feed rate should be equal to the rate of discharge.

- Screen, located directly under the blade, prevents particles to leave the chamber until they are at least the same size as the screen holes. The screen size doesn't necessarily define the particle size of the final product. Depending on rotor speed, particles find various dimension and shape of angle at which they approach the screen. The higher rotor speed will influence the smaller angle under which particles hits the screen. This means that particles will pass through the smaller hole in the screen (see figure 2.9), leading to smaller particle size of the final product. The thickness of the screen has influence on the particle size as well. The thicker the screen, the smaller particle can pass the screen (see figure 2.10) ²⁰.

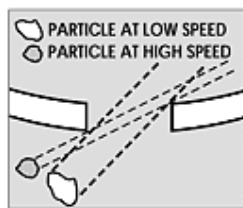


Figure 2.9.: Influence of the rotor speed to particle size ²⁰

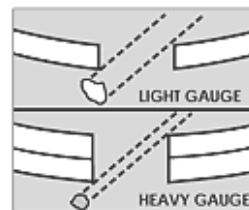


Figure 2.10.: Influence of the screen thickness to particle size ²⁰

- Rotor speed directly affects the particle size range. If all the other variables are the constant, faster rotor speed induces the smaller particle size.

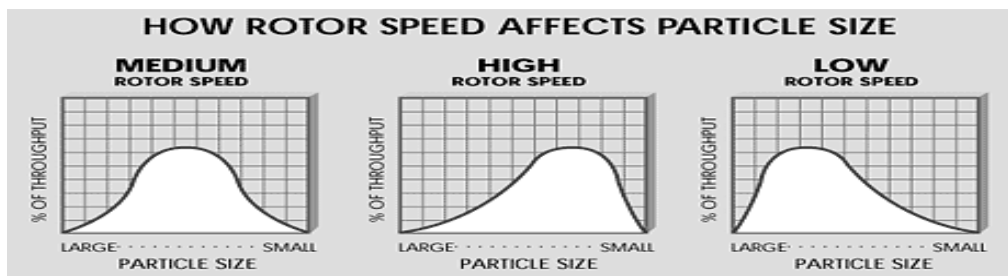


Figure 2.11.: Distribution of the particle size depending to rotor speed ²⁰

As all processes, milling has some advantages and disadvantages, which should be considered before starting with size reduction of the material (see table 2.3.).

Table 2.3.: Advantages and disadvantages of milling ²¹

| Advantages | Disadvantages |
|---|--|
| <ul style="list-style-type: none"> - Increase of surface area (increase dissolution and bioavailability) - Enhance content uniformity (increase number of particles per unit weight) - Improve flowability (irregular shape of the material) - Control particle size distribution | <ul style="list-style-type: none"> - Change in polymorphic form - Possible degradation of the drug |

2.4. Tablets

As it is explained in the beginning, tablets can be produced from a mixture of a powder, or aggregated particles of a powder (granules). Whatever method is used, the resulting tablets should have certain properties.

Tablets have to be enough strong and resistant to abrasion during manufacture, packaging and use, but in the same time active material from tablets must be bioavailable. Bioavailability can be monitored by dissolution and disintegration test ²². In order to achieve these characteristics, active pharmaceutical ingredient is blended with different ingredients having specific functions. The homogeneity of the powder mixture is essential to improve both mechanical and medicinal properties of the tablets.

Although, tablets exist in different forms, the way in which they are produced is in general the same ²³.

When a force is applied on a powder bed, a lot of mechanisms become involved in transformation of the powder into a porous, coherent compact called tablet.

According to Nyström ²⁴ five mechanisms are involved in the powder compaction:

1. Particle rearrangement
2. Elastic deformation of particles
3. Plastic deformation of particles
4. Fragmentation of particles
5. Formation of interparticulate bonds

At the beginning of powder compaction, particles are rearranged, and reduction in volume occurs due to closer packing of powder. Depending on the packing characteristics of particles, at certain load no more rearrangement can take place.

As the pressure is increased, the initial particles change shape or deform and further compression leads to some type of deformation (see figure 2.12). When the load is removed, some particles are able to return to original shape (elastic deformation), whilst other ones are permanently deformed (plastic deformation). The force required to initiate a plastic deformation is noted as yield stress ²⁵. Brittle particles undergo fragmentation, crashing of the original particles into smaller units. A single particle may pass through several of these stages during compaction ^{23,26}.

Some materials consolidate by a plastic deformation (microcrystalline cellulose, starch, sodium chloride), some by fragmentation (crystalline lactose, sucrose, Emcompress), but all materials possess both elastic and plastic component ²⁴.

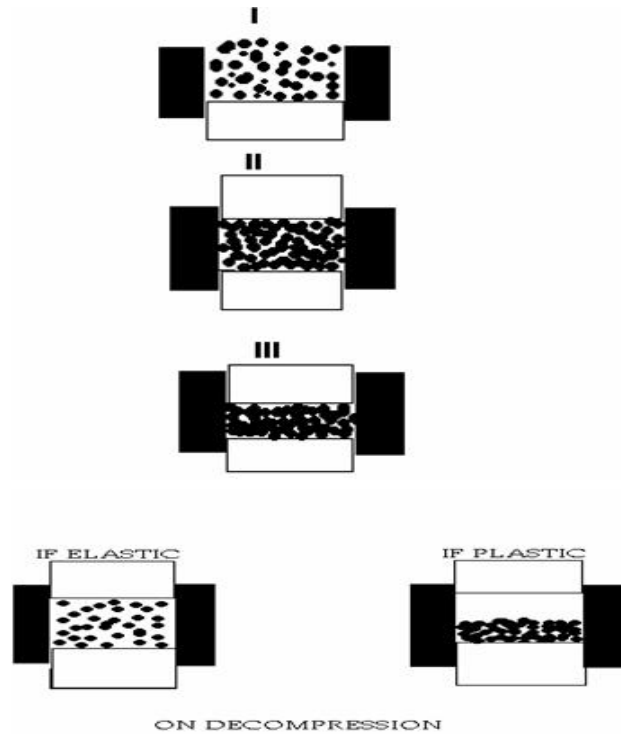


Figure 2.12.: Stages involved in compression (I – III) and decompression ²⁷

2.4.1. Compression Bonding Mechanisms

When particles get together, adhesive forces are developed, which are responsible for the strength of compacts after compression and compaction ⁶.

In compression of dry powders, dominating bonds of interparticular adhesion are ^{6,24} :

- Solid bridges
- Distance attraction forces (intermolecular forces)
- Mechanical interlocking (between irregular shaped particles)

Solid bridges can be formed at the place where there is a particle-particle contact at an atomic level. Due to their structure, solid bridges seem to be relatively strong bonds and tablets containing this type of bonds can be related with prolonged disintegration time.

Intermolecular forces are all bonding forces which coordinate between surfaces separated with some distance and these forces are relatively weak. In this group are involved: Van der Waals forces, electrostatic forces and hydrogen bonding ²⁴.

Material which is bonded with forces of mechanical interlocking has low strength and accelerated disintegration time, but for producing tablets it requires a high

compression forces. This type of bonds induces the hooking and twisting of the packed material.

Mechanical interlocking and Van der Waals forces are the mechanisms which are included in the process of roller compaction so it could be expected that disintegration time of tablets produced by this method is fast.

2.4.2. Properties of Tableting Materials

As it is previously explained materials could consolidate by different type of deformation.

Materials which are undergoing extensively fragmentation during compaction creates a large number of interparticulate contacts point and relatively weak attraction force, which act over distance. However, even weak attraction force are formed, due to the large number of attractions zones relatively strong compacts could be formed. Less fragmenting materials form a less number of contact points between particles and only if strong attraction forces are created, strong compacts could be formed. Extensively plastic materials could develop a large number of attraction forces and form strong compacts.

Due to compression behavior, both fragmenting and plastic behavior materials are considered as bond-forming compression mechanisms. The difference between two mechanisms is that fragmentation affects mainly the number of interparticulate bonding while plastic deformation affects mainly the bonding force of these bonds. This is due to fact that fragmenting material form a large number of bonds, while material with plastic deformation forms a strong attraction force as well.

2.4.3. Mechanical Properties of Tablets

The characterization of compressibility and compactibility of the material has very important role in the tablet manufacturing. Compressibility is an ability of a powder to decrease in volume under pressure, and compactibility is the ability of the material to be compressed into a tablet of specified strength²⁸.

Since the first accurate compaction data were obtained, the use of compaction equations have played an important role to relate the relationship between density or

porosity of the compact, and the applied pressure ^{2,29,30}. Many compaction techniques are used to characterize the consolidation behavior of pharmaceutical solids.

2.4.3.1. Heckel Equation

The most frequently used approach is the analysis of the Heckel plots.

Heckel equation, is established on the postulate that the densification of the bulk powder, that is the reduction in porosity, follows the first order kinetics under applied pressure ²⁹.

According to the analysis, the rate of compact densification (equation 5) with increasing compression pressure is directly proportional to the porosity (equation 6):

$$\frac{d\rho}{dP} = k(1 - \rho) \quad (5)$$

$$\varepsilon = 1 - \rho \quad (6)$$

where ρ is the relative density, and ε is the porosity at a pressure P . The relative density ρ is the ratio of the compact density at pressure P to the density of the material.

The equation can be transformed to:

$$\ln\left(\frac{1}{1 - \rho}\right) = KP + A \quad (7)$$

$$P_y = \frac{1}{K} \quad (8)$$

where ρ is the relative density of the powder compact at a pressure P , constant K is a slope and constant A is an intercept of the linear part from the graph. The reciprocal value of K is material dependent constant P_y (equation 8), known as yield

pressure, which is inversely connected to the ability of the material to deform plastically under pressure^{27,29,31}.

The Heckel plot is linear only at high pressure. According to the character of the material the linearity is noted at different pressures: for plastically deforming materials (Avicel PH grade, Sodium chloride and Sorbitol) at a pressure higher than 20 MPa, whilst for fragmenting materials (Lactose, Dicalcium phosphate) the linear relationship between $\ln(1/(1-\rho))$ and pressure P , occurs at pressure higher than 80 MPa³².

There are two different approaches to obtain density-pressure profiles: “in die” and “out of die”. In the case of the first method, “in die”, dimensions of the tablets are measured during applied pressure, by evaluating punch displacement. The “out of die” method, calculates tablet volume by measuring its dimensions after compression and relaxation.

According to Heckel plots and compaction behavior, material can be classified into three types A, B and C²⁷.

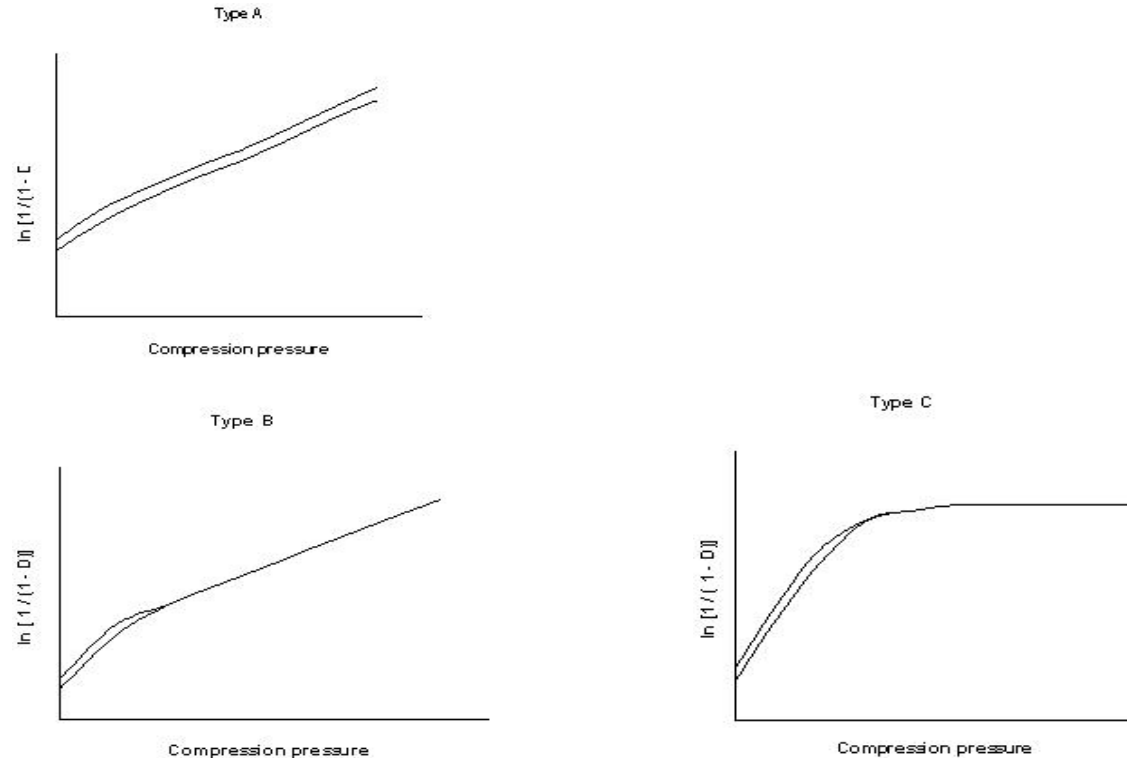


Figure 2.13.: Different types of Heckel plots²⁷

Material type A: materials which deform only by plastic deformation. The plots remaining parallel as the applied pressure is increased (see figure 2.13 A).

Material type B: at the early stages there is a curved region followed by a straight line (see figure 2.13 B). During the compression process the particles are first fragmenting i.e. brittle fracture precedes plastic flow. A typical example of material type B is Lactose.

Material type C: initial sloping linear region become flatten out as the applied pressure is increased (see figure 2.13 C). This type of densification occurs by plastic flow but no initial particle rearrangement is observed.

2.4.3.2. Modified Heckel Equation

Due to the fact that Heckel plot shows linearity only in a region of high pressure, Leuenberger developed a modified Heckel equation which takes into consideration the relation between the pressure susceptibility and relative density of the material.

The modified Heckel equation is especially suitable for low pressure range.

Pressure susceptibility is in a function of porosity and compression pressure (equation 9)³³.

It is known that porosity can be expressed by the relative density $\rho = 1 - \varepsilon$ or in differential form $d\rho = -d\varepsilon$

$$\frac{d\rho}{dP} = \chi_p(1 - \rho) \quad (9)$$

There is a critical porosity ε_c or corresponding relative density ρ_c , where the pressure susceptibility approaches infinity, and in this point powder beds for the first time show the mechanical rigidity. Pressure susceptibility χ_p can be defined only for porosity lower than ε_c , and relative density higher than ρ_c , and these porosity and density can be called critical.

$$\chi_p = \frac{C}{\varepsilon - \varepsilon_c} = \frac{C}{\rho - \rho_c} \quad (10)$$

Combination of equation 9 and 10, and their integration gives a modified Heckel equation (equation 11).

$$P = \frac{1}{C} \left[\rho_c - \rho - (1 - \rho_c) \ln \left(\frac{1 - \rho}{1 - \rho_c} \right) \right] \quad (11)$$

The constant C from modified Heckel equation corresponds to constant K from Heckel equation and indicates ability of the material to deform plastically. The larger value C means that material is more plastic in character.

2.4.3.3. Leuenberger Equation

Compressibility, the ability of the material to decrease in volume under pressure, is only indirect measure of its ability to form tablets²⁸. However, in practice is more important that compression produce a compact of adequate strength. The physical model of powder compression proposed by Leuenberger connects the compressibility and compactibility. Interrelation between these two characteristics can be expressed with equation 12.

$$\sigma_t = \sigma_{Tmax} (1 - e^{-\gamma \sigma \rho}) \quad (12)$$

Where:

σ_T - radial crushing strength at certain pressure (MPa)

σ_{Tmax} - maximum crushing strength (MPa)

γ - compression susceptibility (MPa⁻¹)

ρ - relative density

The equation can be used for a single substance as well as for powder or granules mixtures. Parameter σ_{Tmax} can be used to quantify compactibility and parameter γ to quantify compressibility²⁸.

Table 2.3 presents compressibility and compactibility characterization of the materials according to parameters σ_{Tmax} and γ , respectively³⁴.

Table 2.3.: Classification of the materials according to the type of deformation (compressibility)

| Parameter | Plastic | Brittle |
|--|---------------------|-----------------------|
| Compactibility σ_{Tmax} (MPa) | Small ($0-10^2$) | Large (10^2-10^3) |
| Compressibility γ (MPa) ⁻¹ | Large (10^{-2}) | Small (10^{-3}) |

2.4.4. Factors Affecting Compactibility of Powders

There are several factors which are regarded as very important factors for the compactibility of powders: particle shape, surface texture and particle size.

It is assumed that changes in particle size not only affect the external surface of area of particles, but mechanical properties of particles could be changed as well ³⁵. Generally, a decrease in particle size, affect an increase in mechanical strength of tablets. This phenomenon is usually characteristic for plastic material. However, it was found that in material which undergoes extensive fracture under pressure (brittle material) particles enlargement should less influence mechanical strength of tablets than in the case of plastic material ³⁶.

A widely accepted explanation of this observation is that extensive fracture of particles significantly reduces original particle sizes, hence effectively minimizes or eliminates any difference in original particle size of the material. This was reasonable with studies showed more extensive fragmentation of brittle than plastic material especially at high pressure.

In some ³⁵ studies it was reported that if particle sizes are reduced extremely, conversion from brittle to plastic behavior may take place; it means that modification of mechanical properties of particles could occur.

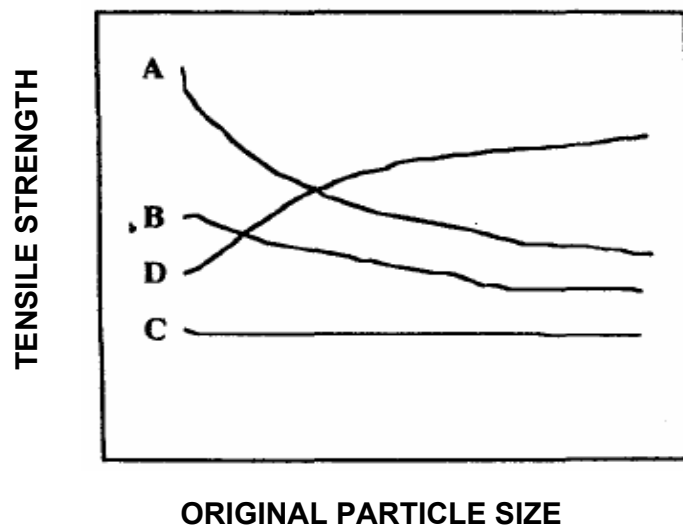


Figure 2.13.: Relationship between original particle sizes and tablet strength: (A, B) increased particle surface deformability with a reduced particle size or marked importance of the numbers of bonds for tablet strength, (C) no particle size effect on particle deformability, (D) increased particle deformability with increasing particle size

2.5. Tablet Press

For producing tablets two basic types of presses are used: single-punch tablets machines (eccentric press) and multistation tablet machines (rotary press). Both types of machines have the same basic functional unit - a set of tooling consisting of a die and an upper and lower punch. The punches, upper and lower, come together in the die that contains powder or granule to form the tablet ²².

2.5.1. Principles of Eccentric Tablet Machine

Eccentric tablet machine is slow and used in product development when raw material is available only in a low quantity. It can produce 40 to 120 tablets per minute ⁶. Within the manufacturing process, tablet formulation is filled from a hopper into a die, and volume of the tablets is determined by the position of the upper and lower punch. The position of the upper punch defines the compression force, while lower punch is responsible for the ejection of compressed tablets. During the compression process on the eccentric press, pressure on upper punch is usually higher than the pressure at lower punch ²⁵.

2.5.2. Principles of Rotary Tablet Machine

Rotary tablet machine is used for high - volume production (up to million tablets per hour). The basic process is that die and punches are situated on a rotating turret and pass through the filling station, precompression and compression rollers and at the end through ejection station ³⁷. Powder is feed by hopper into feed frame under which dies and lower punch receive it. As a result of the upper punch downward movement and upward movement of the lower punch tablets are produced by double side compaction. Process is finished when the tablet is ejected from the die by the extreme upward movement of the lower punch. The productivity of the machine depends on the speed which can be limited by die fill (flow rate) and compressibility of the material.

2.5.3. Compaction Simulator

As a consequence of different working principles between eccentric and rotary tablet presses, results and subsequently developed formulation may not be easily transferable from one machine to another and this can lead to technological problems ³⁸. Varying dwell time, magnitude and rate of applied force, as they even can be found for different brands of machines with the same working principles, can cause major differences in tablet properties as well. Compaction simulator, requiring a small amounts of powder while they all operate with just one pair of punches, running at comparable working principles as rotary tablet press, is the most appropriate machine for compaction process during the early stages of development. Compaction simulators have also proven to be an efficient tool for production trouble-shooting.

First high speed compression simulator and able to reproduce the multiple compression and ejection cycle was developed by Hunter 1976, and in the following years a many different types of simulator were presented.

All simulators are similar in design and construction and often work on hydraulic principles, and they operated either under punch displacement or force control.

Table 2.4.: Comparison of equipment for tableting studies ³⁸

| Feature | Single Station Press | Multi Station Press | Punch and Die Set | Compaction Simulator |
|----------------------------------|----------------------|---------------------|-------------------|----------------------|
| Model production conditions | no | yes | maybe | yes |
| Model other presses | no | no | maybe | yes |
| Small amount of material | yes | no | yes | yes |
| Easy to instrument | yes | no | yes | yes |
| Useful for stress/strain studies | no | no | yes | yes |
| Easy to set up | yes | no | maybe | maybe |
| Equipment inexpensive | yes | no | yes | no |
| Useful for scale up | no | yes | maybe | yes |

2.6. Theophylline

Theophylline (3,7-dihydro-1,3-dimethyl-1H-purine-2,6-dione) is methylxanthine derivative, that is similar in structure to Caffeine and Theobromine, found in coffee, tea and chocolate. It is mainly used in the chronic treatment of bronchial asthma and bronchospastic diseases. Theophylline works as bronchodilator by the relaxation of bronchial smooth muscles. Therapeutic serum concentration of Theophylline is usually in a range from 5 to 15 $\mu\text{m}/\text{ml}$, with a mean of 13 mg/l , while toxicity may appear at concentration over 20 $\mu\text{m}/\text{ml}$ ³⁹.

After Theophylline is directly injected into systematic circulation, it is distributed into different body fluids and tissues. Elimination from the body is done by metabolism and excretion. It is metabolized by the liver in relatively inactive metabolites ⁴⁰. The mean plasma half-life of Theophylline in adults is about 8 hours, although there is a large intra- and interindividual variation, as well as variation with age.

Due to a narrow therapeutic index, it is required to develop a suitable formulation in order to achieve and maintain average serum level of the drug without significant fluctuations.

Theophylline exists either as an anhydrate ($\text{C}_7\text{H}_8\text{N}_4\text{O}_2$) or as a monohydrate ($\text{C}_7\text{H}_8\text{N}_4\text{O}_2 \cdot \text{H}_2\text{O}$).

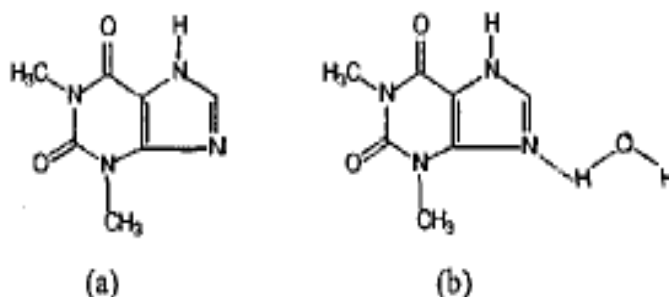


Figure 2.14.: Chemical structure of Theophylline (a) anhydrate and (b) monohydrate⁴¹

Since the physicochemical, mechanical and biological properties of anhydrate and hydrate are not the same, knowledge of the phase transformation of an anhydrate to a hydrate and vice versa is essential for the development of a stable formulation. These transformation can lead to changes in the free energy and thermodynamic activities, and can translate into alter of dissolution and bioavailability of the drug. The

differences in the stability are connected with interaction between crystal water and crystal structure of the drug, which is based on hydrogen bonding ⁴².

Anhydrous Theophylline has two polymorphic forms; form II which is stable at room temperature and form I stable at high temperature ⁴³. It belongs to the orthorhombic crystal system.

According to hydrates classification, which is based on molecular structure, Theophylline monohydrate belong to class II, channel hydrate ⁴¹. It is monoclinic crystal.

Even if the physical form of material is carefully selected for manufacture of certain dosage forms; the processing conditions may change the final solid state of the drug ⁴⁴. Manufacturing of tablets includes different steps as, milling, granulation, drying, and compression and during these processes transformation between two pseudo polymorphic forms or from one polymorph to another, can occur.

During aqueous wet granulation of Theophylline anhydrate, water can be incorporated in crystal lattice and transform anhydrate to monohydrate. When the wet granules are dried hydrate get back to the anhydrous form. Although, at the beginning of wet granulation anhydrate is stable, the end product after drying may, be a metastable polymorph ⁴⁵.

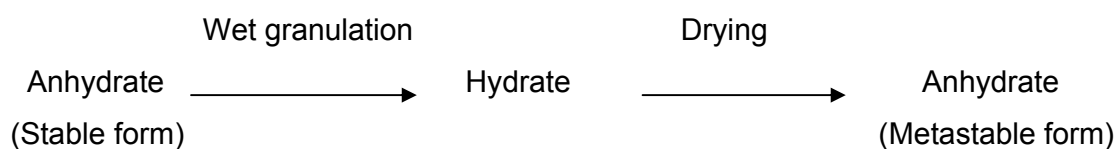


Figure 2.15.: Processing of Theophylline with water

The metastable anhydrous Theophylline is an intermediate product that is produced by the dehydration of the monohydrate, but it was not found as intermediate during the hydration of stable anhydrous Theophylline. During storage, metastable form is converted to stable one, and this conversion is dependent on temperature, water vapor pressure and excipients which are included in formulation ⁴⁶. XRD patterns in a function of temperature could show dehydration of monohydrate and formation of metastable and stable form of anhydrate, respectively, see figure 2.16 ⁴⁵.

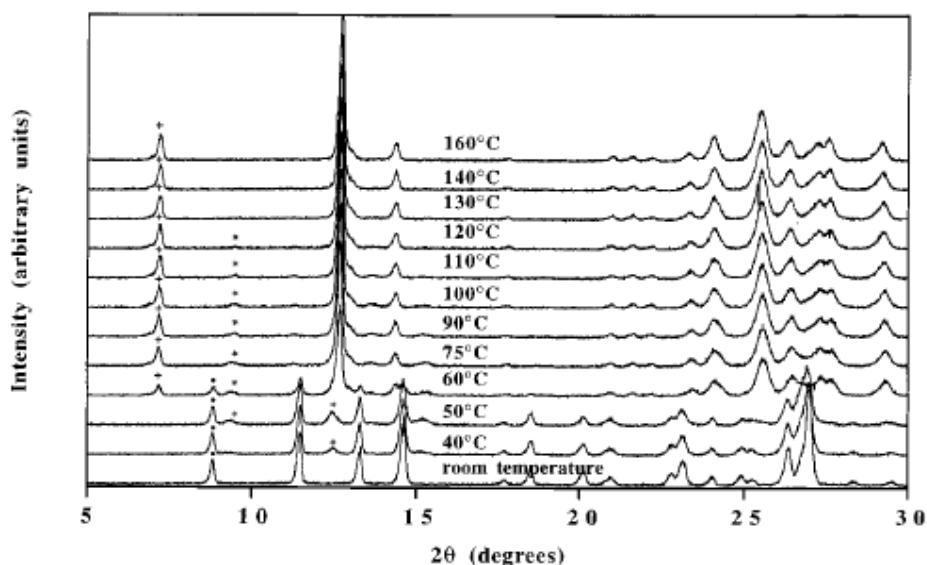


Figure 2.16.: XRD of Theophylline as a function of temperature. The “*”, “+” and “•” marks indicate peaks characteristic to monohydrate, I and II forms of Theophylline, respectively ⁴⁵.

2.7. Polymorphism

It has been known since 18th century that many substances could be obtained in more than one crystal form and since that time the properties of these substances have been studied ⁴⁵. The substances which exhibit different crystalline forms of the same pure drug are called polymorphs. Polymorphs display various physical properties, including those due to different packing and different thermodynamics, spectroscopic, interfacial and mechanical properties.

Some of the physical properties that differ among various polymorphs are listed below:

1. Packing properties

- Molar volume and density
- Refractive index
- Hygroscopicity

2. Thermodynamic properties

- Melting and sublimation temperature
- Enthalpy

- Heat capacity
 - Entropy
 - Free energy and chemical potential
 - Solubility
3. Kinetic properties
- Dissolution rate
 - Rate of solid state reactions
 - Stability
4. Surface properties
- Surface free energy
 - Interfacial tension
5. Mechanical properties
- Hardness
 - Tensile strength
 - Compactibility, tableting
6. Spectroscopic properties
- Electronic transition
 - Vibrational transition
 - Rational transition

Due to stability of various polymers of the same substances, they can be divided in two groups: enantiotropic and monotropic systems.

Different polymorphic forms of the same drug can be transformed to each other at certain conditions of temperature. Enantiotropic polymorphs have a reversible thermodynamic transition temperature where one form is more stable (has the lower free energy content and solubility) above this temperature and the other one is more stable (has the lower free energy content and solubility) below it. This temperature represents the point of the equal solubility of two polymorphic forms. If there is no transition temperature below melting temperature of the polymorphs, than the different forms are monotropic. In this case only one polymorphic form is stable at all temperatures below the melting point and all other polymorphs are unstable.

In addition to different polymorphs, many pharmaceutical solids can exist in amorphous form, as well. Amorphous solids have disordered arranged molecules

and their crystalline lattice nor unit cell could not be distinguishable and as a consequence of this they have zero crystallinity ⁴⁵.

Very often, substances are capable of forming a hydrate under certain conditions of vapor pressure and temperature ⁴¹. Based on their structural characteristics, hydrates can be classified in three groups:

- isolated lattice site water types
- channel hydrates
- ion associated water types

In the crystal structure of an isolated site hydrate the water molecules are isolated from direct contact with other water molecules by the intervening molecules of the drug. Hydrates from the class of channel hydrates have the water molecules located next to each other one direction in the crystal lattice. In ion associated hydrates, the water molecule are coordinated by ions incorporated in the crystal lattice ⁴⁵.

3. Objectives

Granulation with roller compaction is a fast and efficient way of producing granules for development as well as manufacture of tablets⁴⁵. Due to advantages of roller compaction, for processing physically and chemically moisture-sensitive materials since the use of liquid is not required, became very attractive technology in the pharmaceutical industry.

The objectives of this research were:

- influence of roller compaction on pseudo polymorphic/polymorphic forms of Theophylline
- comparison of roller compaction of different pseudo polymorphic forms as well as different particle size of the same polymorphs of Theophylline
- influence of roller compaction on compressibility and compactibility of Theophylline
- influence of different process parameters (compaction pressure) during roller compaction on tablet properties (disintegration, dissolution, compressibility and compactibility)
- influence of roller compaction on disintegration and dissolution rate of Theophylline

4. Materials and Methods

In this study two pseudo polymorphic forms of Theophylline were used, Theophylline anhydrate and Theophylline monohydrate (THMO). Theophylline anhydrate was used in two different particle size, Theophylline anhydrate powder (THAP) and Theophylline anhydrate fine powder (THAFP). All three materials were purchased from BASF ChemTrade GmbH, Germany. Microcrystalline cellulose Avicel PH101 (MCC) was purchased from FMC BioPolymer, US. All other chemicals used in this study were of analytical grade.

4.1. Powder Characterization

4.1.1. Scanning Electron Microscopy (SEM)

SEM images of the powder as well as of the granules were taken using an ESEM Philips XL 30 (Philips, Eindhoven, Netherlands) at a voltage of 10 kV after sputtering with gold.

4.1.2. Density

True density of the powders and granules, in triplicate, was measured by AccuPyc 1330 V2.02 (Micromeritics Instrument Corporation, Norcross, USA). A known weight of the samples was placed into the sample cell. Helium was used as a measuring gas and values were expressed as the mean of five parallel measurements.

Bulk and tap density of powder mixtures and granules were determined using an apparatus Type STAV 2003, (Engelsmann AG, Ludwigshafen, Germany). Measurements were done according to the following method: 50 g of powders and granules gradually were filled in a 250 ml glass cylinder. A volume (V_0) at the beginning was noted and bulk density ρ_{bulk} (g/cm^3) was calculated. After that, the cylinder was tapped for 1250 times, and using this volume (V_{1250}) tap density ρ_{tapped}

(g/cm³) was calculated. Bulk and tap density were used to calculate Carr and Hausner index, see equation 13 and equation 14, respectively.

$$CI = \frac{\rho_{tapp} - \rho_{bulk}}{\rho_{bulk}} \quad (13)$$

$$HI = \frac{\rho_{tapp}}{\rho_{bulk}} \quad (14)$$

Where:

CI – Carr index [%]

ρ_{bulk} – bulk density [g/cm³]

ρ_{tapp} – tapped density [g/cm³]

HI – Hausner index

4.1.3. Moisture content

Moisture content of the materials was measured by Karl fisher titration (Apparatus Karl fisher Titrando, 836 Methrohm, UK). The measurements were carried out with 0.2 g substance according Ph. Eur.

4.1.4. Particle Size Distribution

Particle size and its distribution in volume for all samples were measured by laser diffraction (Malvern Mastersizer 2000, Scirocco 2000). For all samples dry measurement method was done. An adequate amount of each powder was introduced as dispersion produced by air pressure. According to the material properties different pressures were used: for Theophylline anhydrate powder pressure of 0.5 bars, for Theophylline anhydrate powder pressure of 2.0 bars, for Theophylline monohydrate pressure of 2.0 bars and for Cellulose microcrystalline pressure of 2.0 bars. Each sample was measured in triplicate.

4.1.5. Specific Surface Area

Specific surface area was determined by the multipoint (5 points) BET method using Surface area and pore size analyzer (Quantachrome NOVA 2000 E, Florida, USA). Accurately weighed samples were degassed under vacuum at room temperature for 24 h, and measurements were made using nitrogen as the adsorbate and helium as the carrier gas. The amount of gas was measured by volumetric flow procedure. The data are treated according to the Brunauer, Emmet and Teller (BET) adsorption isotherm equation 15⁴⁷:

$$\frac{1}{\left[V \left(\frac{P_0}{P} - 1 \right) \right]} = \frac{C - 1}{V_m C} \frac{P}{P_0} + \frac{1}{V_m C} \quad (15)$$

Where:

P – partial pressure of adsorbate [Pa]

P_0 – saturated of adsorbate at experimental temperature [Pa]

V – volume of gas adsorbed at pressure [cm^3]

V_m – volume of gas adsorbed in monolayer [cm^3]

C – dimensionless constant that is related to the enthalpy of adsorption of the adsorbate gas on the powder sample

The volume of gas absorbed at monolayer V_m was obtained from the slop and intercept of BET plot according to equation 16:

$$V_m = \frac{1}{\text{Slope} + \text{Intercept}} \quad (16)$$

The total surface area of the sample is calculated using equation 17:

$$S_t = \frac{V_m N_a A_{cs}}{M} \quad (17)$$

Where:

S_t – total surface area

N_a – Avogadro's number

A_{cs} – cross-sectional area of the adsorbate

The specific surface area S is finally obtained by dividing total surface area by the sample mass equation 18:

$$S = \frac{S_t}{W} \quad (18)$$

4.1.6. Solubility

Solubility of THAP, THAFP and THMO was determined using the shake flask method at speed of shaking 35 rpm. To assure work under sink conditions, saturated solutions of the model drugs were prepared at a temperature at 25°C. The kinetic of the solubility was monitored by sampling at certain time interval to check transformation of anhydrate to monohydrate in order to monitor differences in solubility of anhydrate and monohydrate form of Theophylline. Aliquots of the solutions were withdrawn and after filtration and appropriate dilution drug content was monitored by UV at 272 nm. The measurement had 72 h equilibration time.

4.1.7. Contact Angle

For the measurement of contact angle the sorption method was used. Measurement was done by Tensiometer K10 (Krüss GmbH, Hamburg, Germany) in combination with Krüss LabDeskt_{TM} software (Version 3.0.1.2509, Krüss GmbH, Hamburg, Germany). The constant weight and volume of the powder were placed in a glass cell with a porous glass base. The measurement of every sample was done in triplicate. The glass cell was fixed to electronic balance integrated in the tensiometer, and brought in contact with vessel containing the test-liquid. Measuring the increase in weight as a function of time and applying the modified Washburn equation (19) allows calculation of the contact angle of the material ⁴⁸.

$$\frac{h}{t} = \frac{c\gamma \cos \theta}{\eta} \quad (19)$$

Where:

h – length of the wetted capillary [cm]

- t – time [s]
 c – constant
 γ – surface tension of the liquid [mN/m]
 θ – contact angle
 η – viscosity of the liquid [mPa s]

Due to the fact that measurement is based on the increasing in mass of sample as function of time, equation (19) can be modified to equation (20):

$$\frac{m^2}{t} = \frac{c\rho^2\gamma\cos\theta}{\eta} \quad (20)$$

Where:

- m – mass of adsorbed liquid [g]
 ρ – density of the liquid [g/cm³]

To determine constant c , measurement with a liquid (n-hexane) that completely wets the sample was carried out, and this constant was entered in to the Washburn equation. For all samples distilled water was used as test liquid.

4.1.7. X – Ray Diffractometry

This method is widely used for the identification of solids phases. The X - ray powder pattern of every crystalline form of compound is unique making this technique particularly suited for the identification of different polymorphic forms of the material. The samples of powder and granules were analyzed by X-Ray diffractometer (Model D 5005 Siemens) with Cu–K α radiation (45 kV x 40 mA). The instrument was operated in a step scan mode and in increment of 0.01°2 θ . The angular range was 5 to 40° 2 θ and counts were accumulated for 10 s at each step.

4.1.8. Differential Scanning Calorimetry (DSC)

DSC is a thermal analysis in which the properties of the material can be defined in function of external applied temperature. This method can be used to determine

some very important characteristics of the material: melting and boiling point, glass transition, vaporization, solid–solid phase transformation, crystallization decomposition, etc ⁴⁹.

DSC measurements of THAP, THAFP and THMO powder were performed (Pyris Diamond 1, Perkin Elmer, Switzerland) in order to characterize and examine polymorphic form of the materials.

Approximately 4 mg of the sample were weighed into 30µl aluminum pan with hole and heated in the DSC from 30°C to 300°C. Heating rate was set to 10°C/min under nitrogen purge.

4.2. Preparation of the Binary Mixtures

Mixtures of (w/w) Theophylline anhydrate powder (THAP), Theophylline anhydrate fine powder (THAFP), Theophylline monohydrate (THMO) and 0, 30, 50, 70, 90 and 100% Microcrystalline cellulose (MCC) respectively, were prepared by mixing the powders during 20 min in a Turbula[®] mixer type T2C (Willy Bachofen AG, Basel, Switzerland).

No lubricant was used for the pure powder as well as binary mixtures.

4.2.1. Characterization of the powder binary mixtures

True density, bulk and tapped density, as well as Carr index and Hausner ratio of the powder binary mixtures were determined by the same method as THAP, THAFP, THMO and MCC separately.

4.3. Roller Compaction

Roller compaction of the materials and binary mixtures were done using Fitzpatrick IR220 Chilsonator[®] (Fitzpatrick, Elmhurst, USA).

According to fact that materials with different particle size were used for compaction, flowability of different Theophylline was measured, by measuring the weight (g) of the material which passes through the roller compactor in time (min). In table 4.1 process parameters of the roller compaction are presented.

Table 4.1.: Process parameters of roller compaction

| | THAP | THAFP | THMO |
|---------------------------|-------------|--------------|-------------|
| Roll speed [rpm] | 3 | 3 | 3 |
| Pressure [bar] | 12 | 12 | 12 |
| Roll force [kN/cm] | 2.6 | 2.9 | 2.6 |
| HFS [rpm] | 18 | 18 | 18 |
| VFS [rpm] | 200 | 200 | 200 |

Roller compaction at these parameters (see table 4.1) was done only for measurement of flow rate of the materials.

According to the fact that the pressure of 12 bars was very low, compactions for all the other investigations were done at parameters as it follows.

Compaction of pure THAP, THAFP, THMO and their binary mixtures with MCC were carried out under standardized conditions (horizontal screw speed - HSV 22 rpm, vertical screw speed - FSV 200 rpm, roll speed 3 rpm and pressure 20 bars). In order to find appropriate rolls, trials with different surface types (smooth, knurled and pocket design) were done. Due to sticky feature of Theophylline, only rolls with smooth surface could be used.

THAP was chosen as a model drug for additional roller compaction under the following conditions: HSV 25 rpm, FSV 200 rpm, roll speed 3 rpm and pressure of 30 bars.

After roller compaction, ribbons were subsequently milled using a L1A Lab Scale FitzMill® (Fitzpatrick, Elmhurst, USA) equipped with 1, 3 mm bar rotor, rasping screen for minimizing fines, and set at a speed of 600 rpm.

4.4. Compacts Characterization

4.4.1. Differential Scanning Calorimetry (DSC)

In order to check is there any influence of roller compaction on polymorphic and pseudo polymorphic forms of THAP, THAFP and THMO, differential scanning calorimetry (DSC Pyris 1, Perkin Elmer) analyze of the compacts was carried. The same method as in the case of powder was used, see chapter 4.1.8.

4.4.2. Porosity of Compacts

The pore size analysis was performed by Mercury porosimeter (PoreSizer 9320, Micromeritics, Norcross, Georgia, USA), measuring the relationship between penetrated volume of mercury and penetration pressure. Five ribbons were measured in the same time in the penetrometer of volume 6.045 cm³. The ribbons were cut into pieces of approximately 1.0 cm with and 2.5 cm length (roll width).

The penetrometer was evacuated to a pressure of 50 mm Hg and then filled with mercury.

The low pressure analysis (manually) and high pressure analysis (automatically) were performed in the pressure ranging 0.5 psi to 30.000 psi, which corresponds to pore diameters ranging from 340 μm to 6 nm.

The mercury porosimeter is based on Washburn equation^{50,51}, (equation 21).

$$P = \frac{-2\gamma \cos \theta}{r} \quad (21)$$

Where:

P – pressure [kPa]

r – pore radius where mercury intrudes

γ – surface tension of mercury [485 mN/m]

θ – contact angle of mercury [130°]

4.5. Granules Characterization

4.5.1. Scanning Electron Microscopy (SEM)

SEM images of the granules were taken with the same method as powders, see section 4.1.1. THAP, THAFP and THMO granules separately, and in the binary mixtures with MCC in the ratio 50% of Theophylline and 50% MCC were measured.

True density, bulk and tapped density of pure material and binary mixtures, were determined according to procedures described in the chapter 4.1.2.

4.5.2. Particle Size Distribution

The size distribution of the granules was evaluated by sieve analysis.

The analysis was performed on 50 g granules, sieved on a sieve shaker (Sieve analyzer – Schieritz and Hauenstein AG, Retsch) for 10 min at level 45, using 90, 125, 180, 250, 355, 500, 710 and 1000 μm sieves. The results were expressed as part of coarse and fines, which was defined as the fraction of particles higher than 1000 μm and smaller than 90 μm ⁵².

4.5.3. X-Ray Diffractometry

The samples of granules were analyzed by X-Ray diffractometer (Model D 5005 Siemens) with Cu-K α radiation (45 kV x 40 mA). The same method as it was previously explained in the Powder characterization, see chapter 4.1.7.

4.5.4. Differential Scanning Calorimetry (DSC)

In order to check is there any influence of roller compaction and milling on polymorphic and pseudo polymorphic forms of THAP, THAFP and THMO, differential scanning calorimetry (DSC Pyris 1, Perkin Elmer) analyze of the granules was carried. The same method as in the case of powder was used, see chapter 4.1.8.

4.6. Tablet Production

In order to check influence of the roller compaction on tablet properties, tablets were produced by direct compression and roller compaction from the same materials.

Tablets (round, flat, 11 mm diameter, 400 mg), for determination of the compactibility (tensile strength, Leuenberger equation) and compressibility (Heckel plot and modified Heckel plot), were prepared from the original and granulated materials and mixtures using Zwick® material tester 1478 (Zwick® GmbH, Ulm, Germany). Preweighed material was filled manually into the die. The compression speed was set to the maximum of 25 mm/min. For each powder system three tablets were compressed at different pressure levels in the pressure range: 10.50, 21.05, 31.50, 42.1, 63.15, 84.21, 105, 26 and 126, 315 MPa (1, 2, 3, 4, 6, 8, 10 and 12 kN).

In order to determine disintegration and dissolution rate, tablets with a constant porosity of $12 \pm 0.5\%$ (round, flat, 10 mm diameter and 350 mg) were prepared using a compaction simulator Presster TM (Metropolitan Computing Corporation). The Korsch 329 machine, 29 press stations was simulated. The gap, thereby compression force, was changed in order to get tablet thickness suitable for a porosity of 12 %. Tableting speed was constant at 5 rpm (0.107 m/s). The process was controlled using Presster® software version 3.8.4 (MCC, New Jersey, USA). Tablet porosity was calculated from the apparent particle density of the material or mixture and the dimensions and weight of the tablet.

Porosity of tablets prepared by one material was calculated according to equation 22:

$$\varepsilon = \left(1 - \frac{\rho_c}{\rho_t} \right) 100 \quad (22)$$

where:

ε – tablet porosity [%]

ρ_c – tablet density [g/cm³]

ρ_t – true density of the material [g/cm³]

Porosity of tablets prepared by binary mixtures of the materials was calculated according to equation 23.

$$\varepsilon = \frac{V_t - (V_a + V_b)}{V_t} 100 \quad (23)$$

Where:

ε – tablet porosity [%]

V_t – tablet volume [cm³]

V_a – volume of part a of the binary mixture [cm³]

V_b – volume of part b of the binary mixture [cm³]

In order to check propriety of the porosity obtained by calculation, porosity of some of the tablets was measured by mercury porosimeter (Porsizer 9320, Micromeritics, Norcross, Georgia, USA), as it is explained in compacts characterization. The measurement was done with three tablets. After compaction tablets were stored 48 h in a closed chamber at relative humidity of 42-44 %.

4.7. Tablet Characterization

4.7.1. Differential Scanning Calorimetry (DSC)

In order to check is there any influence of roller compaction, milling and tableting on polymorphic and pseudo polymorphic forms of THAP, THAFP and THMO, differential scanning calorimetry (DSC Pyris 1, Perkin Elmer) analyze was carried. The same method as in the case of powder was used, see chapter 4.1.8.

4.7.2. Compression Behavior Analysis

4.7.2.1. Heckel and Modified Heckel Equation

Due to double compaction which was done by roller compaction and tableting, compressibility of THAP, THAFP, THMO, MCC and their binary mixtures, before and after compaction was determined. Tablets were prepared as described in the part Tablet Production (see chapter 4.6). The analysis was performed with “out of die”

method. Thickness of tablets h was measured 48 h after manufacturing with thickness gage (Digital caliper).

The pressure of compression was calculated according to equation 24.

$$\text{Compression pressure} = \frac{\text{Compression force}}{\left(\pi \left(\frac{d}{2} \right)^2 \right)} \quad (24)$$

Where d is the diameter of the tablet

Compression properties of tablets prepared by direct compaction (without roller compaction) and tablets prepared by roller compaction at pressure 20 and 30 bars were determined according to Heckel equation (7) and modified Heckel equation (11). The parameters K and A of equation (7) and C and ρ_{rc} of equation (11) were used to characterize the compression behavior of the materials. Reciprocal value of the slope K of the linear region of the Heckel plot, mean yield pressure P_y can be as well used as a measure of materials ability to deform plastically. Several parameters influence the calculation of P_y , and in the same time K and A : operating conditions, type of compression (an uniaxial press, a rotary press, a compaction simulator), compression speed, lubricant (type and amount – if it is used), punch diameter, maximum compression pressure.

This should be taken into account when results are compared between two measurements.

4.7.2.2. Measurement of Radial Tensile Strength

Dimensions of the flat-faced tablets were measured particularly: weight (Balance-AT 460 Delat Range, Mettler Toledo), thickness (Digital caliper) and crushing strength (Tablet Tester 8M, Dr. Schleuniger, Pharmatron Inc, Manchester).

Breaking force was converted into tensile strength according to Newton^{53,54} (equation 25):

$$\sigma = \frac{2F}{\pi dh} \quad (25)$$

where:

σ – radial tensile strength [N/cm]

F – maximal force [N]

d – tablet diameter [cm]

h – tablet thickness [cm]

In order to get compactibility σ_{Tmax} and compressibility γ parameters for individual substances, the Leuenberger equation (equation 12), was applied, see chapter 2.3.3.3. The value of maximal tensile strength at zero porosity of compact σ_{Tmax} , and pressure susceptibility γ were calculated with Mathematica 5.2 program, using non-linear regression. Radial tensile strength (equation 25) at certain forming pressure σ_c was plotted against the product of the compression pressure and relative density of tablets.

4.7.3. Disintegration Time

Tablets for measurement of disintegration time and dissolution rate were prepared as described in the part Tablet compression (see chapter 4.6.). The average disintegration time of 6 tablets was determined in 900 ml water at 37°C (Sotax DT2 Automated Detection, Sotax, Switzerland).

4.7.4. Dissolution Rate

Drug release measurement was performed using USP paddle type II apparatus (Sotax AT 7, Sotax, Switzerland) at 37°C and 50 rpm. The dissolution studies were carried out for 240 min in 900 ml of distilled water, as dissolution medium. First half an hour aliquots of 5 ml were removed every 5 minutes, and the rest of time every 10 min and replaced with the fresh medium to maintain the volume constant. After filtration and appropriate dilution drug content was monitored by UV spectrophotometry at 272 nm.

4.7.5. Statistical Analysis

ANOVA single – factor analysis (0.05) was run for the binary mixtures made from powder, granules and tablets (direct compaction and roller compaction). The purpose of the analysis was detect if there are any statistical differences in characteristics of the powder and granules mixtures as well as characteristics of tablets produced by direct compaction and roller compaction and pressure of 20 and 30 bars. Differences in results are considered as statistical significant in the case if $p < 0.05$.

5. Results and Discussion

5.1. Powder Characterization

5.1.1. Scanning Electron Microscopy

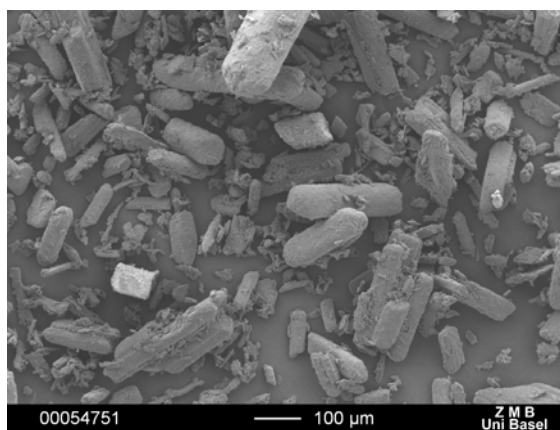


Figure 5.1.: THAP (magnification 100x)

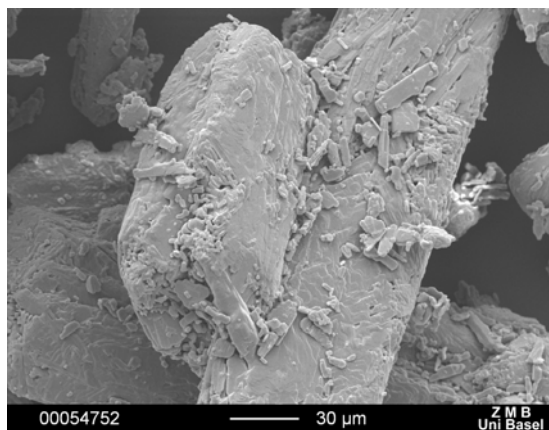


Figure 5.2.: THAP (magnification 500x)

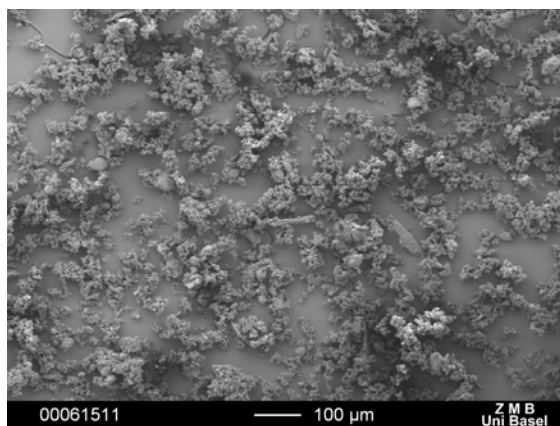


Figure 5.3.: THAFP (magnification 100x)

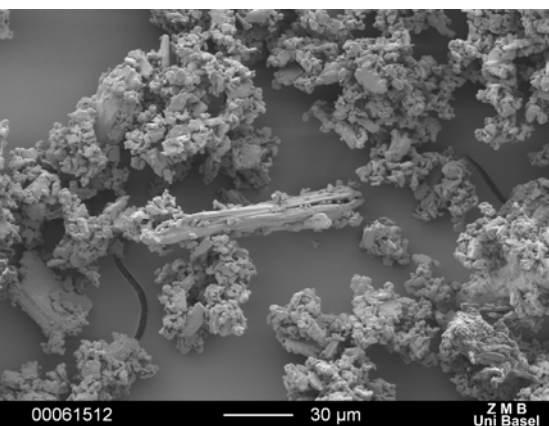


Figure 5.4.: THAFP (magnification 500x)

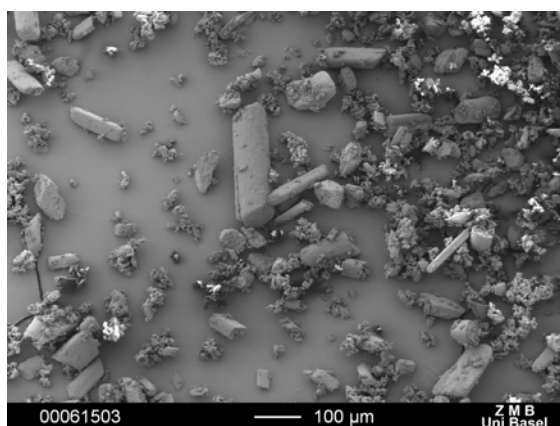


Figure 5.5.: THMO (magnification 100x)

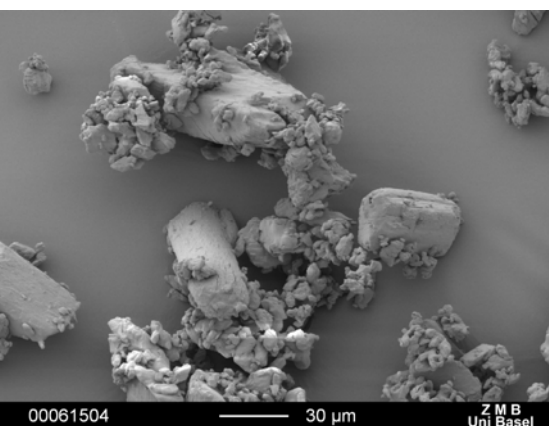


Figure 5.6.: THMO (magnification 500x)

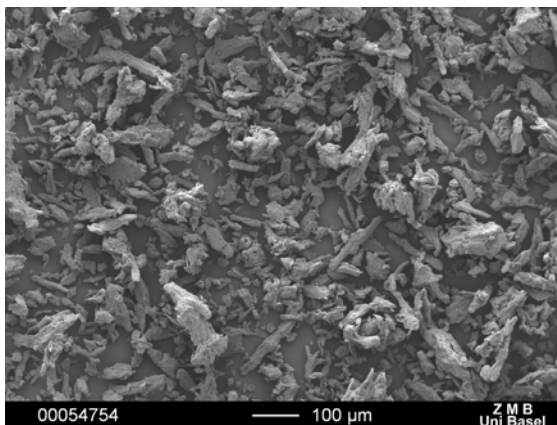


Figure 5.7.: MCC (magnification 100x)

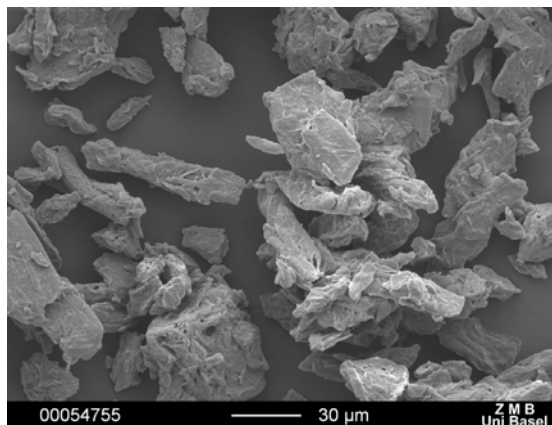


Figure 5.8.: MCC (magnification 500x)

The shape of Theophylline particles was generally elongated, with differences in particle size distribution. THAP had the biggest particles (see table 5.1.4) followed by THMO and THAFP, consecutively. In figure 5.3 and figure 5.4 it could be seen that THAFP formed agglomerates which could have impact on the powder behavior during the technological process of tableting. The scanning electron microscopy (SEM) pictures showed that the particles of MCC have needle shaped fiber. It is well known that particle shape affects the other properties of the material as flowability, compressibility, compactibility, etc.

5.1.2. Density

Results of true, bulk and tapped density of THAP, THAFP, THMO and MCC are summarized in table 5.1.:

Table 5.1.: Powders characterization: true, bulk and tapped density

| Material | True density (n=3; \pm s.d.) [g/cm ³] | Bulk density (n=3; \pm s.d.) [g/cm ³] | Tapped density (n=3; \pm s.d.) [g/cm ³] |
|----------|---|---|---|
| THAP | 1.46 \pm 0.00 | 0.50 \pm 0.01 | 0.63 \pm 0.02 |
| THAFP | 1.47 \pm 0.00 | 0.28 \pm 0.00 | 0.35 \pm 0.00 |
| THMO | 1.47 \pm 0.00 | 0.47 \pm 0.01 | 0.58 \pm 0.01 |
| MCC | 1.58 \pm 0.00 | 0.31 \pm 0.00 | 0.41 \pm 0.00 |

In the literature it is suggested that true density could be used for characterization of the materials regarding polymorphic forms⁵⁵. In the studies of Suzuki et al. 1989,⁴³ and Suihko et al. 2001,⁵⁵ it was presented that true density of Theophylline anhydrate form II (stable form) and form I (metastable) show different values of true density. Suzuki presented that form II shows true density of 1.489 g/cm³ and form I of 1.502 g/cm³, while true density of monohydrate is 1.453 g/cm³. The results of Suihko et al.⁵⁵ were more in agreement with results of this study because the same method of measurement was applied. In their research it was shown that true density of form II is 1.484 g/cm³, form I is 1.522 g/cm³ and for monohydrate 1.470 g/cm³.

True density of THAP, THAFP and THMO are very similar to each other, see table 5.1.1. Results of true density for THAP and THAFP comply to the true density of Theophylline anhydrate polymorphic form II (stable at room temperature) and THMO to the true density of Theophylline monohydrate to the literature value⁵⁵.

Measurement of bulk and tapped density are very important parameters with regard to the planning of a batch size and especially for transferring the batch from development to production size. Especially, attention should be dedicated to the bulk density in respect to planning a granulation bathes (container size, etc). These two parameters depend on a number of factors including particle size distribution, true density, particle shape and cohesiveness due to surface forces including moisture. Therefore, bulk and tapped density of a material can be used to predict both its flow and its compressibility. Using the measured bulk and tapped density and according to equation (13) and (14) Carr index and Hausner ratio were calculated.

Table 5.2.: Powders characterization: Flowability (Carr index and Hausner ratio)

| Material | Carr index (n=3; ± s.d.) [%] | Hausner ratio (n=3; ± s.d.) |
|----------|------------------------------------|--------------------------------|
| THAP | 19.75 ± 0.53 | 1.24 ± 0.25 |
| THAFP | 19.11 ± 1.43 | 1.23 ± 0.02 |
| THMO | 18.88 ± 1.83 | 1.23 ± 0.02 |
| MCC | 22.83 ± 1.40 | 1.29 ± 0.02 |

The powder flowability is influenced by particle size, particle size distribution, particle shape, surface texture, surface energy, moisture content, etc. The values of Carr index and Hausner ratio are directly based on the values for the bulk and tapped density and indirectly represent the flowability of a powder mass. The Carr index values between 5 and 25 % indicates a good flow characteristics, and readings above 25 % generally mean poor flowability⁵⁶. For all four materials Carr index is less than 25%, but flowability of materials was poor. This can be explained by the structure of the powders. SEM pictures, see figure 5.1 to figure 5.8, showed particles shape of the materials which inhibit particle flow. It is well-known that these types of structures, irregular shape, due to relatively high surface area and high interparticle friction, in general do not possess a good flowability⁵⁷. In contrast to the powders with irregular particle shape, spherical particles tend to have a good flowability because the spherical shape reduces interparticle friction. The values of Hausner ratio < 1.25 indicate a good, and > 1.50 poor flow. The same as in the case of Carr index all four materials had Hausner ratio less than 1.5 and higher than 1.25. This means that flowability should be improved by adding glidant⁵⁸.

Even if values of Carr index and Hausner ratio for THAFP were not bigger than for the other materials, its flowability was considerably less regarding to THAP, THMO and MCC. Very poor flowability of THAFP can be explained by the fact that for fine particles in general powder flow is restricted, because the cohesive forces between particles are of the same magnitude as gravitational forces⁵⁹. Therefore, they tend to adhere to each other obstructing flowability of the powder.

Tapped density is related to a specific surface area of the material⁵². In general higher tapped density is connected to a lower specific surface area. The results from these studies are in agreement with this regularity, except THAFP. This phenomenon will be explained in the part with results of specific surface area (see chapter 5.1.4).

5.1.3. Moisture content

Results of moisture content obtained by Karl Fisher titration for THAP, THAFP, THMO and MCC were 0.10%, 0.14%, 8.93% and 4.21 %, respectively.

5.1.4. Particle Size Distribution and Specific Surface Area

Table 5.3.: Powders characterization: particle size distribution and specific surface area of the powders

| Material | Particle size distribution [μm] | Specific surface area (n=3; \pm s.d.) [m^2/g] |
|----------|---|---|
| THAP | d (0.1) < 40.97 d (0.5) < 144.73 d (0.9) < 386.06 | 0.781 \pm 0.046 |
| THAFP | d (0.1) < 2.65 d (0.5) < 7.71 d (0.9) < 38.08 | 1.426 \pm 0.030 |
| THMO | d (0.1) < 5.85 d (0.5) < 27.73 d (0.9) < 107.74 | 1.444 \pm 0.032 |
| MCC | d (0.1) < 20.03 d (0.5) < 58.81 d (0.9) < 135.92 | 1.285 \pm 0.052 |

The particle size distributions of drugs and excipients have a direct effect on a mixing process and on the possible segregation during the mixing process, on the flowability of the materials and the bioavailability of active drug. Regarding all these very important parameters the particle size of the active components as well as excipients has to be carefully controlled.

As it is previously explained (see chapter 5.1.2) small particle size of the powders leads to a poor flowability, while they can improve compactibility of the material. This phenomenon can be explained by the fact that small particles show a big surface area that is responsible for interparticle attraction. Value of specific surface area should be in agreement with particle size distribution, in the way that material with a small particle size has a high specific surface area. Thus, THAFP showing the smallest particle size, specific surface area of this material should be the highest value. Due to very small particles (see table 5.1.4) of THAFP, during the sample preparation for measuring specific surface area particles of powder constantly were agglomerated. This phenomenon could be seen at SEM images, see figure 5.3 and

figure 5.4. Results of specific surface area of THAFP suppose to be the highest value between these materials, but the problem of powder agglomeration led to this incorrect value. This is in accordance with the results of tapped density, where THAFP had lower tapped density than THMO (see table 5.1), what should imply that specific surface area of THAFP should be higher than specific surface area of THMO.

5.1.5. Solubility

Solubility profile of THAP, THAFP and THMO is shown in Figure 5.9. Due to the smallest particle size and the highest specific surface area exposed to a solvent, at the beginning of the measurement the highest value of solubility had THAFP. Since that particle size of THAFP are much lower than particle size of THAP it was expected that difference in solubility of these two materials would be higher. However, SEM images and specific surface area value (see figure 5.3 and table 5.3) indicated that THAFP particles were agglomerated in the original powder bed. When Theophylline anhydrate is exposed to water it immediately starts transformation to monohydrate. This mechanism will be explained in Dissolution rate measurement (see chapter 5.5.5). Figure 5.9 demonstrated the transformation of anhydrate to monohydrate. The difficulty in determining the equilibrium solubility for Theophylline anhydrate is evident in the literature, which reports a very wide range of values⁶⁰. In this study solubility of THAP was determined to be 5.650 mg/ml, of THAFP was 5.736 mg/ml and of THMO was 5.444 mg/ml. The difference between three materials was the time when equilibrium of solubility was reached. THAP showed the maximum solubility rate at 420 min, THAFP at 360 min, and THMO had equilibrium after 48 h. During the time period of transformation of anhydrate to monohydrate, both forms were present in the solution. Consequently, the larger amount of monohydrate induced the lower solubility rate. Once the solid phase transformation was completed, solubility rate of the initially anhydrous form became constant (see figure 5.9).

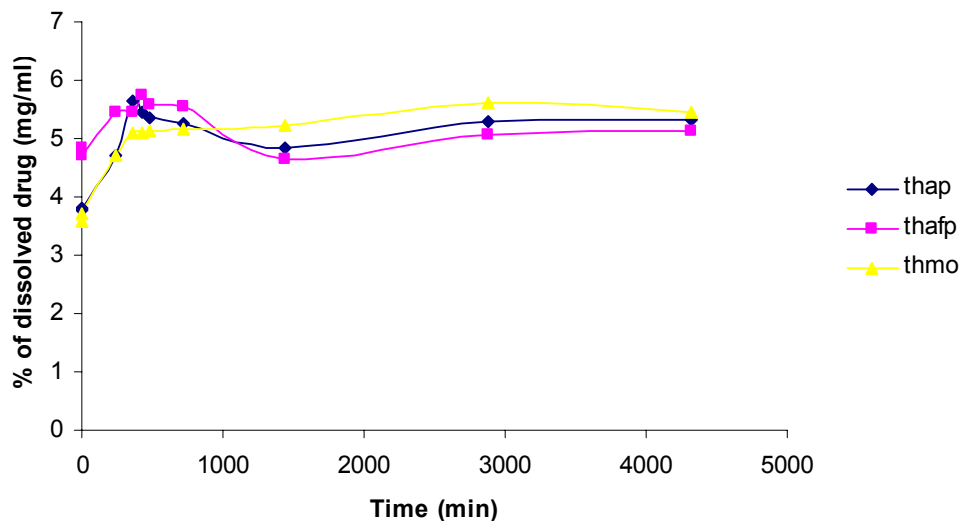


Figure 5.9.: Solubility profile of THAP, THAFP and THMO

5.1.6. Contact Angle

Measurement of contact angle was carried out in order to define which material has the highest wettability. It is well known that contact angle of 0° indicate complete wetting and contact angle of 90° means very poor wettability. The values of contact angle of THAP, THAFP and THMO determined by sorption method are presented consecutively: $50.64 \pm 2.61^\circ$, $52.50 \pm 1.21^\circ$, and $74.63 \pm 2.80^\circ$. In the research of Muster et al. 2005,⁶¹ it was presented that contact angle of Theophylline determined by sorption was $55.0 \pm 2.0^\circ$, what is in agreement with results obtained in this study. THAP and THAFP had almost the same contact angle which is significantly lower than the contact angle of THMO. These results showed that Theophylline anhydrate is more wettable than monohydrate form of Theophylline.

5.1.7. X-Ray Diffractometry

Results of X - ray measurement of THAP, THAFP and THMO powders are presented together with the results obtained for granules, see chapter 5.4.4.

5.1.8. Differential Scanning Calorimetry (DSC)

Results of DSC measurement of THAP, THAFP and THMO powders are presented together with the results obtained for compacts, granules and tablets, see chapter 5.5.1.

5.2. Characterization of the powder binary mixtures

5.2.1. Density and Flowability

Either tablets were produced by direct compaction or roller compaction; the binary mixtures of THAP, THAFP and THMO with MCC were used. In the binary mixture of active substance with excipients, both materials can influence each other and thus initial properties of the powders can be completely changed. Due to the importance of the properties of the incurred mixtures, detailed characterization was carried out.

Table 5.4.: Characterization of the binary mixtures: flowability and true density - binary mixtures THAP + MCC

| % of THAP in the binary mixtures | Carr index [%] (n=3± s.d.) | Hausner ratio (n=3 ± s.d.) | True density [g/cm ³] (n=3 ± s.d.) |
|--|----------------------------------|-------------------------------|--|
| 100% | 19.7 ± 0.538 | 1.25 ± 0.008 | 1.466 ± 0.002 |
| 70% | 28.5 ± 0.919 | 1.40 ± 0.018 | 1.489 ± 0.001 |
| 50% | 26.5 ± 6.736 | 1.35 ± 0.153 | 1.511 ± 0.002 |
| 30% | 23.4 ± 1.512 | 1.30 ± 0.033 | 1.527 ± 0.002 |
| 10% | 21.3 ± 1.402 | 1.27 ± 0.023 | 1.558 ± 0.007 |
| 0% | 22.8 ± 1.401 | 1.30 ± 0.024 | 1.589 ± 0.003 |

Table 5.5.: Characterization of the binary mixtures: flowability and true density - binary mixtures THAFP + MCC

| % of THAFP in the binary mixtures | Carr index [%] (n=3± s.d.) | Hausner ratio (n=3 ± s.d.) | True density [g/cm ³] (n=3 ± s.d.) |
|---|----------------------------------|-------------------------------|--|
| 100% | 19.1 ± 1.43 | 1.24 ± 0.02 | 1.47 ± 0.00 |
| 70% | 33.9 ± 1.44 | 1.51 ± 0.03 | 1.52 ± 0.02 |
| 50% | 29.3 ± 0.91 | 1.41 ± 0.01 | 1.53 ± 0.00 |
| 30% | 30.3 ± 0.51 | 1.43 ± 0.00 | 1.53 ± 0.01 |
| 10% | 27.5 ± 1.51 | 1.38 ± 0.02 | 1.54 ± 0.00 |
| 0% | 22.8 ± 1.40 | 1.30 ± 0.02 | 1.58 ± 0.01 |

Table 5.6.: Characterization of the binary mixtures: flowability and true density - binary mixtures THMO + MCC

| % of THMO in the binary mixtures | Carr index [%] (n=3± s.d.) | Hausner ratio (n=3 ± s.d.) | True density [g/cm ³] (n=3 ± s.d.) |
|--|----------------------------------|-------------------------------|--|
| 100% | 18.9 ± 1.83 | 1.23 ± 0.02 | 1.47 ± 0.00 |
| 70% | 23.9 ± 4.01 | 1.32 ± 0.07 | 1.49 ± 0.01 |
| 50% | 20.9 ± 0.84 | 1.26 ± 0.01 | 1.51 ± 0.02 |
| 30% | 21.3 ± 2.35 | 1.27 ± 0.00 | 1.53 ± 0.00 |
| 10% | 21.5 ± 1.63 | 1.27 ± 0.02 | 1.54 ± 0.00 |
| 0% | 22.8 ± 1.40 | 1.30 ± 0.02 | 1.58 ± 0.01 |

The values of true density of the binary mixtures (THAP, THAFP and THMO) were in between the values of the individual materials. It was increased by increasing the amount of MCC in the mixture. Nagel and Peck 2003⁵⁹, demonstrated that material with high density tend to possess free – flowing characteristics. Comparing density results with the values of Carr index and Hausner ratio (see table 5.4, table 5.5 and table 5.6) it could be observed that in this study that was not the case. Although, Carr index and Hausner ratio are very simple method to determine flow properties, for particles having high adhesiveness, broad size distribution and irregular shape can show the misleading in the obtained results. Changes in true density are very important to be detected for producing tablets of a constant porosity, see chapter 4.6.

True density of the particular material and mixture is suggested to have an effect on the ribbons porosity.

Flowability of the binary mixtures, in respect of Carr index and Hausner ratio, was changed comparing to the pure materials. Variation in flowability was not simple function of Carr index and Hausner ratio of the individual components.

Binary mixtures of 70 % of Theophylline (THAP, THAFP and THMO) and 30 % of MCC had the highest value of Carr index and Hausner ratio, which indicates the lowest flow rate. THAFP in the mixtures with MCC has very poor flowability. For the same reason as in the case of pure material, THAFP in the mixture with MCC showed very poor flowability. Due to very small particle sizes and relatively high surface area during the mixing process THAFP caused the interparticle adhesion with MCC particles. This led to further inhibition of flowability of the mixtures.

5.3. Compact characterization

Due to different particle sizes of THAP, THAFP and THMO, in the process of roller compaction at pressure of 12 bars, different roll gaps were obtained. Compaction pressure of 12 bars was chosen due to properties of the materials during the compaction. At high pressure it was difficult to get a good quality of THMO ribbons. This experiment was done in order to check if all parameters of roller compaction: feeding (HVS), precompaction (FVS), pressure and roll speed, are the same, due to different materials properties (THAP, THAFP and THMO) which size of roll gap and flow rate of will be induced. In order to get valid results all samples were collected 3 min after compaction started. During THAP compaction roll gap was 1.6 – 1.8 mm, for THAFP it was 0.8 – 1.0 mm and for THMO 1.5 – 1.6. Explanation for these results could be found in different particle size distribution and flowability for the materials.

Flow rate measurement of THAP, THAFP and THMO showed following results: 85 g/min, 47 g/min and 83 g/min. THAP with the biggest size of particle had the highest flow rate, followed by THMO and THAFP.

In order to check influence of roller compaction on the tablets properties (compressibility, compactibility, disintegration and dissolution) roller compaction of the original powders and the binary mixtures was done at standard parameters as it is explained in chapter 4.3.

Due to equipment properties, that during compaction roll gap can not be fixed and materials properties, different particle size, and different flow properties, thickness of the ribbons were not equal for all materials during the whole process. In order to get ribbons with the same properties, in the experiments which were done with binary mixtures, they were collected at the moment of the same thickness 1.0 – 1.1 mm.

5.3.1. Differential Scanning Calorimetry (DSC)

Results of DSC measurement of THAP, THAFP and THMO compacts are presented together with the results obtained for powder, granules and tablets, see chapter 5.5.1.

5.3.2. Compact Porosity

Although roller compaction of the THAP, THAFP and THMO and binary mixtures was done with the same parameters, and ribbons with the same thickness were collected, as results of different true density of the used materials (see table 5.4, table 5.5 and table 5.6), porosity of the ribbons were not the same.

Table 5.7.: Compact characterization: porosity of the ribbons - binary mixture THAP + MCC

| % of Theophylline in the binary mixtures | Ribbon porosity [%] | | | |
|---|------------------------|-----------------|-------|-------|
| | THAP (20bar) | THAP (30bar) | THAFP | THMO |
| 100% | 18.70 | 12.36 | 19.29 | 16.56 |
| 70% | 22.14 | 18.64 | 21.53 | 21.90 |
| 50% | 26.35 | 18.66 | 19.39 | 25.81 |
| 30% | 26.05 | 20.02 | 24.52 | 27.14 |
| 10% | 26.55 | 20.50 | 26.32 | 26.07 |
| 0% | 23.82 | 18.86 | 23.83 | 23.80 |

Porosity of the ribbons was an average porosity of the five ribbons measured in the same penetrometer. True density of the powders used for making ribbons had

influence on the ribbons porosity. Increasing the true density led to higher porosity which is in agreement with calculation of the ribbon density according to Hertig and Kleinebudde ⁶². The ribbons produced at pressure of 30 bars showed less porosity comparing to those which are compacted at pressure of 20 bars. This result was expected due to the higher pressure the powder bed was exposed. Further, this higher pressure influenced more uniform porosity although true density of the powders was the same as in the case of 20 bars.

5.4. Granule Characterization

5.4.1. Scanning Electron Microscopy

Granules produced at pressure of 20 bars and milled at 600 rpm are presented in figure 5.8 to figure 5.17.

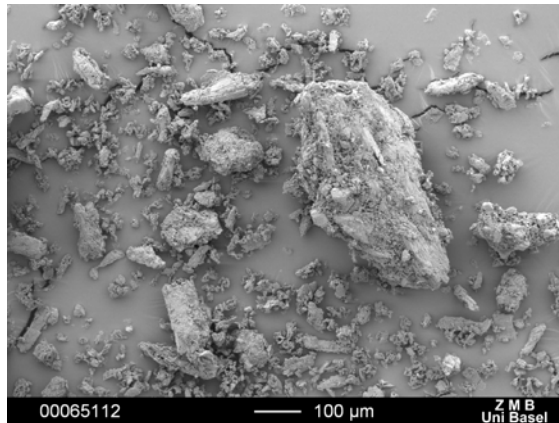


Figure 5.8.: THAP100% (100x)
(20 bar)

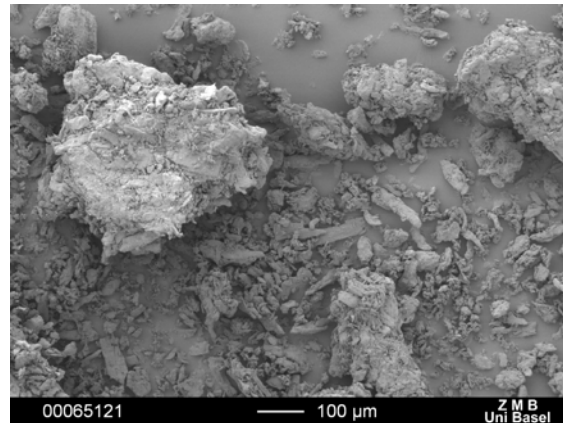


Figure 5.9.: THAP50%+MCC50% (100x)

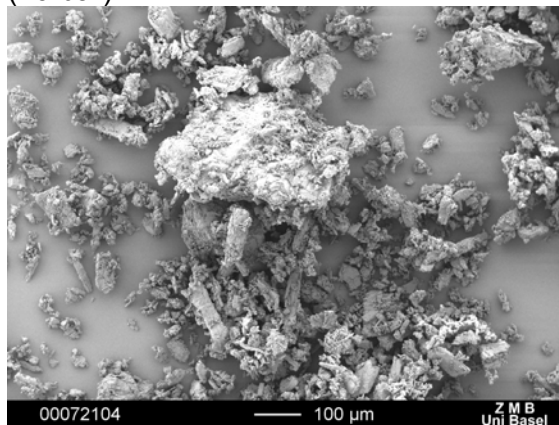


Figure 5.10.: THAP 100% (100x)
(30bar)

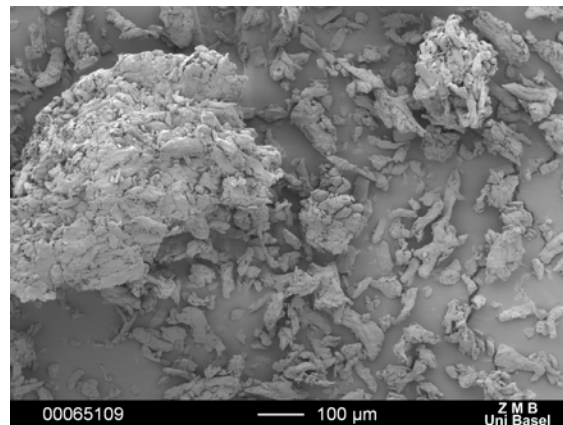


Figure 5.11.: THAP50%+MCC50% (100x)

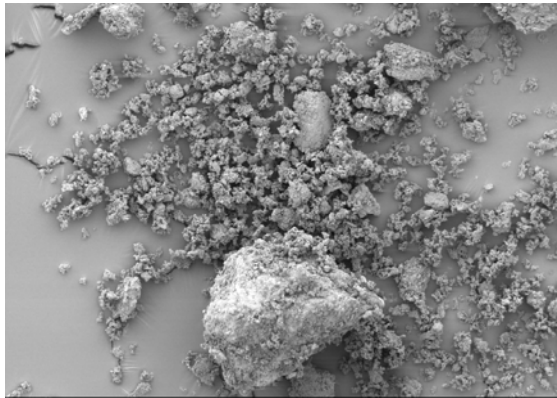


Figure 5.12.: THAFP (100x)

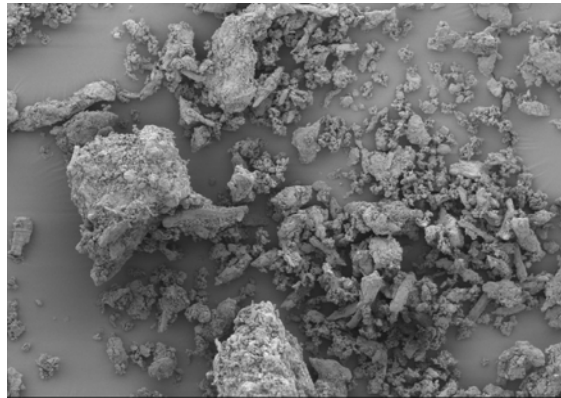


Figure 5.13.: THAFP50%+MCC50%(100x)

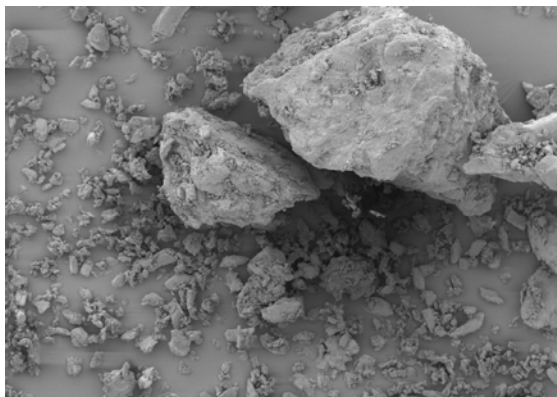


Figure 5.14.: THMO (100x)

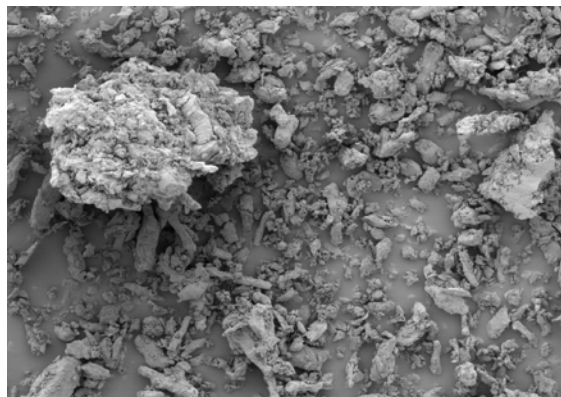


Figure 5.15.: THMO50%+MCC50%(100x)

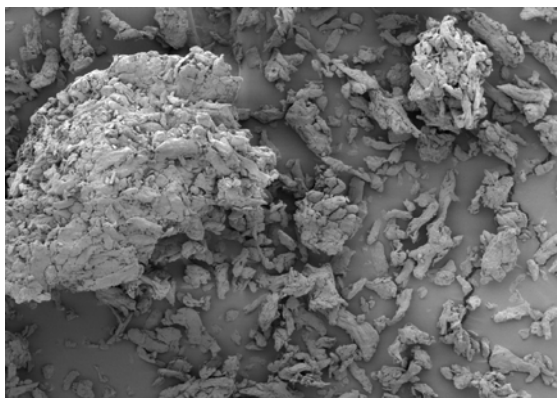


Figure 5.16.: MCC (100x)
(20 bar)

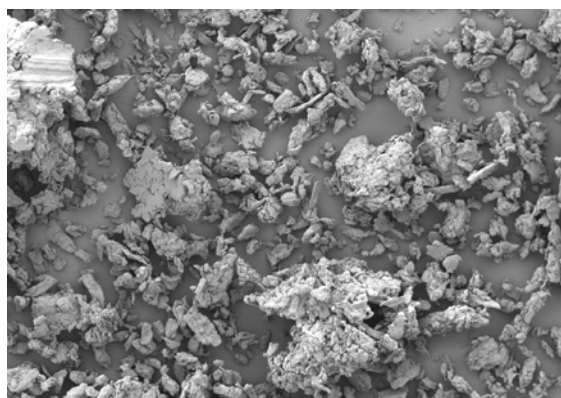


Figure 5.17.: MCC (100x)
(30 bar)

These pictures can be compared with those shown in the chapter Powder characterization, see figures 5.1 to figures 5.8.

During the compaction of the powders and especially milling of the ribbons, particles were cut, but the structure of the materials THAP, THAFP, THMO and MCC was not destroyed.

Compression at pressure of 30 bars did not change particle shape more than compression at pressure of 20 bars.

Although, granules showed much bigger particle size than original powders due to unchanged particle shape and relatively high fraction of fines flowability was still was not good.

5.4.2. Density and Flowability

Table 5.8 to Table 5.11 presented true density and parameters connected to flowability (Carr index and Hausner ratio) of the granules produced at pressure of 20 bars (THAP, THAFP and THMO) and of 30 bars (THAP).

Table 5.8.: Granules characterization: flowability and true density of the binary mixtures THAP + MCC (20 bar)

| % of THAP in the binary mixtures | Carr index [%] (n=3) | Hausner ratio (n=3) | True density [g/cm ³] (n=3) |
|--|----------------------------|------------------------|---|
| 100% | 14.9 ± 0.01 | 1.17 ± 0.00 | 1.51 ± 0.00 |
| 70% | 18.9 ± 1.01 | 1.23 ± 0.01 | 1.52 ± 0.01 |
| 50% | 19.0 ± 2.63 | 1.23 ± 0.03 | 1.53 ± 0.00 |
| 10% | 17.8 ± 0.11 | 1.21 ± 0.00 | 1.54 ± 0.01 |
| 0% | 16.6 ± 1.88 | 1.20 ± 0.02 | 1.56 ± 0.00 |

Table 5.9.: Granules characterization: Flowability and true density of the binary mixtures THAFP + MCC (20 bar)

| % of THAFP in the binary mixtures | Carr index [%] (n=3) | Hausner ratio (n=3) | True density [g/cm ³] (n=3) |
|---|----------------------------|------------------------|---|
| 100% | 15.8 ± 0.01 | 1.18 ± 0.01 | 1.50 ± 0.00 |
| 70% | 17.9 ± 2.51 | 1.22 ± 0.03 | 1.52 ± 0.00 |
| 50% | 18.1 ± 2.12 | 1.21 ± 0.02 | 1.53 ± 0.01 |
| 30% | 19.6 ± 1.32 | 1.20 ± 0.03 | 1.54 ± 0.00 |
| 10% | 18.2 ± 0.30 | 1.22 ± 0.00 | 1.54 ± 0.01 |
| 0% | 16.6 ± 1.88 | 1.20 ± 0.02 | 1.56 ± 0.00 |

Table 5.10.: Granules characterization: flowability and true density of the binary mixtures THMO + MCC (20 bar)

| % of THMO in the binary mixtures | Carr index [%] (n=3) | Hausner ratio (n=3) | True density [g/cm ³] (n=3) |
|--|----------------------------|------------------------|---|
| 100% | 14.3 ± 0.01 | 1.16 ± 0.00 | 1.46 ± 0.01 |
| 70% | 15.3 ± 1.30 | 1.18 ± 0.01 | 1.50 ± 0.01 |
| 50% | 16.1 ± 3.57 | 1.19 ± 0.05 | 1.52 ± 0.00 |
| 30% | 17.3 ± 1.64 | 1.21 ± 0.02 | 1.53 ± 0.00 |
| 10% | 16.9 ± 0.44 | 1.20 ± 0.00 | 1.54 ± 0.00 |
| 0% | 16.6 ± 1.88 | 1.20 ± 0.02 | 1.56 ± 0.00 |

Table 5.11.: Granules characterization: flowability and true density of the binary mixtures THAP + MCC (30 bar)

| % of THAP in the binary mixtures | Carr index [%] (n=3) | Hausner ratio (n=3) | True density [g/cm ³] (n=3) |
|--|----------------------------|------------------------|---|
| 100% | 13.7 ± 0.67 | 1.17 ± 0.00 | 1.50 ± 0.01 |
| 70% | 16.1 ± 1.74 | 1.19 ± 0.02 | 1.51 ± 0.00 |
| 50% | 15.4 ± 1.91 | 1.18 ± 0.02 | 1.52 ± 0.00 |
| 30% | 14.1 ± 1.95 | 1.16 ± 0.00 | 1.53 ± 0.02 |
| 10% | 12.5 ± 3.30 | 1.14 ± 0.04 | 1.54 ± 0.02 |
| 0% | 11.9 ± 1.69 | 1.13 ± 0.02 | 1.54 ± 0.03 |

True density is increased by increasing the amount of MCC in the binary mixtures. Granules made from THAP at pressure of 30 bars showed less true density (see table 5.11) than the granules produced from the same material at pressure of 20 bars (see table 5.10).

Carr index in all cases was less than 25% what implied a good flow rate. However, due to the structure of the materials, and high ratio of fines in the granulate flowability was still not good. SEM pictures showed elongated structure of Theophylline particles and fibrous structure of MCC particles, even after granulation.

Hausner ratio was less than 1.25 what should correspondent to good flowability even without glidant.

Carr index and Hausner ratio of the binary mixtures prepared from the granules were significantly ($p < 0.05$) lower than in the case of the same binary mixtures prepared from the powders. According to these results, flowability of the materials was significantly improved.

By increasing the pressure during the roller compaction process from 20 to 30 bars, flowability of THAP, and its binary mixtures with MCC was significantly increased ($p < 0.05$).

5.4.3. Particle size distribution

Particle size distribution of the granules obtained from the ribbons produced by compaction at 20 and 30 bars were presented as part of fines ($< 90 \mu\text{m}$) and part of coarse ($> 1000 \mu\text{m}$).

Table 5.12.: Granules characterization: particle size distribution

| | 100% | 70% | 50% | 30% | 10% | 0% |
|--------------|-------|-------|-------|-------|-------|-------|
| THAP (20bar) | | | | | | |
| Fine [%] | 1.22 | 0.59 | 0.67 | 7.09 | 6.50 | 17.05 |
| Coarse [%] | 7.57 | 7.21 | 8.91 | 12.01 | 4.95 | 7.91 |
| THAP (30bar) | | | | | | |
| Fine [%] | 6.57 | 8.47 | 7.67 | 9.89 | 13.30 | 8.78 |
| Coarse [%] | 5.97 | 7.34 | 8.33 | 11.01 | 15.42 | 17.92 |
| THAFP | | | | | | |
| Fine [%] | 0.41 | 0.82 | 1.67 | 4.57 | 4.17 | 17.05 |
| Coarse [%] | 8.83 | 9.11 | 8.36 | 10.04 | 12.69 | 7.91 |
| THMO | | | | | | |
| Fine [%] | 8.80 | 9.18 | 19.34 | 17.53 | 17.57 | 17.05 |
| Coarse [%] | 14.69 | 12.79 | 13.17 | 12.55 | 12.79 | 7.91 |

Comparing THAP compacted at two different pressures; it can be observed that granules produced from ribbons compacted at 30bar showed higher fraction of fines and coarse, but this difference was not statistically significant ($p > 0.05$).

Increasing the fraction of Theophylline in the mixtures resulted in less part of fine particles and less part of coarse particles. THAFP had less fines and more coarse than THAP. This can be explained by different particle sizes of these two materials. Material with small particle size (THAFP) had bigger binding area and at the same time produced bigger granules. THMO had the significantly ($p < 0.05$) highest fraction of fines and coarse particles.

Median particle size for THAFP granules was 557.7 μm , for THAP was 450.9 μm , for THMO was 555.5 μm and for MCC was 512.2 μm .

5.4.4. X - Ray Diffractometry

It is well known that Theophylline exists either as anhydrate or monohydrate. Theophylline anhydrate has two polymorphic forms, form II which is stable at room temperature and form I which is stable at high temperatures (see chapter 2.5). In

order to characterize polymorphic and pseudo polymorphic forms and check the influence of roller compaction, milling and tableting to polymorphic/pseudo polymorphic forms X-ray powder diffractometry was applied. The same measurement was done with powder and granules and results were compared.

X-ray powder and granules diffraction patterns were significantly different for the monohydrate and anhydrous form (see figure 5.18, figure 5.19 and figure 5.20) and equivalent to those presented in the literature ⁴⁹. THAP powder and granules produced by roller compaction at pressure of 20 and 30 bars showed characteristics peaks for Theophylline anhydrate form II which is stable at room temperature.

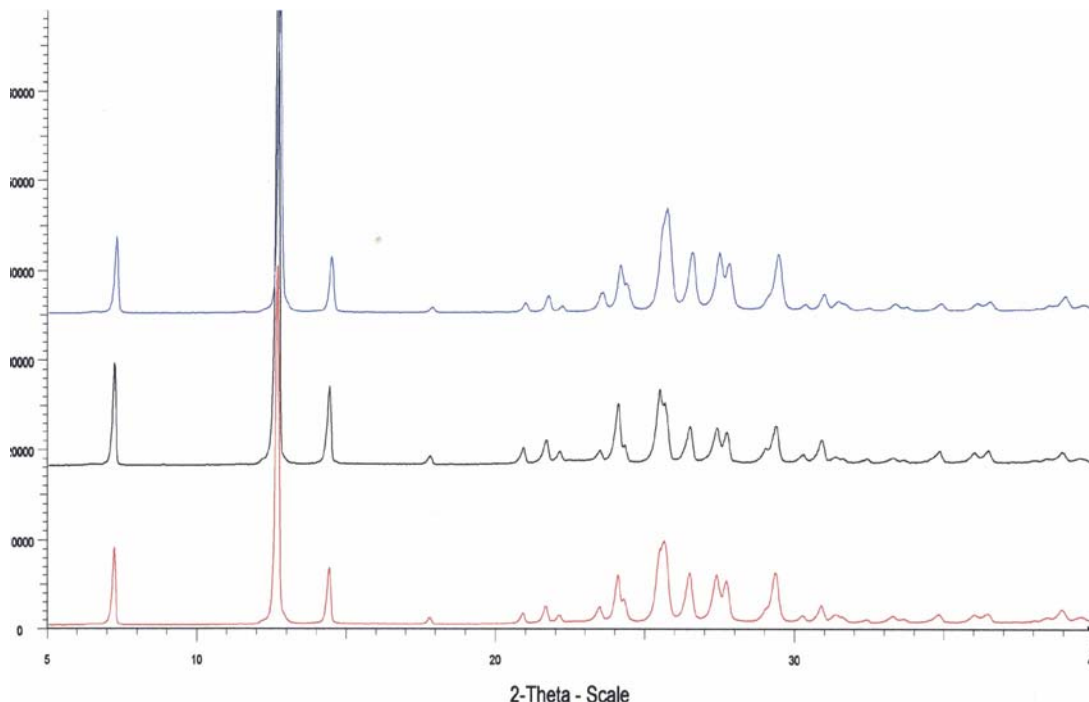


Figure 5.18.: X-ray diffraction patterns of THAP powder (upper), granules produced at pressure of 20 bars (middle) and granules produced at pressure of 30 bars (lower)

Diffraction pattern of THAP showed characteristic peaks of the stable anhydrous Theophylline (form II) at 7.2, 12.6 and 14.5° 2 θ . These characteristic peaks are in agreement with results previously presented in the literature by Airaksinen et al. 2004,⁴⁹ Phadnis and Suryanarayanan 1997,⁴⁵ have described an anhydrous metastable form of Theophylline that has a different X – ray diffraction pattern, with characteristics peaks at 9.4, 11.3, 12.4,13.5 and 15.4° 2 θ .

In Figure 5.18 it could be observed that diffraction patterns of THAP granules (20 and 30 bars) were not changed comparing to THAP powder. Since the diffraction pattern of THAP remained unchanged after roller compaction it could be noticed that roller compaction did not have any influence on the polymorphic form.

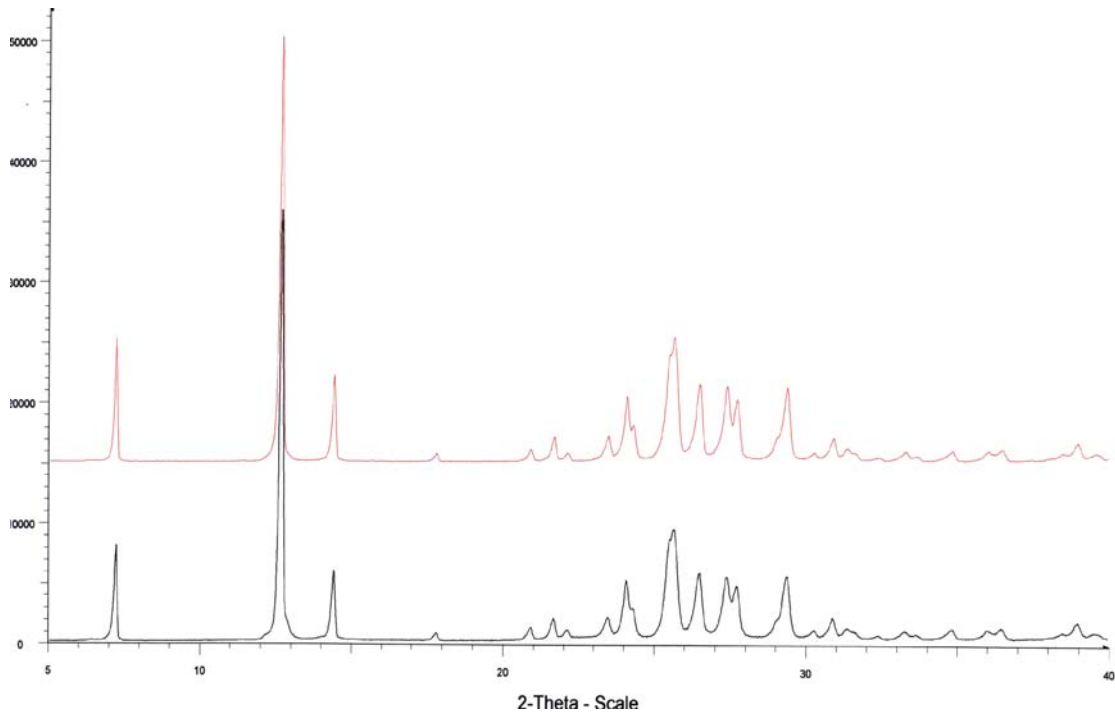


Figure 5.19.: X-ray diffraction patterns of THAFP powder (upper) and granules produced at pressure of 20 bars (lower)

THAFP is the anhydrous form II as well, what could be confirmed by diffraction pattern presented in Figure 5.19. It showed the same characteristic peaks like THAP at 7.2, 12.6 and 14.5° 2θ. After roller compaction diffraction was unmodified, so it indicated that roller compaction had no influence on the polymorphic form of THAFP.

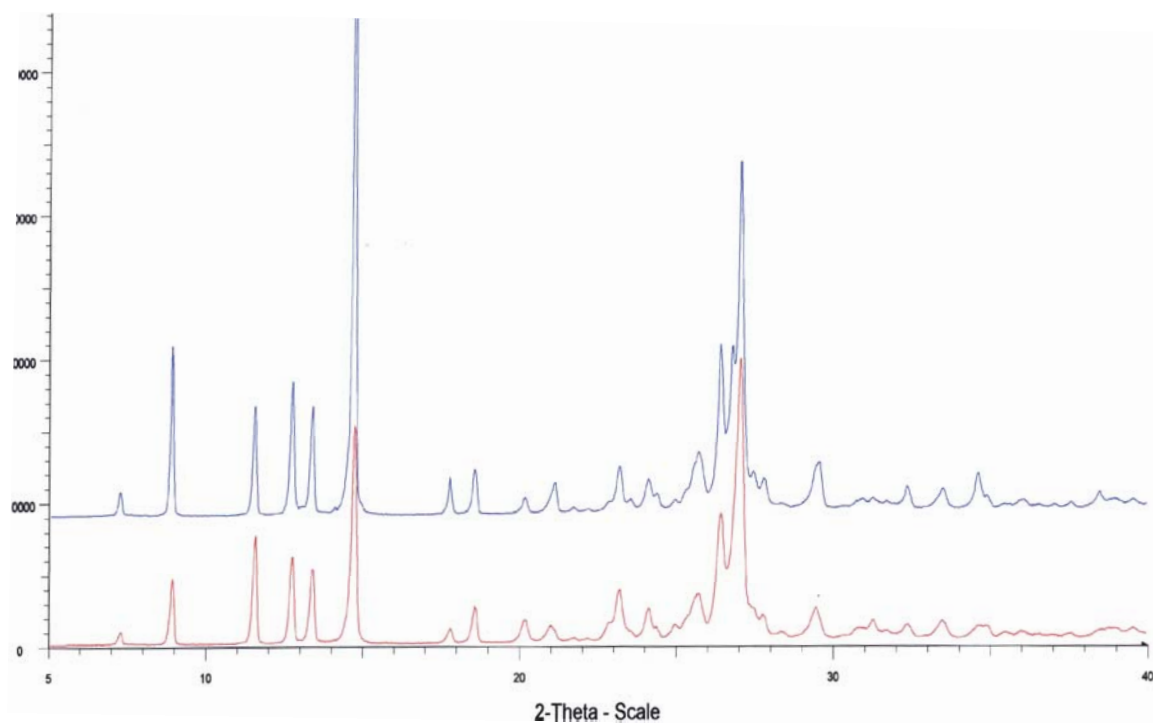


Figure 5.20.: X-ray diffraction patterns of THMO powder (upper) and granules produced at 20 bars (lower)

The X – ray diffraction pattern of THMO was in agreement with that previously presented in the literature ⁴⁹ with characteristics peaks at 8.8, 11.5, 13.3 and 14.7 2θ . In figure 34 it is shown that roller compaction did not have any influence on the diffraction pattern, what implicate that pseudo polymorphic form of THMO was also not changed.

In the chapter 2.5 the way of dehydration of Theophylline monohydrate is shown as a function of temperature (see figure 2.16). This could occur even during compaction under high pressure. However, figure 5.20 confirmed that after roller compaction and milling it still existed as monohydrate.

5.4.4. Differential Scanning Calorimetry (DSC)

Results of DSC measurement of THAP, THAFP and THMO granules are presented together with the results obtained for powder, compacts and tablets, see chapter 5.5.1.

5.5. Tablet Characterization

5.5.1. Differential Scanning Calorimetry (DSC)

In order to check the influence of roller compaction and milling on the structure and polymorphic forms of Theophylline, DSC measurement of pure powders (THAP, THAFP and THMO), ribbons, granules and tablets were performed.

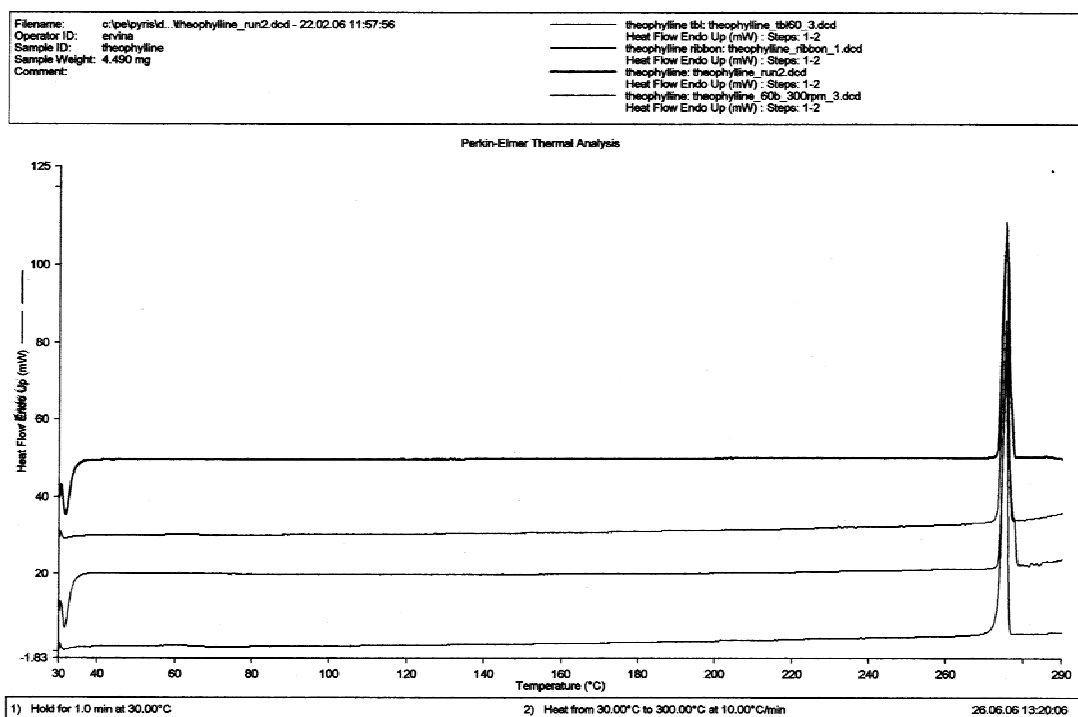


Figure 5.21.: DSC thermogram of THAP, powder, ribbon, granules and tablet (20bar)

According to European Pharmacopoeia melting point of Theophylline is 270 - 274°C. Suzuki et al. 1989,⁴³ prepared separately two polymorphic forms of Theophylline (form II and form I) and made their careful thermochemical analysis. They showed that DSC measurement of these two forms gave different results: form II had a melting point at $273.4 \pm 1.0^\circ\text{C}$ and form I at $269.1 \pm 0.4^\circ\text{C}$. Phadnis and Suryanarayanan 1997,⁴⁵ showed that stable form II had a melting point at 271°C. THAP original powder used in this study showed an endothermic peak at $271.0 \pm 0.5^\circ\text{C}$ and enthalpy $157.2 \pm 3.2 \text{ J/g}$; ribbons produced at pressure of 20 bars had the

same peak at $272.0 \pm 0, 2^\circ\text{C}$ and enthalpy of $152.1 \pm 2.2 \text{ J/g}$; granules obtained from these ribbons had a peak at $271.9 \pm 0.3^\circ\text{C}$, enthalpy of $153.8 \pm 3.3 \text{ J/g}$, and tablets of 12% porosity had a peak at $271.7 \pm 0.2^\circ\text{C}$ and enthalpy of $156.0 \pm 6.5 \text{ J/g}$. The thermograms of THAP powder, ribbon, granules and tablets are presented in figure 5.22.

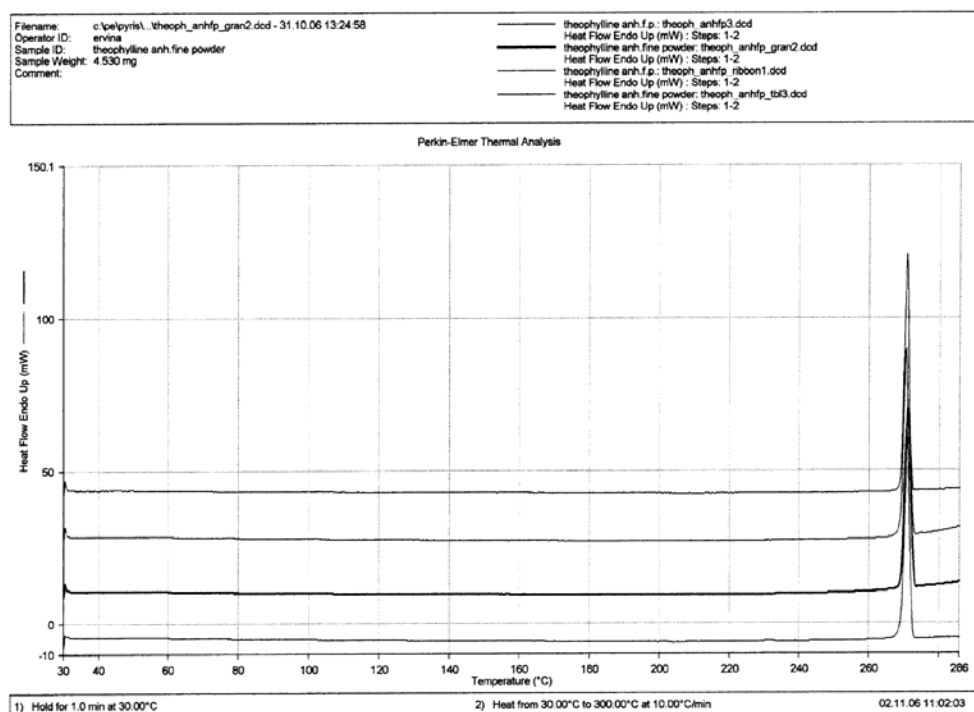


Figure 5.22.: DSC thermogram of THAFP, powder, ribbon, granules and tablet

Analogue to the THAP, THAFP showed the same endothermic peak which is due to the melting point of the material. THAFP pure powder, ribbons, granules and tablets showed peak and enthalpy as follows: $271.3 \pm 0.2^\circ\text{C}$ and enthalpy of $162.8 \pm 3.4 \text{ J/g}$, $271.1 \pm 0.1^\circ\text{C}$ and enthalpy of $160.2 \pm 1.5 \text{ J/g}$, $271.1 \pm 0.1^\circ\text{C}$ and enthalpy of $161.761 \pm 6.3 \text{ J/g}$ and $271.4 \pm 0.2^\circ\text{C}$ and enthalpy of 154.6 J/g , respectively. These results showed that there was no conversion of the polymorphic form during roller compaction and milling.

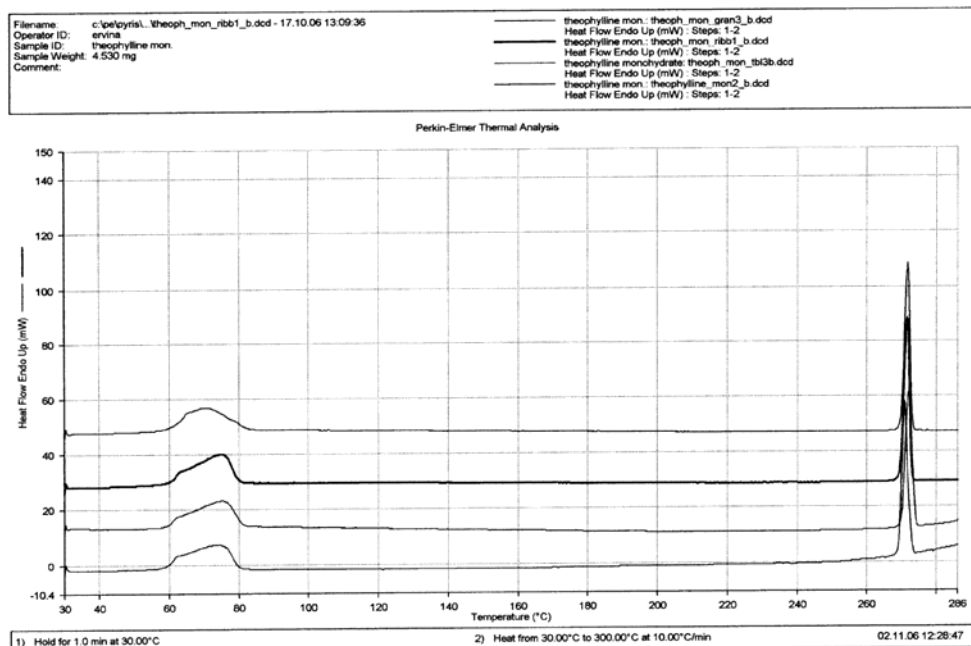


Figure 5.23.: DSC thermogram of THMO, powder, ribbon, granules and tablet

THMO showed first endothermic wide peak around 60 – 80°C due to dehydration and transition of hydrate to anhydrate, second endothermic sharp peak is due to melting of anhydrate. Suzuki et al.1989⁴³, showed that a dehydration of Theophylline monohydrate to anhydrate is at 71°C and further melting of stable anhydrate form is at 273°C.

THMO original powder, used in this study, showed first wide peak and enthalpy at $72.9 \pm 2.2^\circ\text{C}$, $186.1 \pm 14.6 \text{ J/g}$ and second sharp peak end enthalpy at $271.8 \pm 0.2^\circ\text{C}$, $149.4 \pm 1.8 \text{ J/g}$. Ribbons produced by roller compaction at pressure of 20 bars showed these peaks at $75.1 \pm 1.0^\circ\text{C}$, enthalpy of $165.9 \pm 10.3 \text{ J/g}$, and $271.6 \pm 0.2^\circ\text{C}$, enthalpy of $146.9 \pm 6.4 \text{ J/g}$. In the case of granules peak of dehydration was at $76.0 \pm 0.7^\circ\text{C}$, enthalpy of this peak was $170.2 \pm 4.3 \text{ J/g}$, and peak of melting point at $271.6 \pm 0.2^\circ\text{C}$ and enthalpy of $147.0 \pm 0.1 \text{ J/g}$. THMO tablets produced from granules obtained by roller compaction had peak at $73.3 \pm 0.3^\circ\text{C}$, enthalpy of this peak was $164.2 \pm 3.2 \text{ J/g}$. Second sharp peak which corresponded to the melting was at $270.6 \pm 0.1^\circ\text{C}$ and enthalpy was $140.5 \pm 2.4 \text{ J/g}$

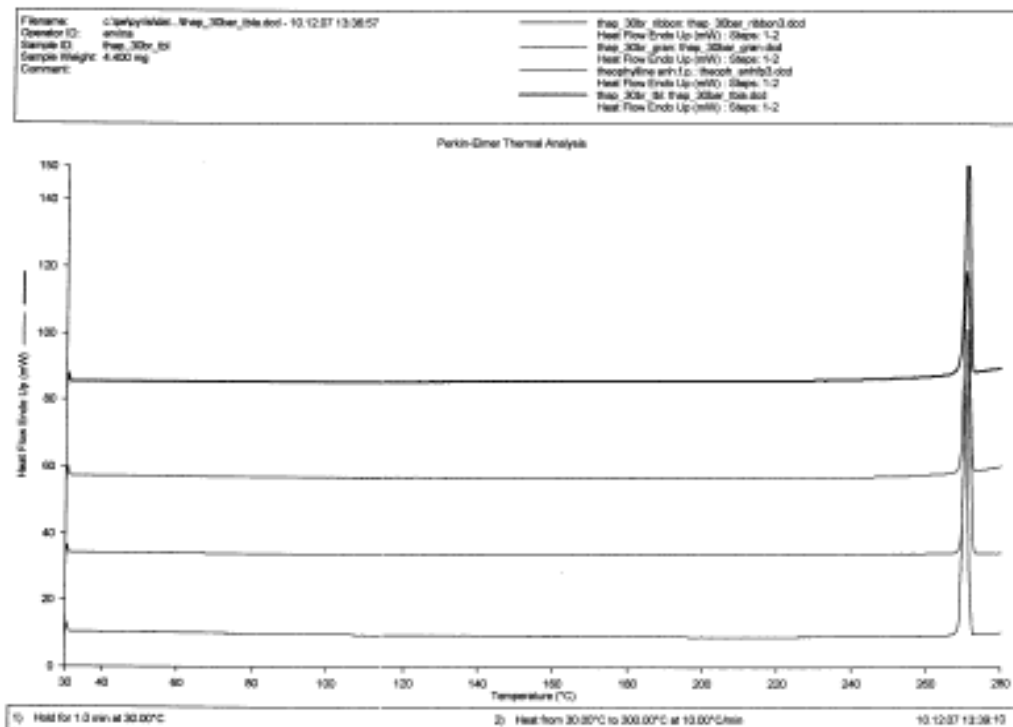


Figure 5.24.: DSC thermogram of THAP, powder, ribbon, granules and tablet (30bar)

THAP compacted at pressure of 30 bars had the same melting point as THAP compacted at pressure of 20 bars, which led to the conclusion that increasing the pressure of compaction did not change the polymorphic form of Theophylline anhydrate. Melting point of THAP ribbons produced at pressure of 30 bars was at $271.2 \pm 0.1^\circ\text{C}$; enthalpy was $153.8 \pm 1.2 \text{ J/g}$. Granules had the endothermic peak at $271.0 \pm 0.5^\circ\text{C}$ and enthalpy of this peak was $133.7 \pm 2.5 \text{ J/g}$, and tablet had the same peak at $271.2 \pm 1.2^\circ\text{C}$ with enthalpy $146.7 \pm 3.5 \text{ J/g}$.

5.5.2. Heckel and Modified Heckel Analysis

During tableting, the bed density or porosity of powder changes as a function of applied compaction force⁶³. Heckel and modified Heckel analysis were performed to study effect of applied pressure on the relative density of a powder bed during compaction and to determine the deformation mechanism of the particular material under the pressure. Due to double compactions which were done by roller compaction and tableting of THAP, THAFP, THMO and their binary mixtures with MCC, compressibility of the materials were investigated with and without roller compaction.

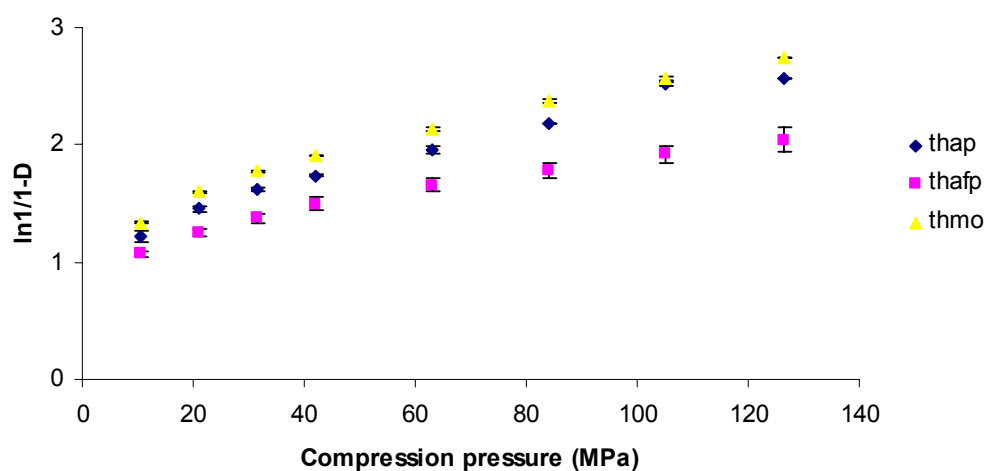


Figure 5.25.: Heckel plot THAP, THAFP and THMO – powder

Figure 5.25 showed that all three plots have a curvature in the region of low pressure 10.5 – 31.5 MPa, what is connected to the fragmentation and rearrangement of the powder. This curvature is followed by the linear portions at pressures higher than 42.1 MPa. It is well accepted that the reciprocal of slope is material dependent constant – yield pressure P_y , which is inversely related to the ability of material to deform plastically under pressure. Low value of P_y indicates a faster onset of plastic deformation²⁷. Parameters K and P_y for THAP were $10.6 \pm 0.1 \times 10^{-3}$ MPa and 94.0 ± 1.3 MPa (see table 5.13), for THAFP were $6.1 \pm 0.2 \times 10^{-3}$ MPa and 162.1 ± 1.5 MPa

(see table 5.16) and for THMO $10.7 \pm 0.2 \times 10^{-3}$ MPa and 92.8 ± 1.7 MPa (see table 5.18).

According to the results obtained by Heckel equation THMO is the most plastic material followed by THAP and THAFP. Figure 5.25 showed that at pressure lower than 42.1 MPa, Heckel plot showed curve which is not taken in account when parameters K and P_y were calculated. The modified Heckel equation is especially suitable for the low pressure range and constants C and ρ_{rc} represent the whole pressure range. Parameters C and ρ_{rc} for THAP were $3.6 \pm 0.1 \times 10^{-3}$ MPa and 0.5 ± 0.1 , for THAFP $2.1 \pm 0.2 \times 10^{-3}$ MPa and 0.5 ± 0.0 , and for THMO $2.8 \pm 0.1 \times 10^{-3}$ MPa and 0.6 ± 0.1 . According to modified Heckel equation and parameter C THAP is the most plastic material followed by THMO and THAFP. The differences in results obtained by Heckel and modified Heckel could be explained by the fact that for the calculation of K and C values not the same pressure range was included.

THAP, THAFP and THMO (see figure 5.25) showed behavior characteristic for material type B²⁷ which means that initial curved region is followed by straight line. This would be more noticeable if lower compression force and more point in this region would be used.

Suihko et al. 2001,⁵⁵ studied properties of the tablets produced from different Theophylline form. Stable and metastable form of Theophylline anhydrate and Theophylline monohydrate were studied. In the research it is presented that under compression all modifications of Theophylline deforms primarily by plastic flow. The results from this study showed that Theophylline at low compaction range underwent fragmentation, followed by plastic flow which occurred at the higher compaction pressure.

Table 5.13.: Heckel and modified Heckel parameters for characterization of the compression behavior of THAP, MCC and their binary mixtures – direct compression

| % of THAP in the binary mixture | K [10 ⁻³ MPa] n=3 | A n=3 | Py [MPa] n=3 | R ² | C [10 ⁻³ MPa] n=3 | ρ _{rc} n=3 | R ² |
|---------------------------------------|------------------------------------|-------------|--------------------|----------------|------------------------------------|------------------------|----------------|
| 100% | 10.66 ± 0.12 | 1.30 ± 0.02 | 94.05 ± 1.35 | 0.967 | 3.64 ± 0.01 | 0.54 ± 0.00 | 0.995 |
| 70% | 10.50 ± 0.26 | 1.07 ± 0.01 | 95.27 ± 2.37 | 0.994 | 4.84 ± 0.08 | 0.40 ± 0.00 | 0.998 |
| 50% | 10.60 ± 0.26 | 0.97 ± 0.03 | 94.37 ± 2.32 | 0.991 | 5.45 ± 0.23 | 0.33 ± 0.01 | 0.999 |
| 30% | 11.70 ± 0.43 | 0.77 ± 0.02 | 85.54 ± 3.25 | 0.996 | 6.21 ± 1.12 | 0.25 ± 0.05 | 0.998 |
| 10% | 11.26 ± 0.15 | 0.87 ± 0.01 | 89.85 ± 2.02 | 0.989 | 6.68 ± 0.14 | 0.25 ± 0.00 | 0.999 |
| 0% | 9.33 ± 0.28 | 0.77 ± 0.01 | 107.21 ± 3.37 | 0.969 | 5.40 ± 0.64 | 0.32 ± 0.03 | 0.996 |

Table 5.14.: Heckel and modified Heckel parameters for the characterization of the compression behavior of THAP, MCC and their binary mixtures – granules (20bar)

| % of THAP in the binary mixture | K [10 ⁻³ MPa] n=3 | A n=3 | Py [MPa] n=3 | R ² | C [10 ⁻³ MPa] n=3 | ρ _{rc} n=3 | R ² |
|---------------------------------------|------------------------------------|-------------|--------------------|----------------|------------------------------------|------------------------|----------------|
| 100% | 7.33 ± 0.15 | 1.37 ± 0.15 | 136.39 ± 2.82 | 0.998 | 1.88 ± 0.05 | 0.61 ± 0.01 | 0.998 |
| 70% | 8.03 ± 0.05 | 1.25 ± 0.01 | 124.48 ± 0.89 | 0.993 | 2.59 ± 0.00 | 0.53 ± 0.00 | 0.998 |
| 50% | 9.50 ± 0.20 | 1.09 ± 0.01 | 105.29 ± 2.21 | 0.994 | 3.50 ± 0.12 | 0.46 ± 0.03 | 0.995 |
| 30% | 10.90 ± 0.17 | 0.89 ± 0.01 | 96.93 ± 1.78 | 0.998 | 4.06 ± 0.10 | 0.32 ± 0.00 | 0.997 |
| 10% | 10.30 ± 0.51 | 0.93 ± 0.03 | 101.03 ± 4.73 | 0.997 | 5.15 ± 0.42 | 0.39 ± 0.02 | 0.998 |
| 0% | 9.50 ± 0.36 | 0.85 ± 0.02 | 105.36 ± 3.94 | 0.997 | 4.69 ± 0.23 | 0.30 ± 0.01 | 0.996 |

Table 5.15.: Heckel and modified Heckel parameters for the characterization of the compression behavior of THAP, MCC and their binary mixtures – granules (30bar)

| % of THAP in the binary mixture | K [10 ⁻³ MPa] n=3 | A n=3 | Py [MPa] n=3 | R ² | C [10 ⁻³ MPa] n=3 | ρ _{rc} n=3 | R ² |
|---------------------------------------|------------------------------------|-------------|--------------------|----------------|------------------------------------|------------------------|----------------|
| 100% | 6.96 ± 0.28 | 1.37 ± 0.01 | 143.70 ± 5.81 | 0.997 | 1.74 ± 0.20 | 0.61 ± 0.01 | 0.997 |
| 70% | 7.76 ± 0.47 | 1.12 ± 0.03 | 129.06 ± 0.89 | 0.993 | 2.40 ± 0.09 | 0.55 ± 0.02 | 0.993 |
| 50% | 8.46 ± 0.25 | 1.16 ± 0.01 | 118.18 ± 3.53 | 0.996 | 2.97 ± 0.06 | 0.50 ± 0.02 | 0.996 |
| 30% | 9.66 ± 0.61 | 1.00 ± 0.06 | 103.73 ± 6.69 | 0.998 | 3.46 ± 0.03 | 0.37 ± 0.02 | 0.998 |
| 10% | 9.56 ± 0.72 | 1.25 ± 0.01 | 104.91 ± 4.73 | 0.995 | 4.55 ± 0.03 | 0.45 ± 0.03 | 0.995 |
| 0% | 9.80 ± 0.10 | 0.85 ± 0.02 | 105.41 ± 4.96 | 0.993 | 4.30 ± 0.02 | 0.38 ± 0.01 | 0.993 |

As it is explained before, parameters K and P_y calculated by Heckel equation are measures of material's ability to deform plastically. The binary mixtures of THAP and MCC (powder and granules produced at compression pressure of 20 and 30 bars) behaved in the same way as pure THAP and MCC, which means at low pressure (10.5 – 31.5 MPa) they showed no linearity because of fragmentation and rearrangement of the particles followed by linear part of the plot at higher pressure (42.1 – 126.3 MPa). According to Heckel equation the most compressible and in the same time the most plastic is the binary mixture of THAP 30% + MCC 70%, followed by the mixture of THAP 10% + MCC 90% (see table 5.13). The same results were obtained with tablets made from granules produced by roller compaction at pressure of 20 (see table 5.14) and 30 bars (see table 5.15). As an addition to the Heckel, that observes only the linear part of the plot, modified Heckel equation take the entire pressure range into account. The highest compressibility parameters C showed the binary mixture of THAP 10% + MCC 90%, followed by the mixture of THAP 30% + MCC 70%. The critical relative density ρ_{rc} for the mixture THAP 10% + MCC 90% (see table 5.13) was the lowest among all samples and what indicated that this mixture forms rigid compacts at the smallest relative density. According to these results it could be seen that Heckel plot has limitations to characterize powder materials. Due to the powder characteristics that at low pressure it undergo compression by fragmentation first, which is followed by plastic deformation, and the fact that Heckel equation consider only linear part of the plot, it could occur that material is not well characterized.

Results obtained with Heckel, as well as modified Heckel equation, showed that after roller compaction compressibility parameters of THAP, MCC and their binary mixtures have been changed. The yield pressure P_y of THAP powder was 94.0 ± 1.3 MPa, for THAP granules produced at pressure of 20 bars was 136.3 ± 2.8 MPa and for THAP granules produced at pressure of 30 bars was 143.7 ± 5.8 MPa. From these results and figure 5.26 it could be seen that there was a difference in behavior of THAP under pressure, in the way that roller compaction decreased the ability of plastic deformation. The results of modified Heckel plots confirmed this phenomenon because the constant C of THAP powder, granules produced at pressure of 20 bars and granules of 30 bars was decreased (see table 5.13, table 5.14 and table 5.15).

Although, differences in compressibility behavior of THAP original powder and granules was observed it was not statistically significant.

MCC during roller compaction according to Heckel equation showed different behavior because P_y of powder was 107.2 ± 3.3 MPa, for granules produced at pressure of 20 bars 105.3 ± 3.9 MPa, and for granules produced at pressure 30 bars 105.4 ± 4.9 MPa. This indicated that granules showed more plastic behavior than powder, but this difference was not statistically significant ($p < 0.05$). From the Figure 5.37 and Figure 5.38 it could be seen that there was a difference in behavior of MCC powder and granules under pressure, but this difference was more expressed at low pressure which Heckel equation does not consider. Therefore, results of modified Heckel equation approved that MCC powder was more plastic than MCC granules (see table 5.13, table 5.14 and table 5.15).

It is well known that due to a good compressibility and compactibility properties, MCC is widely used excipients in direct compaction and roller compaction as well. In the literature it is possible to find a lot of different data regarding compressibility parameters for this material.

Xiarong et al. 2006,⁶⁴ studied effect roller compaction on mechanical properties of tablets. It was shown that P_y of MCC powder is 81.7 MPa, while after roller compaction it is increased to the value of 107.0 MPa. From this result it could be seen that yield pressure of MCC was increased after roller compaction, what means that material showed less plastic behavior. If these results are compared with results obtained in this study it could be observed that there is a contradictory observation. Previously (see chapter 4.7.2.1), it was explained that a lot of parameters as: operating conditions, type of compression, compression speed, lubricant, punch diameter, maximum compression pressure, may have influence on the value of yield pressure. This fact should be taken into account when results of different studies are compared and small variations in the obtained results can be justified.

Ilkka and Paronen 1993,²⁹ in their study showed that P_y for AVICEL PH 101 is 106 MPa. In the research of Medina 2005,³² it was demonstrated that yield pressure of the same material is 94.1 MPa. All these results approximately are in agreement with results obtained in this study.

The results in table 5.13, table 5.14 and table 5.15 showed that goodness of fit was always better for modified Heckel equation, independent whether powder or granules

were analyzed. This confirmed that the results obtained from modified Heckel equation gave more accurate results.

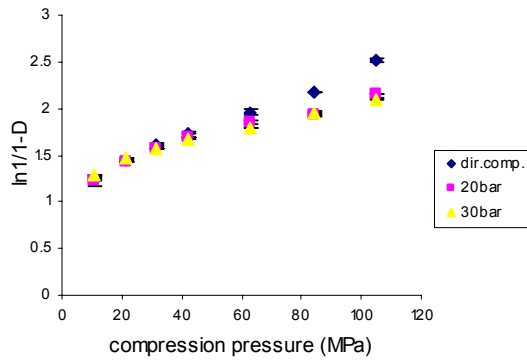


Figure 5.26.: Heckel plot – THAP 100%

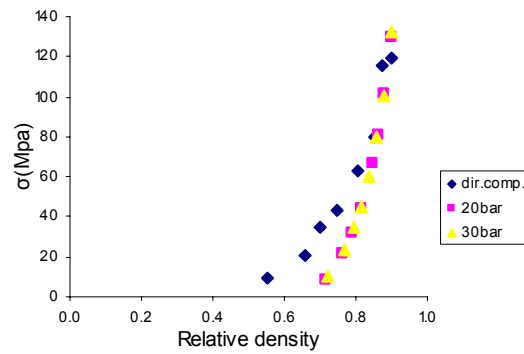


Figure 5.27.: Modified Heckel plot – THAP100%

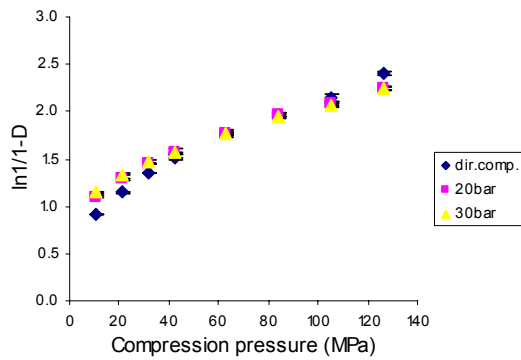


Figure 5.28.: Heckel plot – binary mixture THAP70% + MCC30%

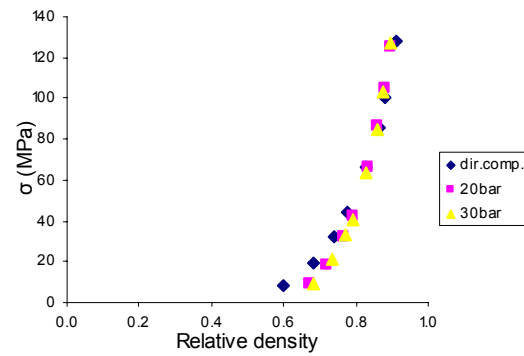


Figure 5.29.: Modified Heckel plot – binary mixture THAP70% + MCC30%

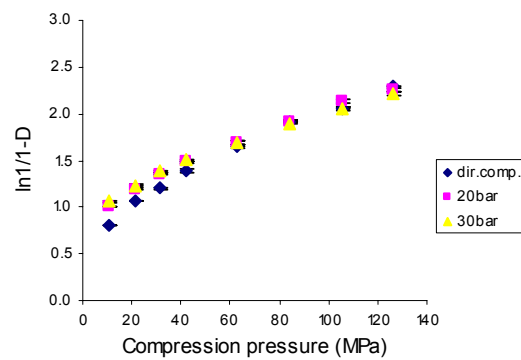


Figure 5.30.: Heckel plot - binary mixture THAP50% + MCC50%

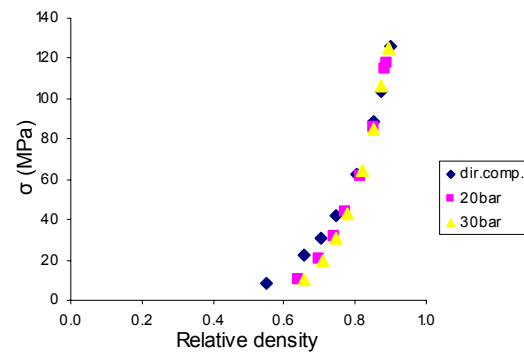


Figure 5.31.: Modified Heckel plot – binary mixture THAP50% + MCC50%

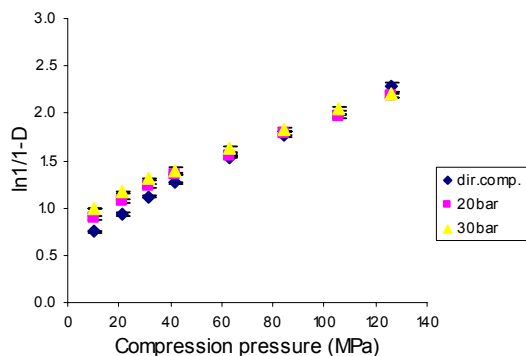


Figure 5.32.: Heckel plot – binary mixture THAP30% + MCC70%

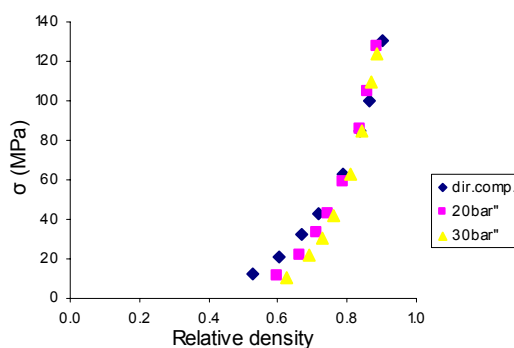


Figure 5.33.: Modified Heckel plot – binary mixture THAP30% + MCC70%

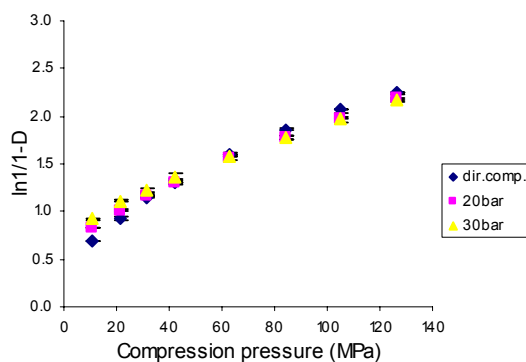


Figure 5.34.: Heckel plot – binary mixture THAP10% + MCC90%

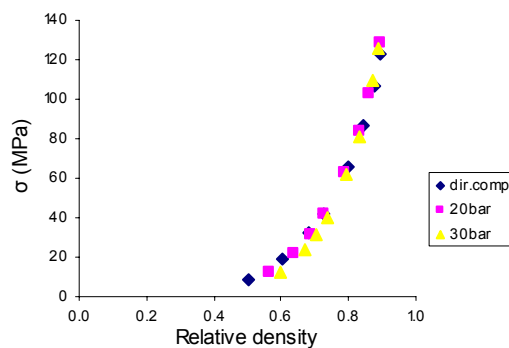


Figure 5.35.: Modified Heckel plot – binary mixture THAP10% + MCC90%

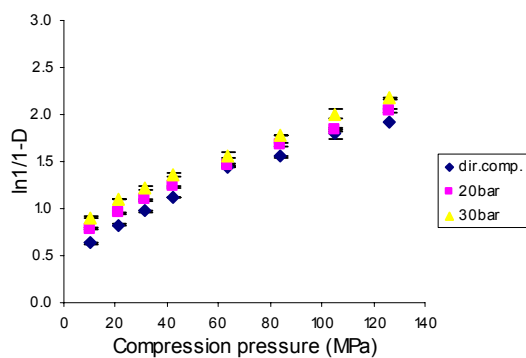


Figure 5.36.: Heckel plot – MCC 100%

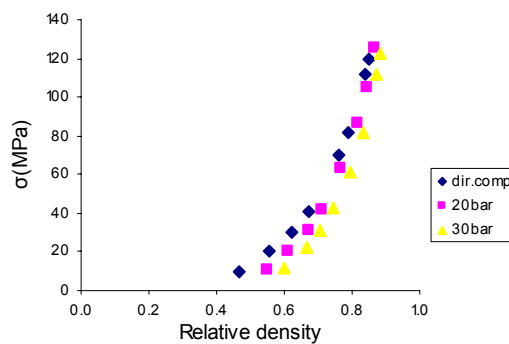


Figure 5.37.: Modified Heckel plot – MCC 100%

THAFP

In an equivalent way like in the case of THAP, Heckel and modified Heckel plots were done for THAFP tablets produced from the powder and granules produced at pressure of 20 bars.

Table 5.16.: Heckel and modified Heckel parameters for the characterization of the compression behavior of THAFP, MCC and their binary mixtures – direct compression

| % of THAFP in the binary mixture | K 10 ⁻³ [MPa] n=3 | A n=3 | Py [MPa] n=3 | R ² | C [10 ⁻³ MPa] n=3 | ρ _{rc} n=3 | R ² |
|--|------------------------------------|-------------|--------------------|----------------|------------------------------------|------------------------|----------------|
| 100% | 6.16 ± 0.28 | 1.23 ± 0.02 | 162.17 ± 1.52 | 0.996 | 2.10 ± 0.01 | 0.55 ± 0.00 | 0.999 |
| 70% | 9.26 ± 0.05 | 1.04 ± 0.08 | 107.94 ± 0.65 | 0.999 | 3.22 ± 0.56 | 0.46 ± 0.00 | 0.996 |
| 50% | 10.10 ± 0.60 | 0.99 ± 0.05 | 99.27 ± 5.90 | 0.994 | 5.34 ± 1.29 | 0.35 ± 0.05 | 0.995 |
| 30% | 11.26 ± 1.16 | 0.85 ± 0.08 | 86.38 ± 4.82 | 0.992 | 7.80 ± 0.26 | 0.20 ± 0.01 | 0.997 |
| 10% | 10.75 ± 0.07 | 0.87 ± 0.00 | 93.02 ± 0.61 | 0.998 | 7.25 ± 0.12 | 0.21 ± 0.01 | 0.998 |
| 0% | 9.33 ± 0.28 | 0.77 ± 0.01 | 107.21 ± 3.37 | 0.969 | 5.40 ± 0.64 | 0.32 ± 0.03 | 0.996 |

Table 5.17.: Heckel and modified Heckel parameters for the characterization of the compression behavior of THAFP, MCC and their binary mixtures – granules 20 bar

| % of THAFP in the binary mixture | K [10 ⁻³ MPa] n=3 | A n=3 | Py [MPa] n=3 | R ² | C [10 ⁻³ MPa] n=3 | ρ _{rc} n=3 | R ² |
|--|------------------------------------|-------------|--------------------|----------------|------------------------------------|------------------------|----------------|
| 100% | 5.69 ± 0.30 | 1.33 ± 0.02 | 167.88 ± 8.46 | 0.998 | 1.27 ± 0.03 | 0.62 ± 0.00 | 0.998 |
| 70% | 8.90 ± 0.05 | 1.20 ± 0.00 | 112.38 ± 2.21 | 0.994 | 2.79 ± 0.14 | 0.53 ± 0.00 | 0.998 |
| 50% | 8.53 ± 0.25 | 1.17 ± 0.01 | 119.53 ± 1.63 | 0.983 | 3.06 ± 0.36 | 0.50 ± 0.01 | 0.998 |
| 30% | 10.30 ± 0.36 | 1.04 ± 0.02 | 97.16 ± 3.35 | 0.997 | 4.79 ± 0.19 | 0.41 ± 0.01 | 0.999 |
| 10% | 10.28 ± 0.55 | 0.97 ± 0.03 | 97.27 ± 5.34 | 0.983 | 4.72 ± 0.56 | 0.37 ± 0.02 | 0.998 |
| 0% | 9.50 ± 0.36 | 0.85 ± 0.02 | 105.36 ± 3.94 | 0.997 | 4.69 ± 0.23 | 0.30 ± 0.01 | 0.999 |

THAFP and the binary mixtures with MCC showed the same behavior as THAP, curvature at low pressure and linear part at higher pressure range. According to yield pressure P_y from the Heckel analysis, constant C and critical relative density ρ_{rc} from the modified Heckel equation it could be concluded that the most plastic mixture is the binary one of THAFP 30% + MCC 70% either powder or granules were observed (see table 5.16 and table 5.17). Although, in the previous section of THAP it was shown that results obtained from Heckel and modified Heckel equation did not give results that the same material showed the most plastic behavior with both equation, THAFP approved that these two methods suit for some materials. This means that the material which showed the highest value of the constant K of the Heckel equation in the same time showed the highest value of the constant C of modified Heckel equation. Yield pressure P_y for THAFP powder and granules were 162.170 ± 1.527 MPa and 167.886 ± 8.467 MPa consecutively. Constant C and ρ_{rc} obtained by modified Heckel equation for THAFP powder were as followed $2.1 \pm 0.1 \times 10^{-3}$ MPa and 0.5 ± 0.1 MPa. Results of constants C and ρ_{rc} obtained for granules were $1.2 \pm 0.3 \times 10^{-3}$ MPa and 0.6 ± 0.0 . Comparing compressibility parameters (see table 5.16 and table 5.17) obtained from the tablets produced by direct compaction and roller compaction (20 bar) compressibility of THAFP after roller compaction is decreased but this difference is not significant ($p < 0.05$).

The results in table 5.16 and table 5.17 showed that goodness of fit was always better for modified Heckel equation independent whether powder or granules were analyzed.

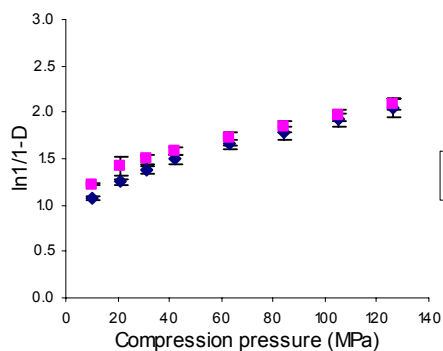


Figure 5.38.: Heckel plot – THAFP 100%

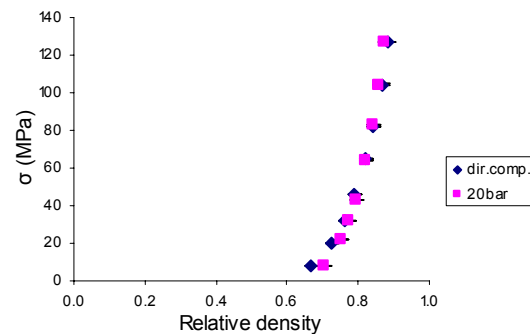


Figure 5.39.: Modified Heckel plot – THAFP100%

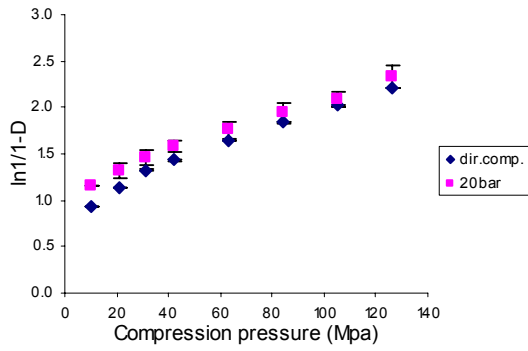


Figure 5.40.: Heckel plot – binary mixture THAFP70% + MCC30%

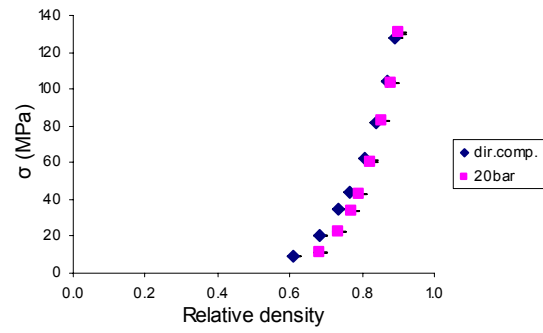


Figure 5.41.: Modified Heckel plot – binary mixture THAFP70% + MCC30%

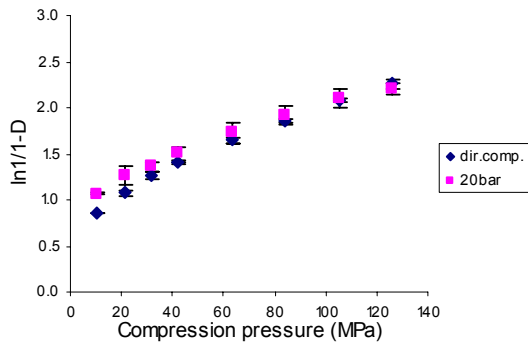


Figure 5.42.: Heckel plot – binary mixture THAFP50% + MCC50%

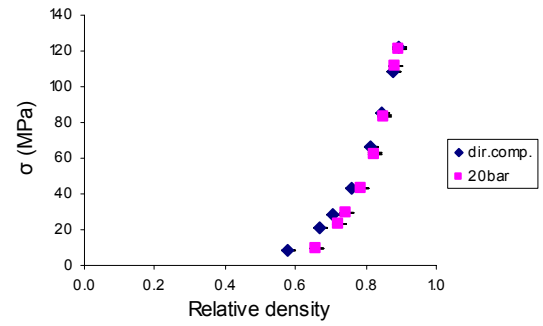


Figure 5.43.: Modified Heckel plot – binary mixture THAFP50% + MCC50%

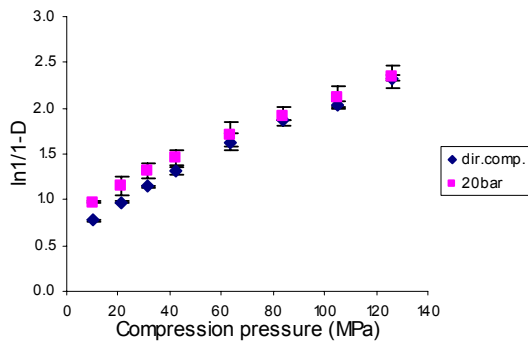


Figure 5.44.: Heckel plot – binary mixture THAFP30% + MCC70%

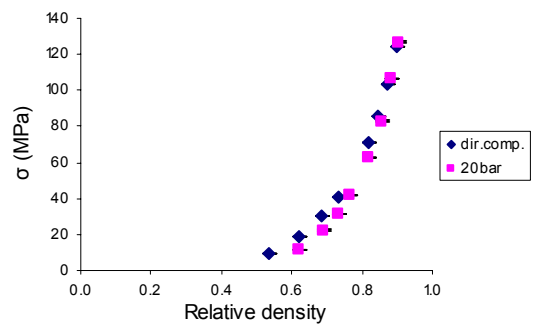


Figure 5.45.: Modified Heckel plot – binary mixture THAFP30% + MCC70%

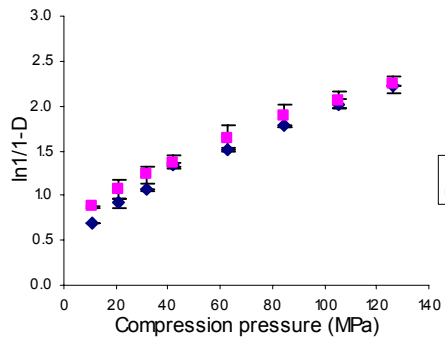


Figure 5.46.: Heckel plot - binary mixture THAFP10% + MCC90%

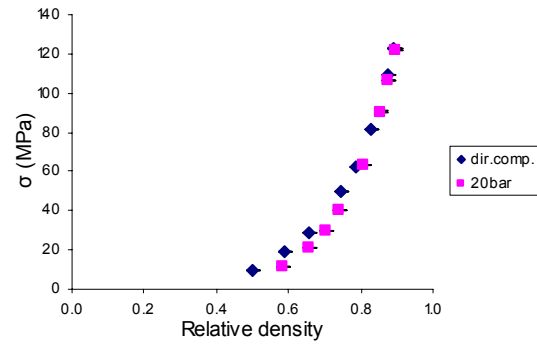


Figure 5.47.: Modified Heckel plot – binary mixture THAFP10% + MCC90%

THMO

Results of compressibility behavior for THMO powders and granules produced at pressure of 20 bars are presented in table 5.18 and table 5.19 as well as in the figure 5.47 to figure 5.57.

Table 5.18.: Heckel and modified Heckel parameters for the characterization of the compression behavior of THMO, MCC and their binary mixtures – direct compression

| % of THMO in the binary mixture | K [10 ⁻³ MPa] n=3 | A n=3 | Py [MPa] n=3 | R ² | C [10 ⁻³ MPa] n=3 | ρ _{rc} n=3 | R ² |
|---------------------------------------|------------------------------------|-------------|--------------------|----------------|------------------------------------|------------------------|----------------|
| 100% | 10.76 ± 0.20 | 1.50 ± 0.00 | 92.89 ± 1.78 | 0.996 | 2.80 ± 0.07 | 0.62 ± 0.00 | 0.999 |
| 70% | 9.43 ± 1.38 | 1.31 ± 0.23 | 107.43 ± 5.17 | 0.991 | 4.91 ± 0.01 | 0.44 ± 0.00 | 0.999 |
| 50% | 10.95 ± 0.25 | 1.03 ± 0.03 | 91.37 ± 2.95 | 0.991 | 5.89 ± 0.12 | 0.35 ± 0.00 | 0.998 |
| 30% | 11.13 ± 0.28 | 0.88 ± 0.02 | 89.96 ± 2.36 | 0.989 | 6.19 ± 0.15 | 0.25 ± 0.03 | 0.998 |
| 10% | 10.76 ± 0.15 | 0.80 ± 0.03 | 91.89 ± 0.64 | 0.996 | 6.41 ± 0.06 | 0.22 ± 0.00 | 0.998 |
| 0% | 9.33 ± 0.28 | 0.77 ± 0.01 | 107.21 ± 3.37 | 0.969 | 5.40 ± 0.64 | 0.32 ± 0.03 | 0.996 |

Table 5.19.: Heckel and modified Heckel parameters for the characterization of the compression behavior of THMO, MCC and their binary mixtures – granules 20bar

| % of THMO in the binary mixture | K [10 ⁻³ MPa] n=3 | A n=3 | Py [MPa] n=3 | R ² | C [10 ⁻³ MPa] n=3 | ρ _{rc} n=3 | R ² |
|---------------------------------------|------------------------------------|-------------|--------------------|----------------|------------------------------------|------------------------|----------------|
| 100% | 12.20 ± 0.88 | 1.40 ± 0.06 | 82.26 ± 6.20 | 0.992 | 3.94 ± 0.45 | 0.57 ± 0.02 | 0.998 |
| 70% | 9.03 ± 0.15 | 1.23 ± 0.01 | 110.72 ± 1.86 | 0.993 | 3.43 ± 0.06 | 0.50 ± 0.00 | 0.999 |
| 50% | 10.53 ± 0.35 | 1.08 ± 0.02 | 95.00 ± 3.15 | 0.994 | 4.53 ± 0.30 | 0.42 ± 0.01 | 0.998 |
| 30% | 10.63 ± 0.28 | 0.99 ± 0.02 | 97.77 ± 2.80 | 0.995 | 4.65 ± 0.22 | 0.38 ± 0.01 | 0.999 |
| 10% | 10.20 ± 0.88 | 0.90 ± 0.01 | 94.39 ± 2.67 | 0.996 | 5.43 ± 0.19 | 0.31 ± 0.00 | 0.999 |
| 0% | 9.50 ± 0.36 | 0.85 ± 0.02 | 105.36 ± 3.94 | 0.997 | 4.69 ± 0.23 | 0.30 ± 0.01 | 0.999 |

In contrast to two other materials (THAP and THAFP), THMO showed more plastic behavior under pressure after roller compaction calculated by Heckel and modified Heckel equation. Yield pressure P_y of THMO powder was 92.8 ± 1.7 MPa, and for THMO granules produced at pressure of 20 bars was 82.2 ± 6.2 MPa, and lower P_y indicated more plastic behavior of the material. Modified Heckel equation gave results which led to the same conclusion. Compressibility constants C and ρ_{rc} for THMO powder were $2.8 \pm 0.1 \times 10^{-3}$ MPa and 0.6 ± 0.0 , for THMO granules were $3.9 \pm 0.4 \times 10^{-3}$ MPa and 0.5 ± 0.2 . Even if THMO and MCC according to Heckel equation were more compressible and more plastic after roller compaction, the binary mixtures of these materials showed an opposite behavior (see table 5.18 and table 5.19).

Analogous to THAP, the most compressible according to Heckel equation was the binary mixture of THMO 30% + MCC70% (see table 5.18 and table 5.19), but according to modified Heckel equation it was the mixture THMO10% + MCC 90%. All results showed that modified Heckel equation gave better goodness of fit.

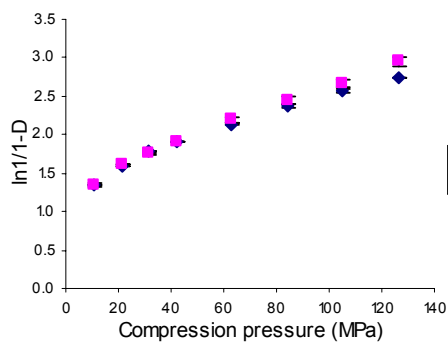


Figure 5.48.: Heckel plot – THMO 100%

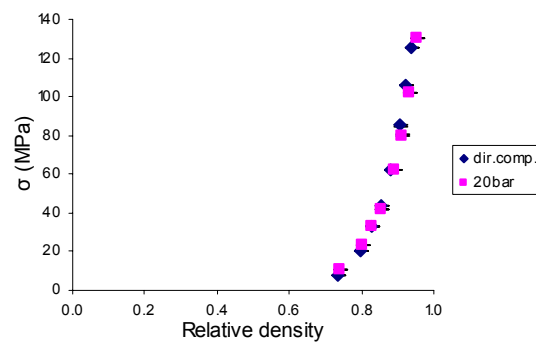


Figure 5.49.: Modified Heckel plot – THMO100%

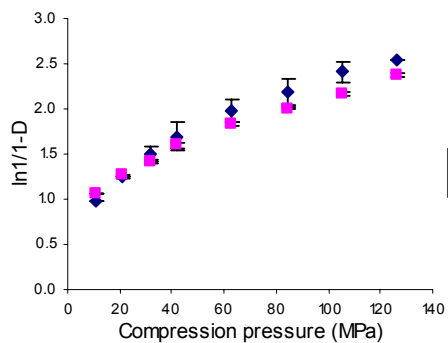


Figure 5.50.: Heckel plot – binary mixture THMO70%+MCC30%

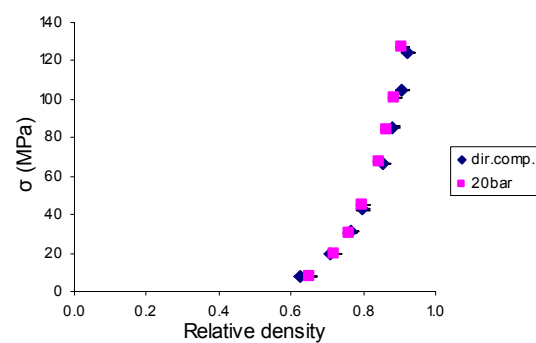


Figure 5.51.: Modified Heckel plot – binary mixture THMO70%+MCC30%

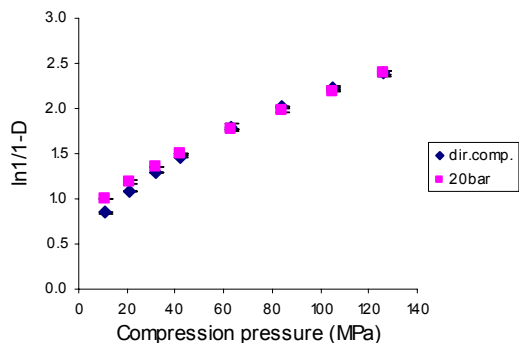


Figure 5.52.: Heckel plot – binary mixture THMO50% + MCC50%

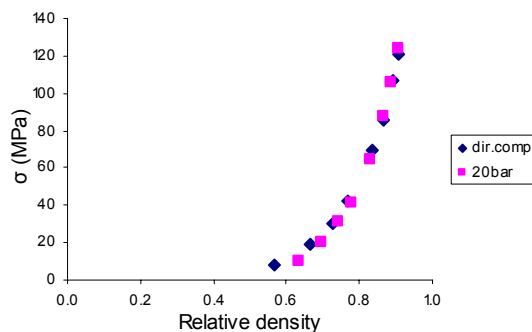


Figure 5.53.: Modified Heckel plot – binary mixture THMO50% + MCC50%

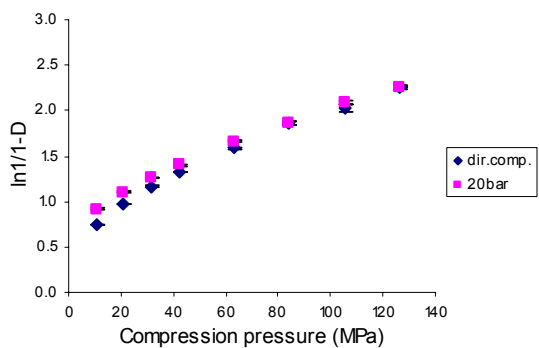


Figure 5.54.: Heckel plot - binary mixture THMO30% + MCC70%

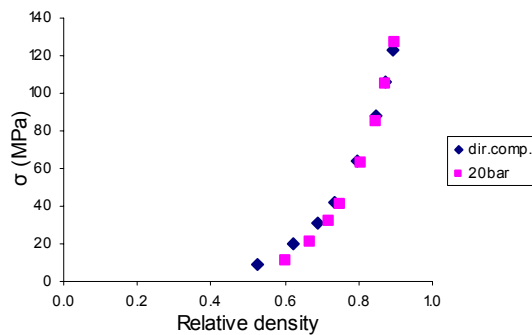


Figure 5.55.: Modified Heckel - plot binary mixture THMO30% + MCC70%

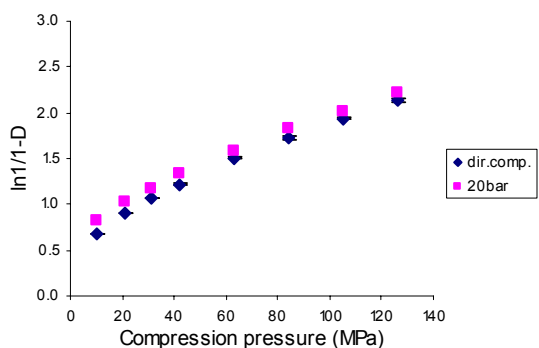


Figure 5.56.: Heckel plot – binary mixture THMO10% + MCC90%

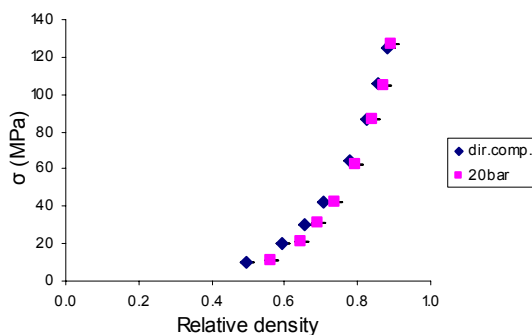


Figure 5.57.: Modified Heckel plot – binary mixture THMO10% + MCC90%

5.5.3. Tensile strength

Tablets produced in the pharmaceutical industry commonly consist of more than one component. The mechanical strength of tablets depends on formulation and processing parameters. Although, the same process parameters are used, the strength of tablets compressed from binary mixtures can often not be predicted from the compaction properties of individual material. Reasons for this phenomenon are interactions between materials which may occur during compaction process⁶⁵.

In the literature it is very often discussed about decreasing of tensile strength of tablets produced by roller compaction compared with other technique⁶². This phenomenon, reducing tabletability of powder after roller compaction, is termed “loss of reworkability” or “loss of tabletability”.

This is due to the limited binding potential which is partially consumed in the first compression step by increasing particle size and decreasing specific surface area of the material. Materials with plastic deformation properties are particularly sensitive to loss of tabletability. However, if granules undergo extensive fracture under pressure, effect of granule size enlargement on tabletability of granules prepared by roller compaction should be much less³⁶. Explanation for this phenomenon could be found in the fact that fracture of particles significantly reduces original particles size, thereby minimizes or eliminates any difference in original particle size of the material.

Tensile strength of the tablets made from powder and granules were measured in order to check influence of roller compaction on tablet hardness. The same pressure range 1 – 12 kN (10.2 – 126.6 MPa) was used for all materials and binary mixtures.

According to the fact that THAFP (90% less than 38.085 μm) had a lower particle size than THAP (90% less than 386.09 μm), tensile strength of tablets produced from THAFP should be much higher than tensile strength of THAP tablets. Because of the smaller particle size THAFP showed a higher specific surface area, which is a criterion for increased particle bonding in tablets. Surprising was that THAFP tablets did not show significantly higher mechanical strength regarding tablets prepared from THAP, except at very low compression pressure. Tensile strength of THAFP at compression force 1 kN and 12 kN (lowest and highest compression pressure) was

$34.2 \pm 6.7 \text{ N/cm}^2$ and $233.4 \pm 4.5 \text{ N/cm}^2$, and for THAP $19.2 \pm 1.6 \text{ N/cm}^2$ and $260.2 \pm 14.4 \text{ N/cm}^2$, consecutively.

In the research of Hertig and Kleinebudde 2007,⁶² it was reported that decreasing in particle sizes of Theophylline and MCC results in stronger tablets and even if tablets are produced by roller compaction tensile strength is still dependent of the particle sizes of the original materials. This was explained by more available binding points due to the larger surface area. As it is previously shown that THAFP used in this study was agglomerated, differences in the obtained results can be clarified. THMO powder formed tablets with higher tensile strength than THAP and THAFP in the whole compression range, except at high compression force 12 kN. This could be explained, that at high force THMO dehydrated and lost its tabletability. DSC results showed that THMO in tablets with 12 % porosity (4.5 kN) did not loose a water, but it is assumed to be possible that at very high pressure it undergoes dehydration.

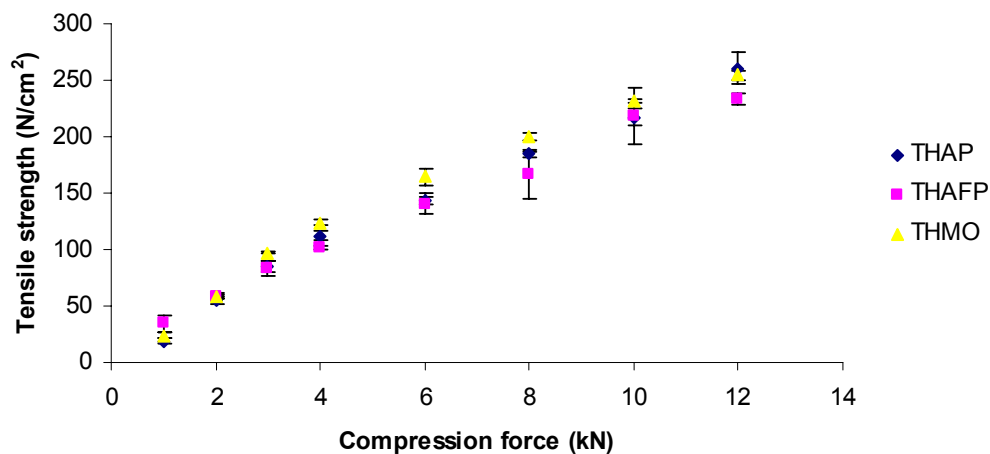


Figure 5.58.: Tensile strength of THAP, THAFP and THMO – powder

THAP

Although, according to Heckel equation THAP and MCC showed the same behavior under compression with nearly the same P_y (see table 5.13), what classified them to the group of plastic material, they showed different behavior regarding changing of tensile strength after roller compaction.

The average values of tensile strength including standard deviation and the corresponding pressures of compression are shown in table 7.1, Appendix.

In figures 5.59 to figure 5.64 tensile strength [N/cm²] of the tablets produced from THAP, MCC and their binary mixtures was plotted against the compression force. The tensile strength of tablets showed linear dependence on compression force produced either by direct compaction or roller compaction (20 and 30 bars).

Tensile strength of tablets produced from THAP powder at compression force 12 kN was 260.6 ± 7.1 N/cm², from THAP granules (20 bars) was 237.8 ± 6.7 N/cm², from THAP granules (30 bars) was 227.9 ± 9.4 N/cm². From these results it could be seen that roller compaction decreased the tensile strength of tablets, especially at higher compression pressure (30 bars). However, difference in tensile strength of MCC tablets produced by direct compaction and roller compaction was even more noticeable than in the case of THAP. Direct compaction tablets produced at compression force 12 kN showed tensile strength of 672.0 ± 10.6 N/cm², while tensile strength of tablets produced by roller compaction at pressure of 20 bars was 367.1 ± 3.2 N/cm², and at pressure of 30 bars was 331.8 ± 10.8 N/cm².

Decrease in re-working potential was described in literature as work hardening^{62,64}. Hertig and Kleinebudde 2007,⁶² used the ratio of tensile strength of tablets produced from powder to tensile strength of tablets resulting from granules of the same material to describe the extent of this phenomenon (equation 26).

$$TS_{ratio} = \frac{TS_{granules}}{TS_{powder}} \quad (26)$$

A low *TS* ratio indicates a high loss in compactibility, i.e. a poor re-working potential. THAP granulated at compression pressure of 20 bars (compacted at compression force 12 kN), had a *TS* ratio of 0.91, and the same material compacted at pressure of 30 bars had a ratio of 0.87. According to these results, roller compaction had no significant effect on the re-working potential of THAP and even alteration of roller compaction pressure did not decrease it significantly. In the case of MCC *TS* ratio for material compacted at pressure of 20 bars was 0.55, and at pressure of 30 bars was 0.49. Malkowska and Khan 1983,⁶⁶ studied the effect of slugging on the properties of MCC tablets and they found that re-working potential was decreased as well. In this article it was explained that this phenomenon was probably caused by work hardening, which is defined as the resistance to permanent deformation of material increasing with the amount of deformation⁶⁶. This trend to reduce tensile strength

after roller compaction is well known for plastic material and since that it is more noticed in the case of MCC, it could be considered as more plastic material (see figure 5.65). Although, strength of MCC tablets was decreased by roller compaction, increasing the pressure of compaction did not significantly influence the tensile strength of tablets. Figure 5.59 to figure 5.64 showed that by increasing the amount of MCC in the binary mixtures the difference in tensile strength between tablets produced by direct compression and roller compaction was increased. This could be explained by the fact that plastic deformation of particles during roller compaction introduces a significant amount of defects to the particles.

In the research of Hertig and Kleinebudde 2007,⁶² it is presented that after roller compaction of the mixtures Theophylline and MCC tensile strength is decreased. However, the ratio of Theophylline and MCC in the mixtures affects the changes of tensile strength in the way that increasing of Theophylline in the mixture has a positive effect on work hardening, what is in agreement with the results of this study.

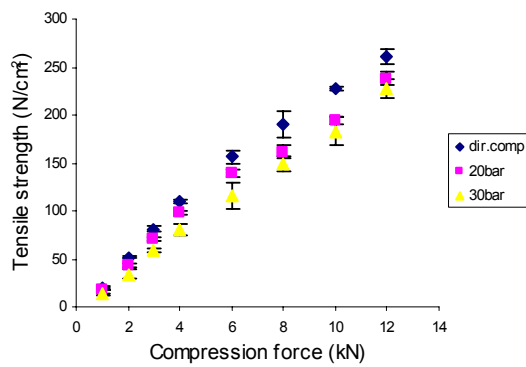


Figure 5.59.: Tensile strength – THAP 100%

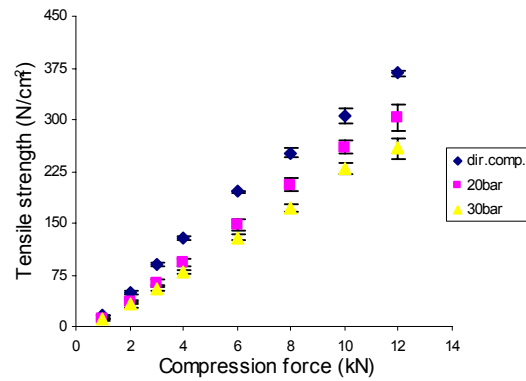


Figure 5.60.: Tensile strength – binary mixture THAP70% +MCC30%

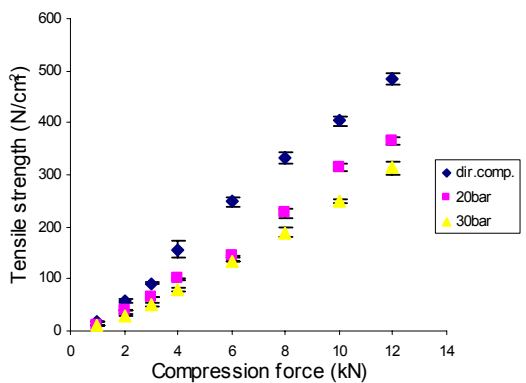


Figure 5.61.: Tensile strength – binary mixture THAP50% + MCC50%

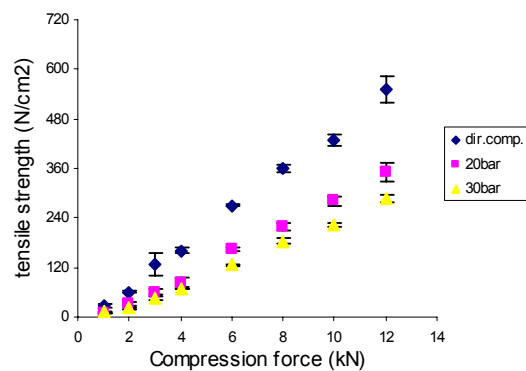


Figure 5.62.: Tensile strength – binary mixture THAP30% + MCC70%

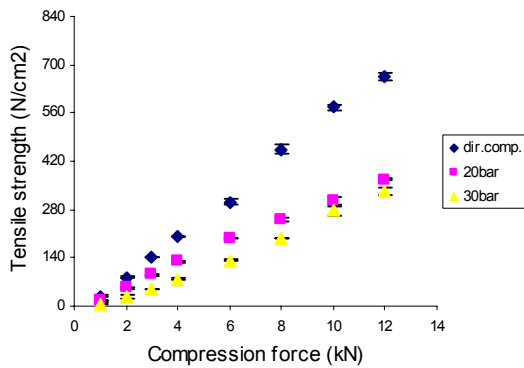


Figure 5.63.: Tensile strength – binary mixture THAP10% + MCC90%

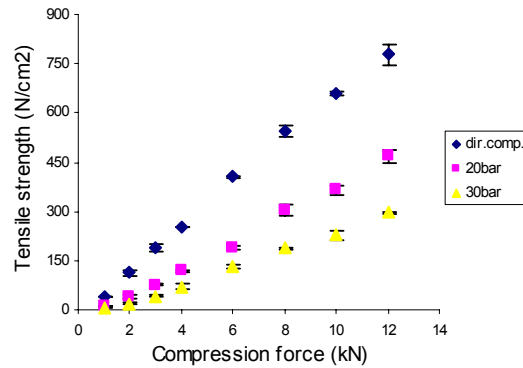


Figure 5.64.: Tensile strength – MCC 100%

If tensile strength of the tablets produced at certain compression force (12 kN) are compared, it could be observed that strength of tablets prepared from mixtures of THAP and MCC was not a simple function of strength of the individual components in the tablets. The values of tensile strength for the powder mixtures of 100%, 70%, 50%, 30%, 10% and 0% of THAP and rest of MCC were 260.6 ± 14.4 N/cm², 367.1 ± 3.2 N/cm², 484.1 ± 11.7 N/cm², 551.75 ± 3.21 N/cm², 778.3 ± 15.3 N/cm² and $665. \pm 10.6$ N/cm², subsequently. It is interesting to note that the mixture of THAP 10% + MCC 90% produced tablets with higher tensile strength than individual material. This phenomenon that tensile strength of tablets produced from the powder mixture is higher than strength of tablets produced from separate components is characteristically for the mixture of two materials which consolidate by different mechanism. Garr and Rubinstein⁶⁷ examined the tabletability of MCC and dicalcium phosphate hydrate mixtures in direct compaction and after slugging. They found that the best tablets were produced within the range of 66 – 99% MCC and 10 – 33% dicalcium phosphate hydrate. It is well known that MCC shows plastic deformation and dicalcium phosphate hydrate brittle behavior under pressure. Results obtained in this study showed the same trend, because the mixture with the best tablets was in this range.

Figure 5.65 showed the effect of different concentration of THAP and MCC in the mixture on tablet tensile strength (direct compaction, roller compaction at pressure of 20 and 30 bars). According to this result and the fact that after roller compaction

tensile strength of THAP was not decreased significantly, it could be hypothesized that THAP consolidated by fragmentation more than plastic deformation.

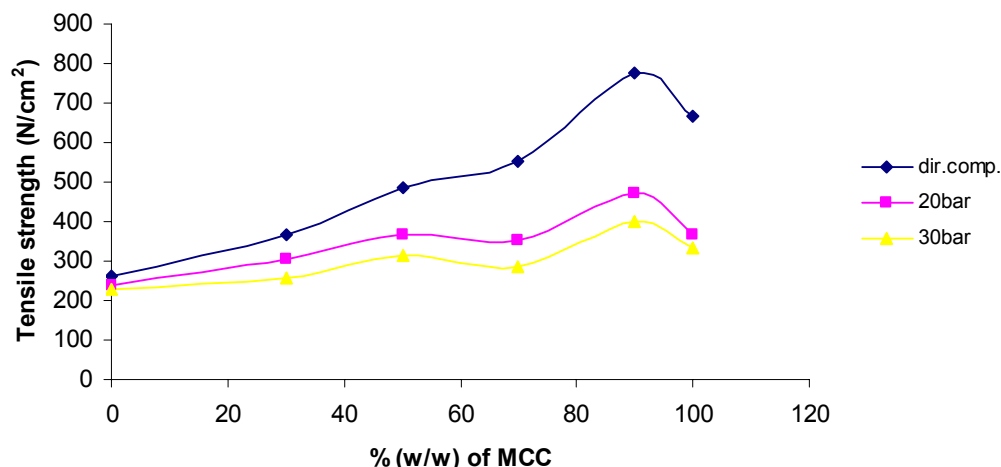


Figure 5.65.: The effect of MCC mass (w/w) on radial tensile strength for THAP/MCC mixtures

Figure 5.65 showed that tensile strength of MCC tablets was significantly decreased after roller compaction, while THAP tablets had almost the same strength either they were prepared by direct compression and roller compaction. Also, in figure 5.65 it is presented that THAP 10% + MCC 90% mixture had highest tensile strength.

THAFP

Analogous to THAP, tensile strength of tablets prepared from THAFP (powder and granules) and binary mixtures with MCC was plotted against the compression force. A linear dependence of tensile strength relating to compression force was observed. Tensile strength of tablets prepared from THAFP at compression force of 12 kN was 233.4 ± 4.5 N/cm², for THAFP granules (20 bars) was 208.4 N/cm². Roller compaction slightly decreased mechanical strength of tablets, however not statistically significant ($p > 0.05$). Comparing this reduction in tablet strength with MCC tablets, it could be observed that THAFP showed different behavior when it was exposed to pressure.

In figure 5.66 to figure 5.71 it could be seen that by increasing amount of MCC in the binary mixture tensile strength was significantly decreased.

It was previously explained that yield pressure P_y from Heckel equation and constant C from modified Heckel equation are measure of the materials plasticity in the way that lower P_y and higher C presents the materials with plastic behavior under pressure. Due to the fact that P_y for THAFP powder was 162.170 ± 1.5 MPa and constant C was $2.1 \pm 0.0 \times 10^{-3}$ MPa, and the same parameters for MCC were 107.2 ± 3.3 MPa and $5.4 \pm 0.6 \times 10^{-3}$ MPa, and since it is well known that MCC shows plastic deformation under pressure, it could be observed that THAFP showed significantly less plastic behavior than MCC.

TS ratio, as measure of re-workability for THAFP was 0.89, what is very high and due to this tensile strength of tablets prepared from granules was not affected by changing the particle size and specific surface area of particles.

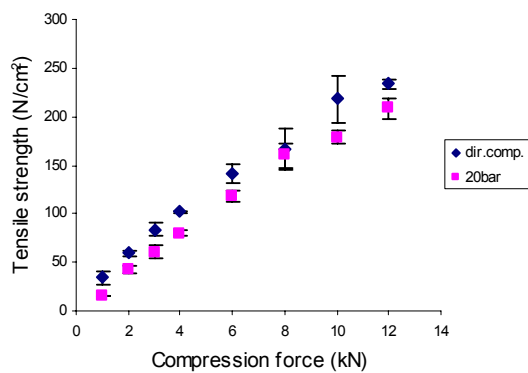


Figure 5.66.: Tensile strength – THAFP 100%

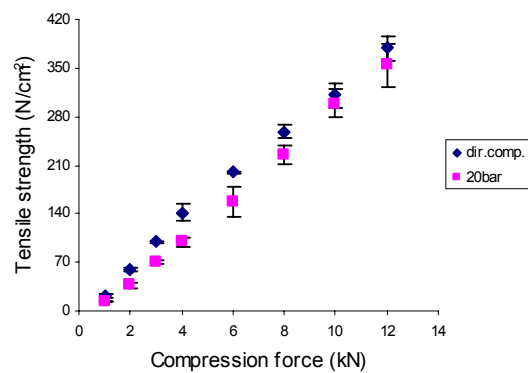


Figure 5.67.: Tensile strength – binary mixture THAFP70% + MCC30%

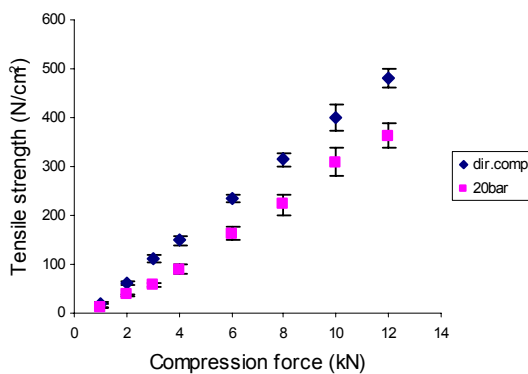


Figure 5.68.: Tensile strength – binary mixture THAFP50% + MCC50%

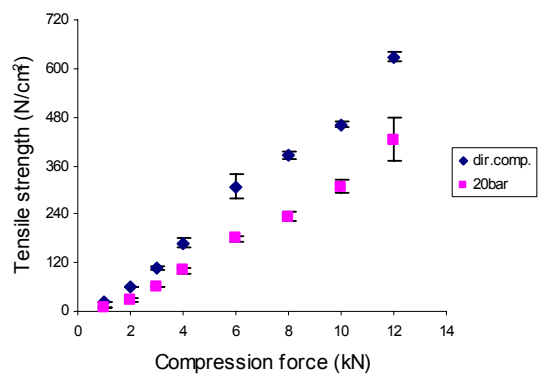


Figure 5.69.: Tensile strength – binary mixture THAFP30% + MCC70%

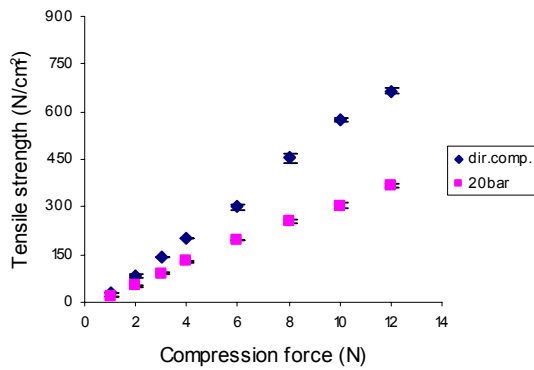


Figure 5.70.: Tensile strength – binary mixture THAFP10% + MCC90%

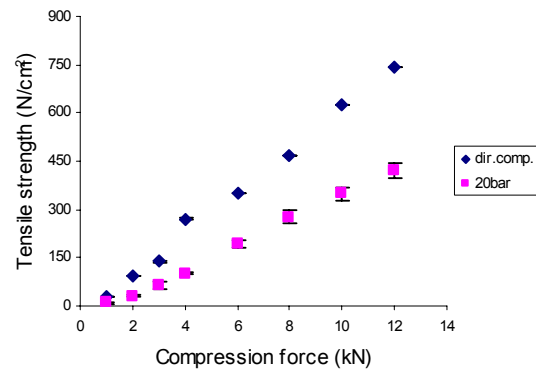


Figure 5.71.: Tensile strength – MCC100%

Tensile strength of the mixture THAFP 10% + MCC 90% was higher than tensile strength of pure MCC (see figure 5.72). The same trend occurred in tablets prepared by direct compaction and roller compaction. In figure 5.66 it could be observed that tensile strength of THAFP appeared to be particle size independent, while the compactibility of MCC decreased by increasing the particle size by roller compaction (see figure 5.71).

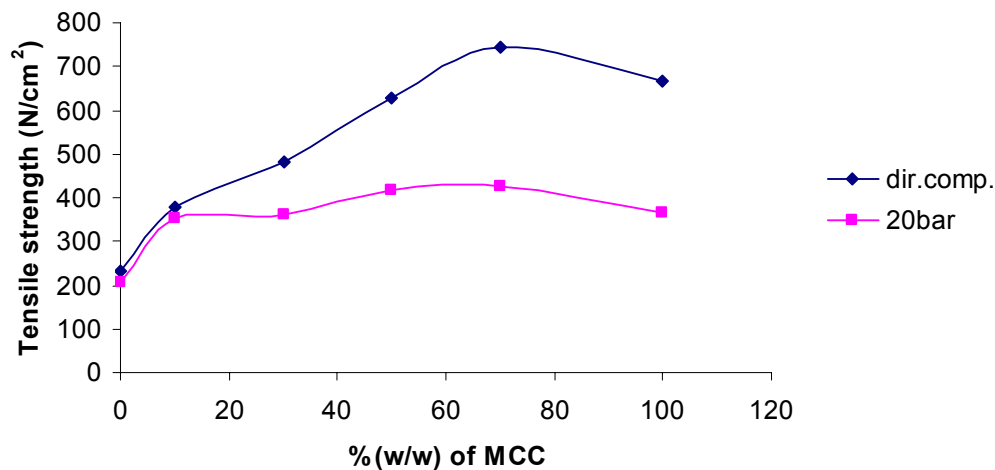


Figure 5.72.: The effect of MCC mass (w/w) on radial tensile strength for THAFP/MCC mixtures

THMO

Tensile strength of THMO tablets was plotted against the compression force and analogous to THAP, THAFP and MCC a linear dependence was found.

Figure 5.73 showed that the difference in tensile strength of THMO tablets produced by direct compression and roller compaction at low compression force (1 – 4 kN) was higher than at high compression force. In contrast to THMO, tablets produced from MCC and binary mixtures composed of MCC, at low compression force, it was shown that tensile strength of tablets produced by two different methods were more similar, than at higher compression force.

Increasing the amount of MCC in the binary mixture the resulted difference was more significant.

TS ratio for tablets produced at compression force of 12 kN (the same as it was calculated for the other materials) was 0.95, but calculated for the force of 4 kN was 0.60.

Sy-Juen Wu and Sun 2007,³⁶ showed that for brittle material there is a critical compaction pressure where particle size started to slightly influence tensile strength of tablets. They were studied different materials and showed that a corresponding critical pressure for Lactose is 100 MPa, for Anhydrous Dibasic Calcium Phosphate is 140 MPa and for Mannitol is 100 MPa. How pressure was increasing differences in tensile strength were bigger. Results obtained for THMO were contradictory to the study of Wu and Sun. The highest difference in tensile strength of THMO tablets produced by direct compaction and roller compaction was at pressure 42.1 MPa, see figure 5.73.

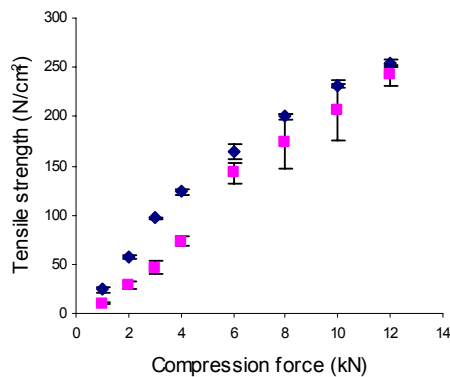


Figure 5.73.: Tensile strength – THMO 100%

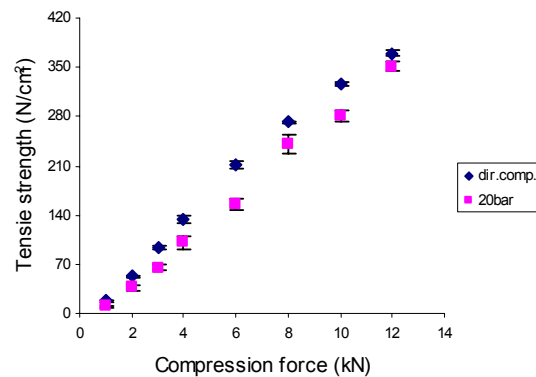


Figure 5.74. Tensile strength – binary mixture THMO70% + MCC30%

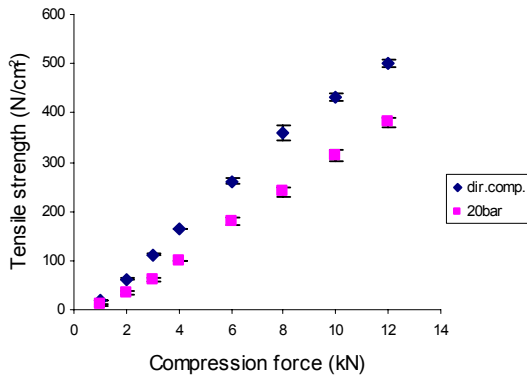


Figure 5.75.: Tensile strength – binary mixture THMO50%+MCC50%

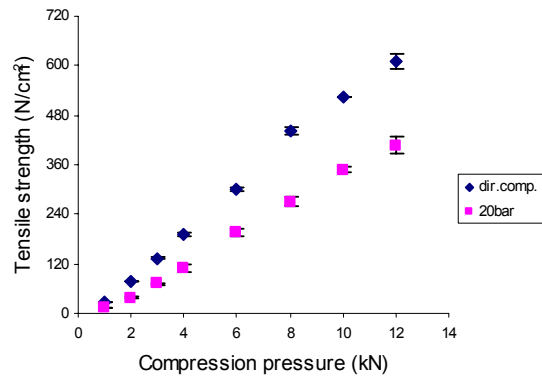


Figure 5.76.: Tensile strength – binary mixture THMO30% + MCC70%

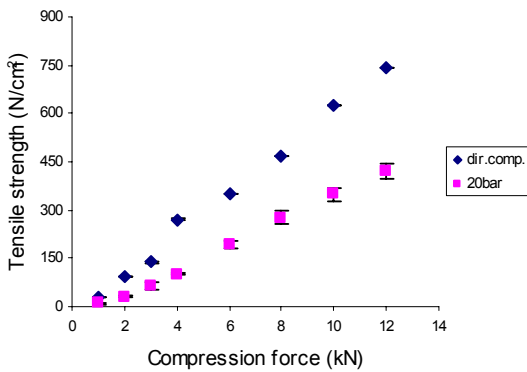


Figure 5.77.: Tensile strength – binary mixture THMO10% + MCC90%

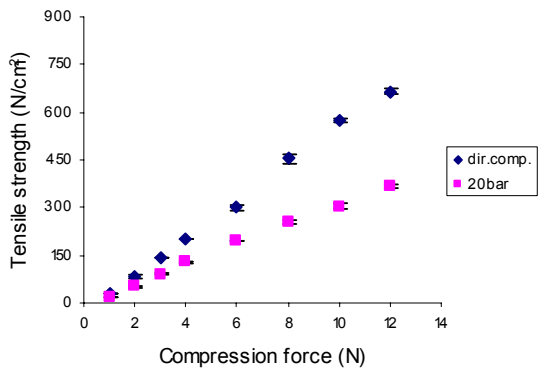


Figure 5.78.: Tensile strength – MCC100%

Binary mixtures of THMO and MCC showed difference in tablet tensile strength of tablets prepared by direct compaction and roller compaction. This difference was increased by increasing the amount of MCC in the mixture. Analogues to THAP and THAFP the binary mixture THMO 10% + MCC 90% showed the highest tensile strength, either tablets produced by direct compaction or roller compaction were examined (see figure 5.77).

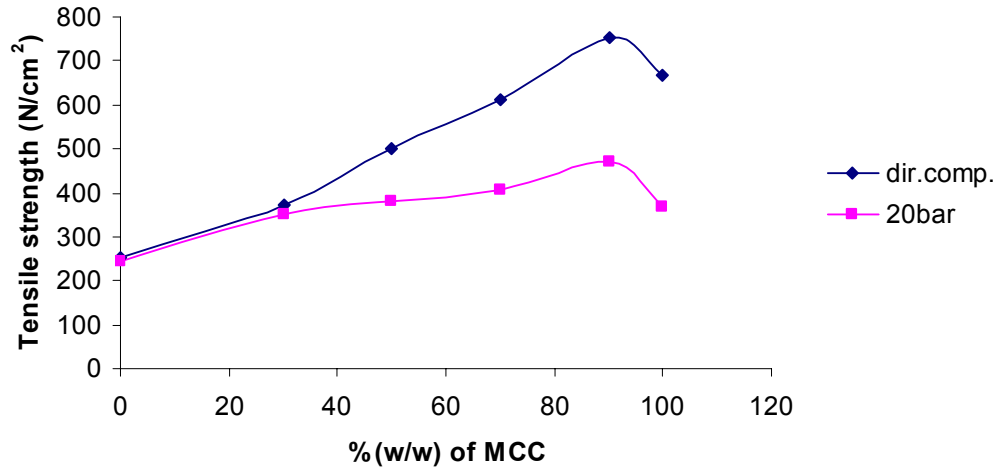


Figure 5.77.: The effect of MCC mass (w/w) on radial tensile strength for THMO/MCC mixtures

5.5.4. Leuenberger Equation - Compressibility and Compactibility

Applying different mathematical equation, in order to check compressibility and compactibility of THAP, THAFP, THMO and MCC powder and granules, obtained results could not entirely characterize the materials. In order to find a correlation with previous methods, Leuenberger equation was applied (equation12).

Radial tensile strength σ_T at certain forming pressure σ_c was plotted against the product of the compression pressure and relative density of tablets, see figure 5.78.

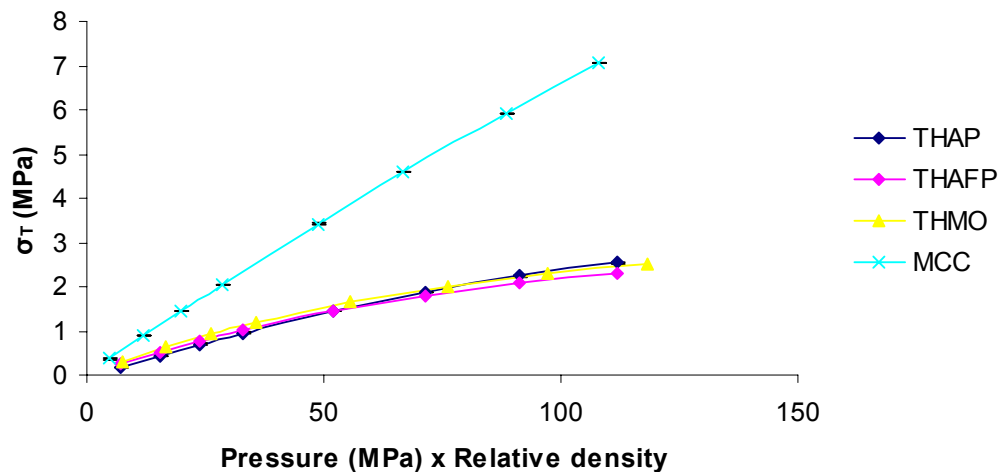


Figure 5.78.: Tensile strength of THAP, THAFP, THMO and MCC according to Leuenberger equation

Figure 5.78 showed that THAP, THAFP and THMO would reach the plateau of the maximal tensile strength at lower compression pressures than MCC. In this figure it could be seen that higher compression pressure should be applied to reach maximal the tensile strength for MCC. This could be confirmed with results in table 5.20.

The parameter σ_{Tmax} is theoretical maximal possible tensile strength for a compact whose porosity is equal to zero and γ compression susceptibility is a specific constant that describes compressibility. Material with low σ_{Tmax} show relatively poor compactibility, and even if high compression pressure is applied this value can not be exceeded. A high γ value means that at low compression pressure maximal tensile strength could be achieved²⁸.

Due to results of σ_{Tmax} , MCC is the most compactable material with extremely high maximum tensile strength of 29.9 ± 1.8 MPa. THAP, THAFP and THMO had a maximal tensile strength of 3.1 ± 0.2 MPa, 3.9 ± 0.6 and 3.9 ± 0.6 MPa respectively, and showed approximately the same compactibility. MCC showed the highest tensile strength σ , what is in agreement with these results.

According to pressure susceptibility parameter, THAP, THAFP and THMO will reach maximal tensile strength much faster than MCC. This could be noted in figure 5.78.

Pressure susceptibility parameter for THAP, THAFP, THMO and MCC were $8.9 \pm 0.0 \times 10^{-3} \text{ MPa}^{-1}$, $11.7 \pm 0.3 \times 10^{-3} \text{ MPa}^{-1}$, and $12.7 \pm 0.0 \times 10^{-3} \text{ MPa}^{-1}$ and $2.5 \pm 0.0 \times 10^{-3} \text{ MPa}^{-1}$, respectively.

Since, constant K of Heckel equation, as well as, compression susceptibility γ describes the compressibility of the materials they should show the same order of magnitude.

If these two constants are compared it could be seen that THAP and THMO showed a higher value K (see table 5.13 and table 5.18) than MCC (see table 5.13), what was in agreement with results of γ . Somehow constant K of THAFP (see table 5.16) was lower than K of MCC and according to γ THAFP is more compressible one.

THAP

Table 5.20.: The compression susceptibility parameter $\gamma \times 10^{-3}(\text{MPa})^{-1}$, and the maximum tensile strength σ_{Tmax} (MPa) of THAP, MCC and their binary mixtures – direct compression

| n=3 ± s.d. | $\gamma \times 10^{-3}$ [MPa ⁻¹] | σ_{Tmax} [MPa] | R ² |
|------------|---|--------------------------|----------------|
| 100% | 8.97 ± 0.06 | 3.170 ± 0.02 | 0.999 |
| 70% | 4.62 ± 0.01 | 8.862 ± 0.02 | 0.998 |
| 50% | 2.66 ± 0.25 | 17.865 ± 0.59 | 0.998 |
| 30% | 3.10 ± 0.26 | 18.214 ± 1.48 | 0.999 |
| 10% | 5.18 ± 0.08 | 17.496 ± 0.25 | 0.999 |
| 0% | 2.45 ± 0.01 | 29.994 ± 1.85 | 0.998 |

Tablets resulting from the binary mixtures of THAP and MCC showed remarkable tensile strength. All mixtures showed maximum tensile strength and pressure susceptibility values in between these parameters of pure THAP and MCC. The mixture THAP 10% + MCC 90% had relatively high value of pressure susceptibility $5.1 \pm 0.1 \times 10^{-3} \text{ MPa}^{-1}$ what is in agreement with the results of Heckel equation and the very high value of constant K . The results of maximal tensile strength indicated that MCC is the most compactable material, but figure 5.79 showed that at certain compression pressure (10.2 - 120.6 MPa) tensile strength of the mixture THAP 10% + MCC 90% was higher. This means that the mixture, with high pressure susceptibility value, will reach the maximum tensile strength significantly faster than pure MCC. If higher compression pressure would be used for this experiment it would be more manifestly when maximal tensile strength is reached. However, even with this pressure range in figure 5.79 it could be observed that the mixture of THAP10% + MCC 90% will reach the maximum tensile strength before MCC. MCC plot is more linear and it needs higher pressures to reach the plateau.

In the literature ⁶ as example of material with good and low compression properties Acetyl salicylic acid and Paracetamol were chosen. The maximum crushing strength and pressure susceptibility of Acetyl salicylic acid were 2.4 MPa and $7.5 \times 10^{-3} \text{ MPa}^{-1}$ and 0.4 MPa and $3.5 \times 10^{-3} \text{ MPa}^{-1}$ for Paracetamol.

According to these results and value of σ_{Tmax} and γ , shown in table 5.20, all examined materials suppose to be used in direct compression.

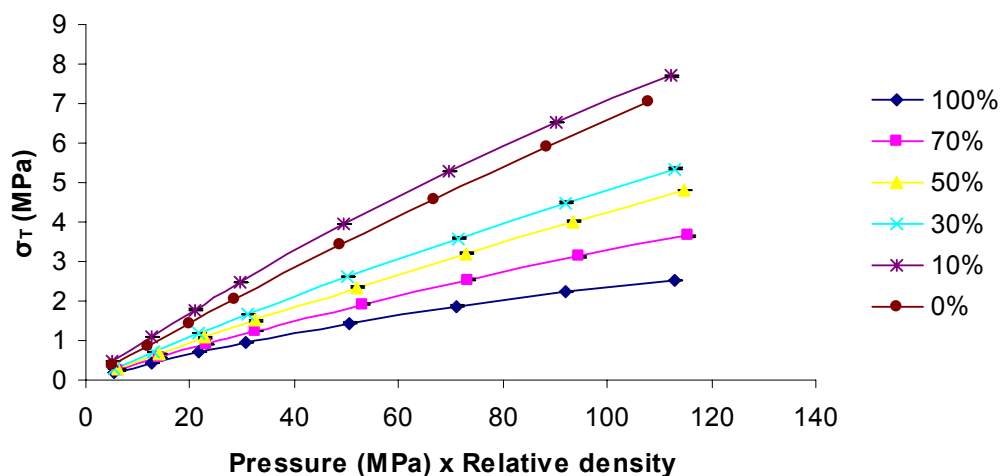


Figure 5.79.: Tensile strength of THAP and MCC binary mixtures (Leuenberger equation)

Maximal tensile strength and pressure susceptibility parameter of THAP tablets produced by direct compaction were 3.1 ± 0.2 MPa and $8.9 \pm 0.2 \times 10^{-3}$ MPa⁻¹; tablets produced by roller compaction at pressure of 20 bars were 3.9 ± 0.0 MPa and $7.8 \pm 0.1 \times 10^{-3}$ MPa⁻¹ and for THAP compacted at pressure of 30 bars 2.8 ± 0.1 MPa and $8.2 \pm 0.2 \times 10^{-3}$ MPa⁻¹. According to these results it could be observed that all three materials at very similar compression pressure will reach almost the same maximal tensile strength.

Roller compaction did not significantly change compressibility and compactibility of THAP. Results obtained by Heckel and modified Heckel equation, as well as tensile strength measurements were in agreement with this.

In contrary to THAP, compressibility and compactibility parameters of MCC were changed after roller compaction. Maximal tensile strength and pressure susceptibility of MCC tablets produced by direct compression were 29.9 ± 1.8 MPa and $2.4 \pm 0.0 \times 10^{-3}$ MPa⁻¹, while the same parameters of tablets produced by roller compaction were $7.5 \pm$ MPa and 5.9×10^{-3} MPa⁻¹. Maximal tensile strength, which compact could reach when it has zero porosity, was extremely decreased. In the same time according to the fact that pressure susceptibility was increased, that tensile strength could be achieved at lower compression pressures. Figure 5.80 and figure 5.81 showed radial tensile strength THAP and MCC tablets (direct compaction and roller compaction) plotted against the product of compression pressure and relative density of the

compacts. It could be noted that compacts produced from powder by direct compaction showed a higher crushing strength at certain pressure than tablets prepared from the granules. The differences in crushing strength are more remarkable in the case of MCC than THAP.

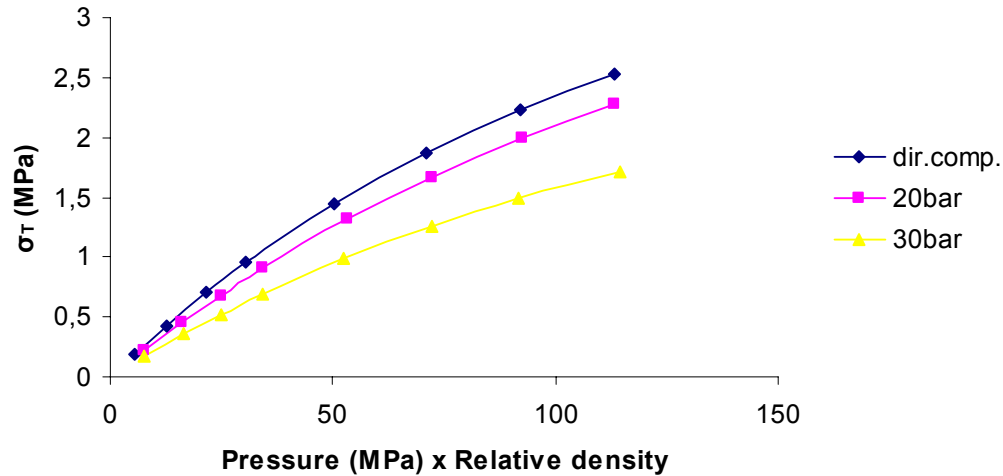


Figure 5.80.: Tensile strength of THAP tablets (direct compaction and roller compaction)

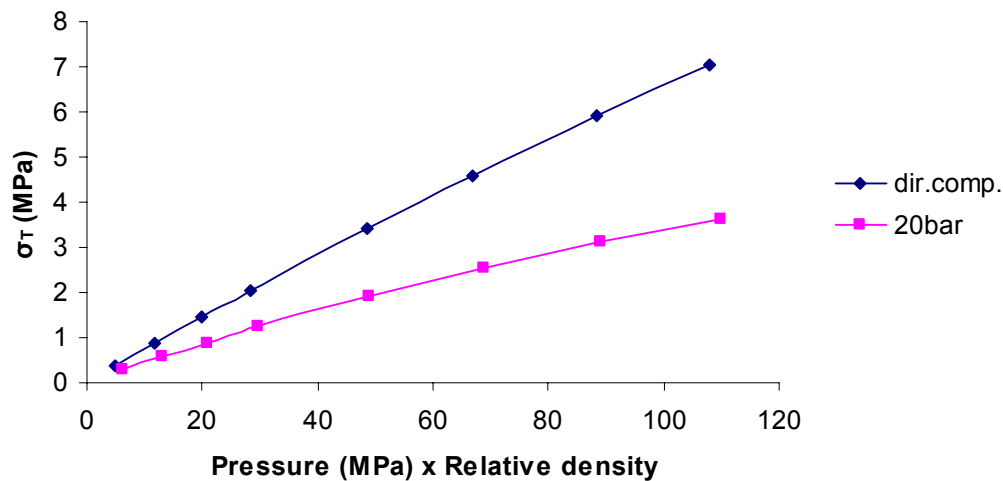


Figure 5.81.: Tensile strength of MCC tablets (direct compaction and roller compaction)

Fitting of the plot obtained by Leuenberger equation was done by nonlinear regression. Due to the fact that the used pressure range for producing tablets was

not enough high to reach plateau for tensile strength, results of the binary mixtures tablets produced by roller compaction could not be evaluated by this equation. During the calculation of maximal tensile strength and pressure susceptibility parameters by Mathematica 5.2 program due to insufficient applied pressure to get adequate nonlinear regression mistake was occurred and accuracy of the results was not appropriate. Because of these problems, results for the tablets prepared by roller compaction are not presented.

THAFP

Table 5.21.: The compression susceptibility parameter $\gamma \times 10^{-3}(\text{MPa})^{-1}$, and the maximum tensile strength σ_{Tmax} (MPa) of THAFP, MCC and their binary mixtures – direct compression

| n=3 ± s.d. | $\gamma \times 10^{-3}$ [MPa ⁻¹] | σ_{Tmax} [MPa] | R ² |
|------------|---|--------------------------|----------------|
| 100% | 11.78 ± 0.00 | 3.97 ± 0.06 | 0.999 |
| 70% | 5.78 ± 0.36 | 7.82 ± 0.42 | 0.999 |
| 50% | 2.24 ± 0.26 | 21.49 ± 2.26 | 0.999 |
| 30% | 2.10 ± 0.26 | 22.61 ± 2.63 | 0.997 |
| 10% | 3.02 ± 0.04 | 25.42 ± 0.39 | 0.999 |
| 0% | 2.45 ± 0.01 | 29.99 ± 1.85 | 0.998 |

As amount of MCC in the binary mixture was increased, maximal tensile strength was increased as well, and in the same time pressure susceptibility was decreased. This leads to the conclusion that MCC was responsible for compactibility and THAFP for compressibility of the tablets.

Maximal tensile strength and pressure susceptibility of THAFP tablets prepared by direct compaction were 3.9 ± 0.6 MPa and $11.7 \pm 0.0 \times 10^{-3}$ MPa⁻¹; and for tablets prepared by roller compaction were 3.7 ± 0.1 MPa and $7.3 \pm 0.3 \times 10^{-3}$ MPa⁻¹, respectively. According to these results it could be noted that during roller compaction compactibility was not changed while compressibility was decreased. The same maximal tensile strength which could be attained in compact with zero porosity for tablets prepared by direct compression may be reached with the lower compression pressure than tablets produced by roller compaction. *K* value of Heckel equation for THAFP after roller compaction was slightly reduced (see table 5.16 and table 5.17) while tensile strength of the tablets with and without roller compaction was

almost the same (see figure 5.66). This is in conformity with the results obtained by Leuenberger equation, where pressure susceptibility-compressibility index was decreased and maximal tensile strength-compactibility index was almost unchanged. Even if compactibility was reduced after roller compaction, THAFP granules still have a very good compressibility and compactibility characteristics.

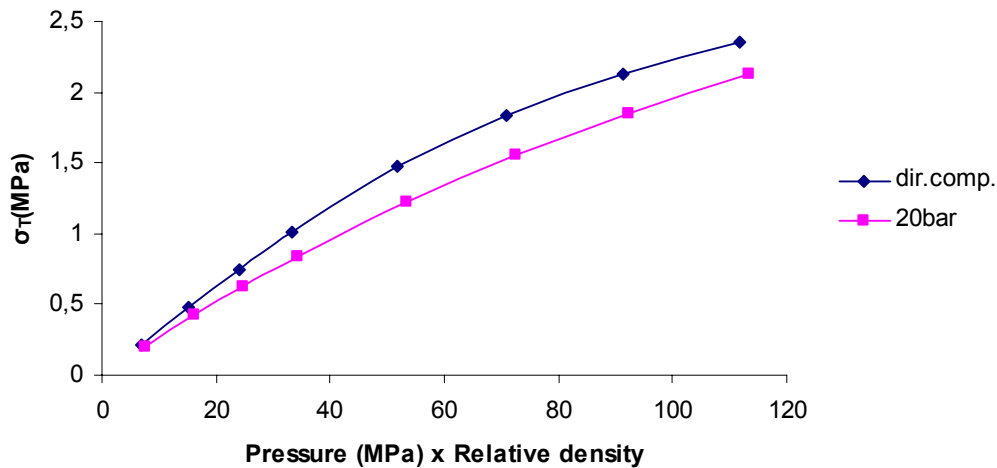


Figure 5.82.: Tensile strength of THAFP tablets (direct compaction and roller compaction)

Table 5.21 showed that maximal tensile strength and pressure susceptibility of the binary mixtures were between these parameters for THAFP and MCC. Even if MCC had a higher maximal tensile strength than binary mixture THAFP 10% + MCC 90%, Figure 93 showed that at certain pressure range (10.2 - 120.6 MPa) that the mixture had higher tensile strength σ_T . Important is that MCC could reach a higher tensile strength (29.9 ± 1.8 MPa) when compacts with zero porosity are produced from both materials, but the mixture THAFP 10% + MCC 90% can reach maximal tensile strength (25.4 ± 0.6 MPa) at lower compression pressure. These results are in agreement with the results of Heckel equation and tensile strength, and means that MCC is more compactable (see table 7.4, Appendix) and the mixture THAFP 10% + MCC 90% is more compressible (see table 5.16).

The binary mixtures of THAFP and MCC granules could not be evaluated by Leuenberger equation, due to the same reason as THAP. Non linear regression did not fit to the results and error occurred.

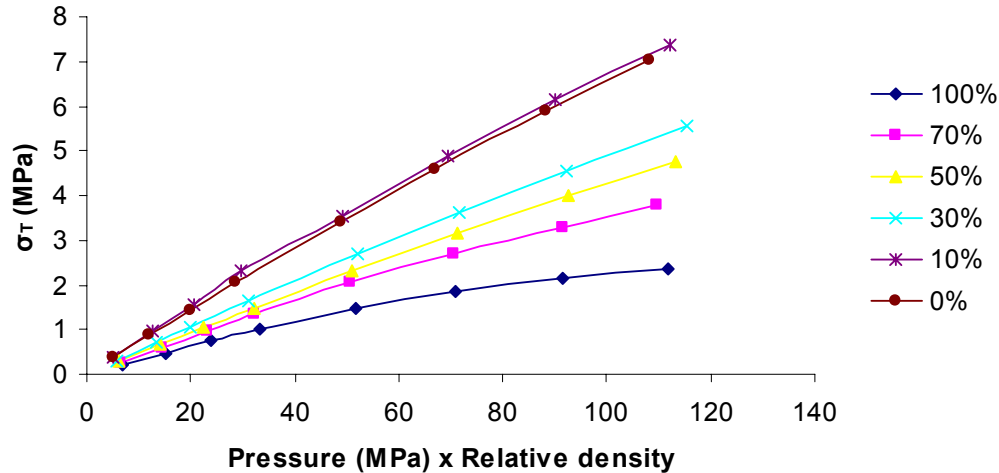


Figure 5.83.: Tensile strength of THAFP and MCC binary mixtures (Leuenberger equation)

THMO

Table 5.22.: The compression susceptibility parameter $\gamma \times 10^{-3}(\text{MPa})^{-1}$, and the maximum tensile strength σ_{Tmax} (MPa) of THMO, MCC and their binary mixtures – powder

| n=3 ± s.d. | $\gamma \times 10^{-3}$ [MPa ⁻¹] | σ_{Tmax} [MPa] | R ² |
|------------|---|--------------------------|----------------|
| 100% | 12.79 ± 0.00 | 3.25 ± 0.00 | 0.999 |
| 70% | 5.49 ± 0.00 | 7.96 ± 0.01 | 0.999 |
| 50% | 3.82 ± 0.14 | 14.24 ± 0.34 | 0.999 |
| 30% | 3.78 ± 0.12 | 17.76 ± 0.53 | 0.999 |
| 10% | 5.31 ± 0.06 | 16.89 ± 0.17 | 0.999 |
| 0% | 2.45 ± 0.01 | 29.99 ± 1.85 | 0.998 |

Analogues to THAP and THAFP, THMO had higher pressure susceptibility than MCC, while MCC has extremely higher maximal tensile strength. Value of pressure susceptibility parameter for THMO indicating that maximal tensile strength could be achieved at low compression pressure. Maximal tensile strength and pressure susceptibility of THMO powder were 3.2 ± 0.0 MPa and $12.7 \pm 0.0 \times 10^{-3}$ MPa⁻¹; the same parameters for THMO granules were 2.1 ± 0.0 MPa and $11.3 \pm 0.4 \times 10^{-3}$ MPa⁻¹. According to these results compressibility and compactibility of THMO after roller compaction were slightly decreased (see figure 5.84). In contrast to these results, constant K of Heckel equation after roller compaction was increased from 10.7 ± 0.2

$\times 10^{-3}$ MPa (see table 5.18) to $12.2 \pm 0.8 \times 10^{-3}$ MPa (see table 5.19). Heckel equation showed that compressibility of THMO after roller compaction was improved comparing to powder, however Leuenberger equation gave a contradictory result. In the previous chapter it was discussed that sometimes different mathematical equation could give different results and could lead to different conclusion. Maximal tensile strength after roller compaction was decreased, but not significantly and this is in agreement with results of tensile strength (see table 7.6 and table 7.7, Appendix).

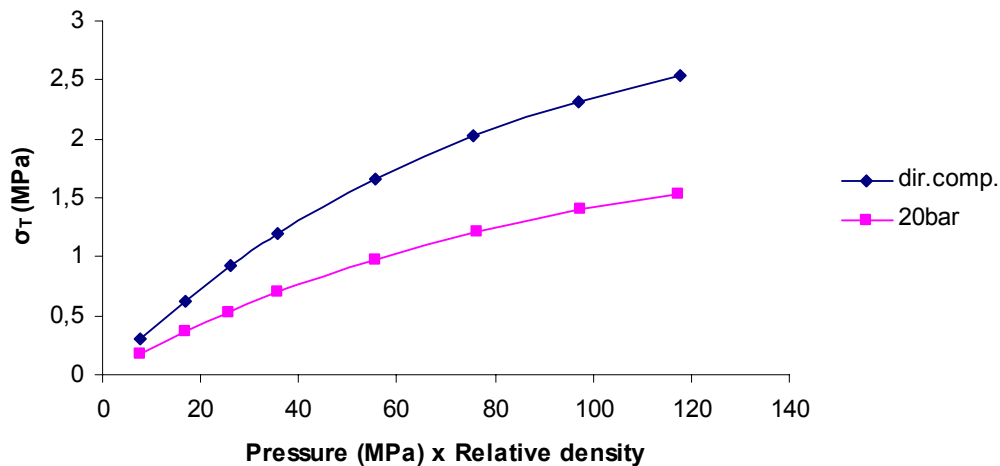


Figure 5.84.: Tensile strength of THMO tablets (direct compaction and roller compaction)

Nevertheless, maximal tensile strength of the binary mixture THAP 30% + MCC 70% was higher (17.7 MPa) than maximal tensile strength of the mixture THAP 10% + MCC 90% (16.8 MPa), tensile strength of the second mixture at certain compression pressure was much higher (see figure 5.85). Due to higher pressure susceptibility (5.3×10^{-3} MPa) the mixture THAP 10% + MCC 90% at lower compression pressure will reach the maximal tensile strength than mixture THAP 30% + MCC 70% (3.7×10^{-3} MPa). Observing maximal tensile strength and pressure susceptibility of the whole mixtures and individual powders (see table 5.22) THMO was the most compressible and MCC most compactable material. These results are not in agreement with Heckel, modified Heckel equation (see table 5.19) and tensile strength value (see table 7.6, Appendix), where the mixture THAP 10% + MCC 90% was the most compressible and the most compactable material.

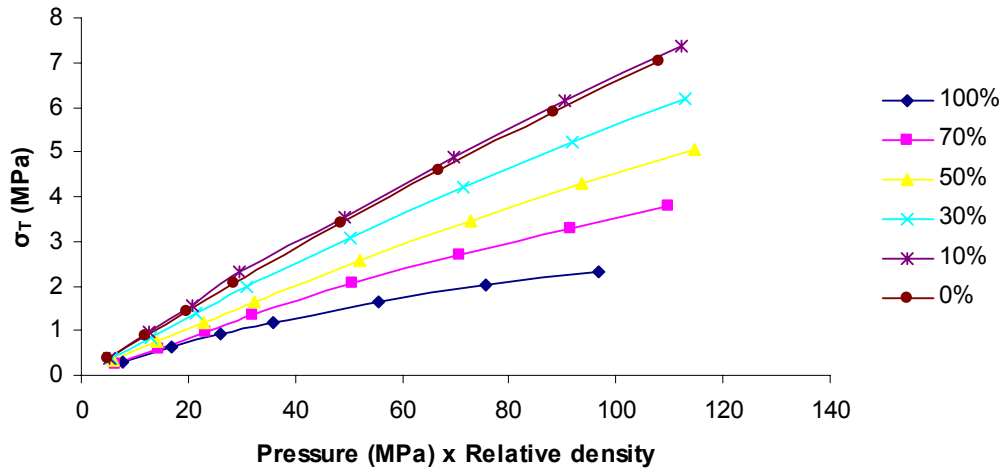


Figure 5.85.: Tensile strength of THMO and MCC binary mixtures (Leuenberger equation)

5.5.5. Disintegration time

In many cases fast disintegration of tablets is the first step of reaching high bioavailability of drugs, especially low water soluble drugs. Disintegration time can be influenced by the addition of a certain amount of tablet disintegrants ²⁸.

Table 5.23.: Experimentally determined values of disintegration time of the binary mixtures THAP/MCC

| % THAP in the binary mixture (w/w) | Disintegration time [min] n=6 ± s.d. | | |
|--|--|--------------|---------------|
| | Direct compression | 20 bar | 30 bar |
| 100% | 89.47 ± 16.49 | 71.47 ± 3.25 | 58.70 ± 15.56 |
| 90% | 48.98 ± 4.26 | 42.78 ± 3.74 | 35.25 ± 5.62 |
| 80% | 0.19 ± 0.01 | 0.14 ± 0.06 | 0.11 ± 0.02 |
| 70% | 0.30 ± 0.06 | 0.22 ± 0.08 | 0.13 ± 0.01 |
| 50% | 0.49 ± 0.29 | 0.26 ± 0.03 | 0.18 ± 0.01 |
| 30% | 5.41 ± 3.45 | 0.39 ± 0.06 | 0.20 ± 0.01 |
| 10% | 11.07 ± 4.34 | 0.58 ± 0.31 | 0.23 ± 0.02 |
| 0% | 11.64 ± 0.57 | 1.42 ± 0.09 | 0.32 ± 0.03 |

Disintegration time of THAP tablets produced by direct compaction and roller compaction at pressure of 20 and 30 bars was very slow because Theophylline has no any disintegrant properties and tablets were more dissolvable. Due to disintegration property of MCC, adding a certain amount of MCC improved the disintegration time of THAP tablets. Table 5.23 showed that the critical amount of MCC to improve disintegration significantly was 20% either using direct compaction or roller compaction.

If disintegration time of tablets produced by direct compaction and roller compaction are compared it was obvious that in the case of roller compaction disintegration time was extremely faster. This could be explained by the fact that tablets produced by roller compaction disintegrated to granules very fast and tablets produced direct compression were more dissolvable. Increasing a content of THAP in the binary mixture with MCC, differences in disintegration time of tablets prepared by direct compaction and roller compaction was decreased. Increasing the compaction

pressure during roller compaction from 20 to 30 bars slightly improved disintegration, but this was not significant as it was in the case of direct compaction.

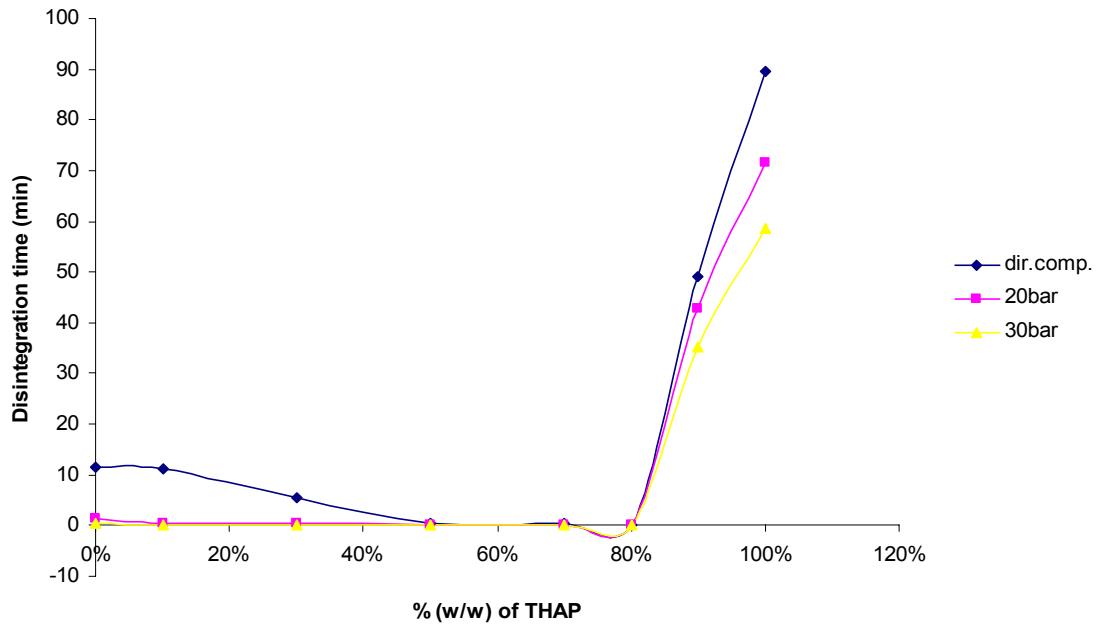


Figure 5.86.: Disintegration time of the binary mixtures THAP/MCC

THAFP

Table 5.24.: Experimentally determined values of disintegration time of the binary mixtures THAFP/MCC

| % THAFP in the binary mixture (w/w) | Disintegration time [min] n=6 ± s.d. | |
|---|--|--------------|
| | Direct compression | 20 bar |
| 100% | 95.56 ± 5.24 | 87.04 ± 5.57 |
| 90% | 57.25 ± 9.05 | 41.31 ± 2.31 |
| 80% | 1.14 ± 0.73 | 0.16 ± 0.13 |
| 70% | 0.97 ± 0.03 | 0.18 ± 0.03 |
| 50% | 1.12 ± 0.56 | 0.22 ± 0.03 |
| 30% | 2.01 ± 0.30 | 0.25 ± 0.03 |
| 10% | 4.96 ± 0.50 | 0.37 ± 0.09 |
| 0% | 11.64 ± 0.57 | 1.42 ± 0.09 |

Analogous as THAP, tablets produced from individual THAFP had very slow disintegration time due to the same reason that was previously explained. Disintegration time for direct compacted and roller compacted THAFP tablets were 95.56 and 87.04 minutes, respectively. According to smaller particle size (see table 5.3) of the original powder, tablets made from THAFP suppose to have faster disintegration time than THAP tablets. Results presented in table 5.23 and table 5.24 showed the contrary situation. In the chapter 5.1.4 it was explained that during the storage and transport, and due to very small particle size of THAFP the material was agglomerated and even after the sieving step it was impossible to separate the particles. MCC significantly influenced disintegration time and in the case of tablets prepared by direct compression this influence was extremely obvious when 20% and more of MCC was added to THAFP.

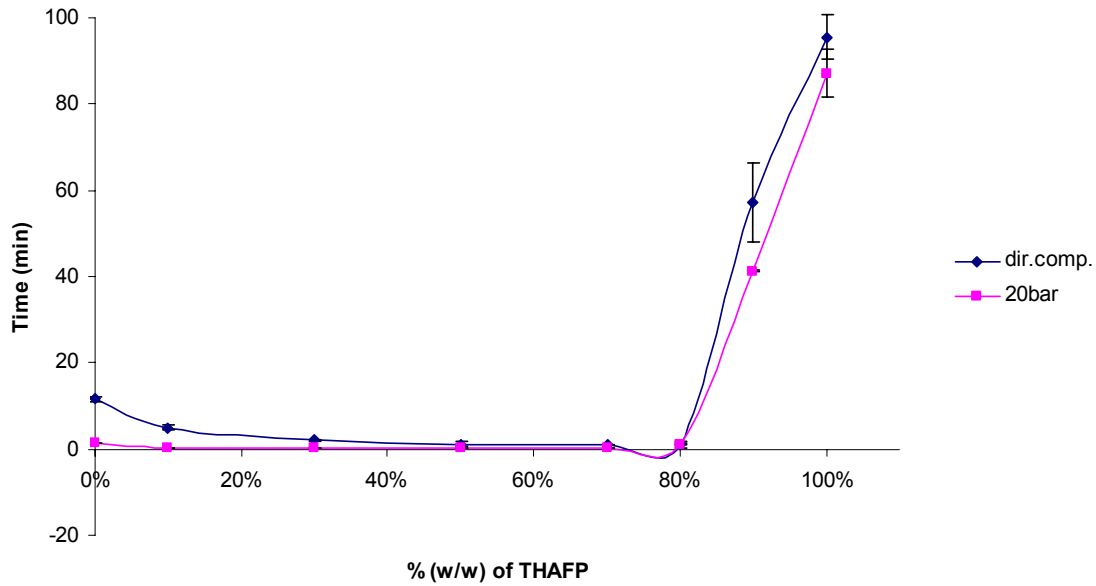


Figure 5.87.: Disintegration time of the binary mixtures THAFP/MCC (direct compaction and roller compaction)

Table 5.24 and figure 5.87 showed that the fastest disintegration time was achieved with the mixture THAFP 70% + MCC 30%. After this critical concentration of MCC, disintegration time slowly started to increase, and in the case of the mixture containing 90% of THAFP and 10% MCC it was very slow. Analogues to THAP, disintegration time of tablets prepared by direct compaction was various upon the concentration of MCC, while roller compacted tablets had very similar disintegration time for all mixtures except one with 10% of MCC. These differences in the case of tablets produced by roller compaction were not significant, because disintegration of all the mixtures was extremely fast.

THMO

Table 5.25.: Experimentally determined values of disintegration time of the binary mixtures THMO/MCC

| % THMO in the binary mixture (w/w) | Disintegration time [min] n=6 ± s.d. | |
|--|--|---------------|
| | Direct compression | 20 bar |
| 100% | 87.63 ± 6.37 | 75.52 ± 6.37 |
| 90% | 48.22 ± 6.13 | 47.00 ± 11.34 |
| 80% | 1.34 ± 0.87 | 0.20 ± 0.02 |
| 70% | 2.88 ± 2.29 | 0.34 ± 0.77 |
| 50% | 3.09 ± 1.30 | 0.59 ± 0.10 |
| 30% | 3.29 ± 0.59 | 0.62 ± 0.07 |
| 10% | 5.43 ± 0.34 | 1.05 ± 0.25 |
| 0% | 11.64 ± 0.57 | 1.42 ± 0.09 |

Disintegration time of the tablets prepared from the binary mixtures THMO and MCC was significantly improved after roller compaction (see table 5.25). In an equivalent way as THAP and THAFP after roller compaction tablets disintegrated to granules very fast, since tablets produced by direct compaction did not show this phenomenon. Pure THMO tablets even after roller compaction had very slow disintegration time, almost the same as the tablets prepared by direct compaction. This was due to the properties of THMO, which was dissolving more than disintegrated. Analogues to THAP and THAFP, by adding MCC in tablets disintegration time was extremely increased. The fastest disintegration time was achieved with the mixture of THMO 80% + MCC 20% for both techniques. This mixture had disintegration time for tablets prepared by direct compaction of 1.3 ± 0.8 min and tablets prepared by roller compaction 0.20 ± 0.0 min. By decreasing the amount of MCC from 20% to 10% disintegration time was extremely reduced, 48.2 ± 6.1 min and 47.0 ± 11.3 min, respectively.

Changing the concentration of MCC and Theophylline (THAP, THAFP and THMO), regardless it was decreased or increased disintegration time was reduced, but differences which were obtained by increasing the amount of MCC from 20% to 80 % were not significant. This phenomenon showed that 20% of MCC was critical concentration regarding disintegration time of the tablets.

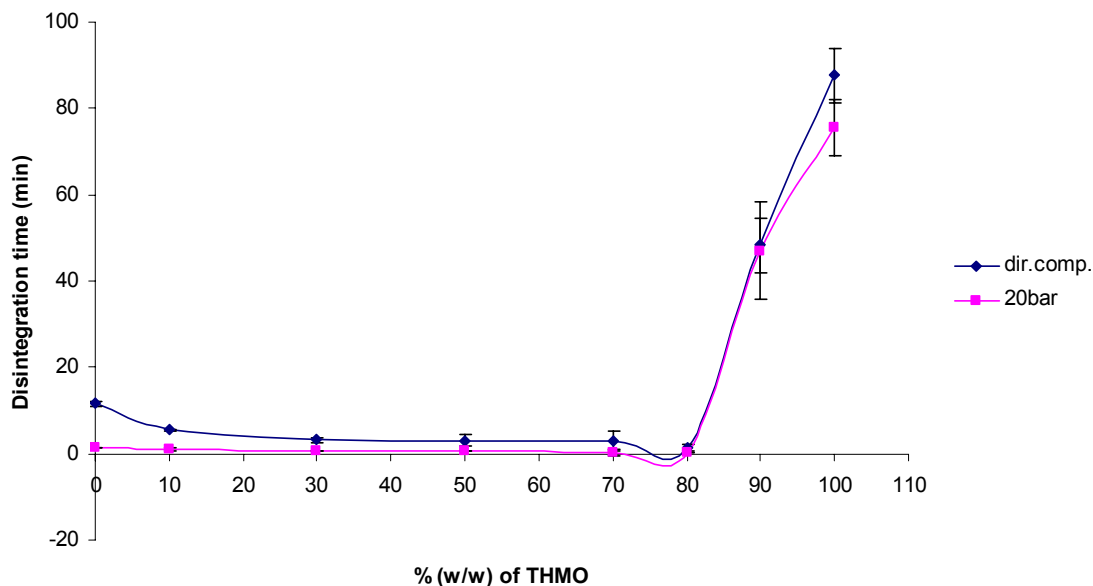


Figure 5.88.: Disintegration time of the binary mixtures THMO/MCC

5.5.5. Dissolution Rate

Evaluation of dissolution rates of drug is very important in the development, formulation and quality control of pharmaceutical dosage forms. Such evaluation is especially important in the case of polymorphic systems. In this case bioavailability variation may arise from difference in solubility. In the present study measurement of dissolution rate was carried out in order to check influence of roller compaction process on the properties of tablets as well as presence of different pseudo polymorphs and different particle size of the same polymorphs. Due to the fact that dissolution rate is very dependent on tablet porosity, special attention was dedicated to production of tablets (direct compaction and roller compaction) with the constant porosity of 12 ± 0.5 % (see chapter 4.6.). Differences in true density which was presented in Chapters Characterization of The Binary Mixtures and Characterization of Granules (see chapter 4.2.1 and chapter 4.5) had a key role in tablet porosity.

Dissolution rate is influenced by particle size in the way that small particles indicate a high dissolution rate. This is due to fact that small particles have a high specific surface area exposed to the solvent, allowing a greater number of particles to dissolve more rapidly.

According to the phenomenon mentioned above dissolution rate of THAFP was higher than dissolution rate of THAP. However, taking into account that particle size of THAP was much higher (see table 5.3) than particle size of THAFP, dissolution rate was not much influenced by particle size (see figure 5.91). Montel et al ⁶⁸ showed that Theophylline with very small particle size had lower dissolution rate than one with higher particle size. They proved by microscopy studies the presence of agglomerates in the tablet with the smallest particle size. In general, agglomerated particles are undesirable because they reduce the surface area leading to the slower dissolution rate. SEM images (see figure 5.3 and figure 5.4) and results of specific surface area (see table 5.3) showed that THAFP was agglomerated. Even after sieving it was impossible to get separated particles.

It has been noted from the earliest dissolution work that for many substances the dissolution rate of an anhydrous form exceeds the corresponding hydrate. This observation was explained by thermodynamics, were it was reasoned that the drug in the hydrates form possessed a lower activity and it would be more stable than corresponding anhydrate form.

During dissolution Theophylline anhydrate underwent a transformation to monohydrate. Aaltonenon 2007, ⁶⁹ showed that this transformation started almost immediately after the tablets are exposed to water, see figure 5.89. The dissolution rate of the initially anhydrous Theophylline decreased as the amount of monohydrate form occurred. Figure 5.90 shows that during transformation dissolution of both forms occur. Consequently, the larger the amount of monohydrate, the slower dissolution rate and once the transformation is complete dissolution rate becomes constant (6 min, see figure 5.90) ⁶⁹.

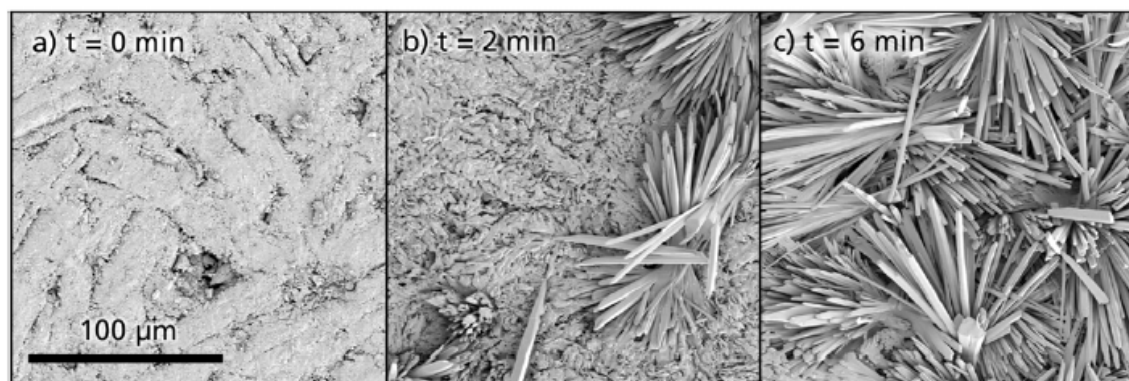


Figure 5.89.: SEM images of Theophylline anhydrate tablet during dissolution ⁶⁹.

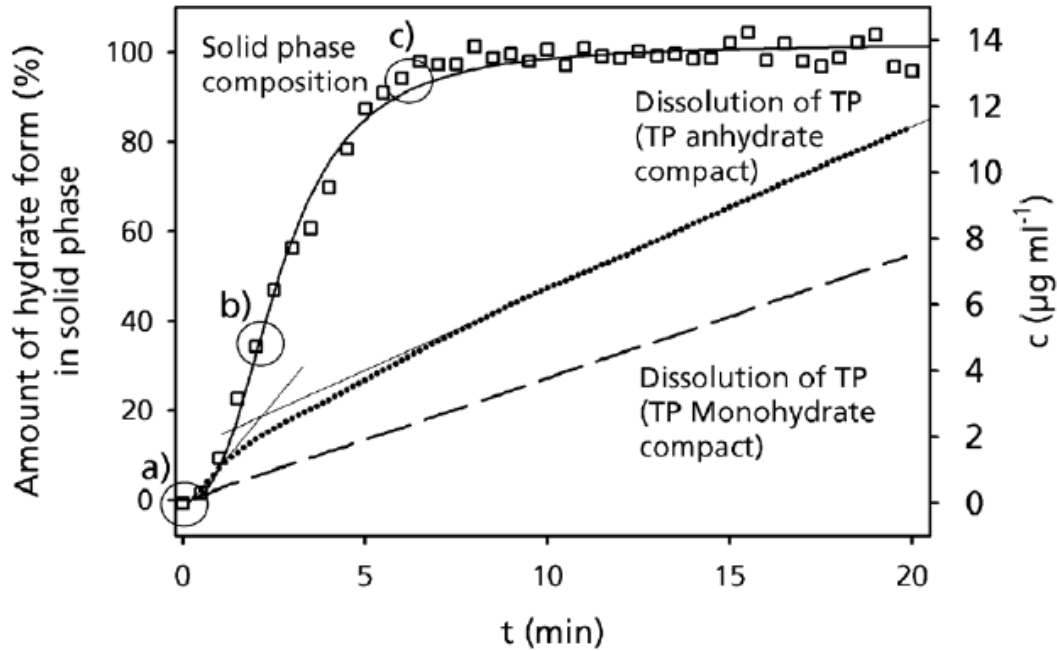


Figure 5.90.: Dissolution rate of Theophylline anhydrate and Theophylline monohydrate tablets as time points ⁶⁹

Results obtained in this study showed that dissolution rate of THMO was slightly lower than dissolution rate of THAP and THAFP, even anhydrate still was transformed to monohydrate. It is shown (see figure 5.3) that after 6 minutes all anhydrate form was transformed to monohydrate. However, as sampling in this study was done every 5 minutes it means that during whole dissolution measurement Theophylline was in the monohydrate form. Differences in dissolution rate between THAP, THAFP and THMO could be explained by differences in particles shape and specific surface area of THMO (see figure 5.5) and monohydrate which was obtained by monohydrate crystal growth on the initially anhydrous surface (see figure 5.89).

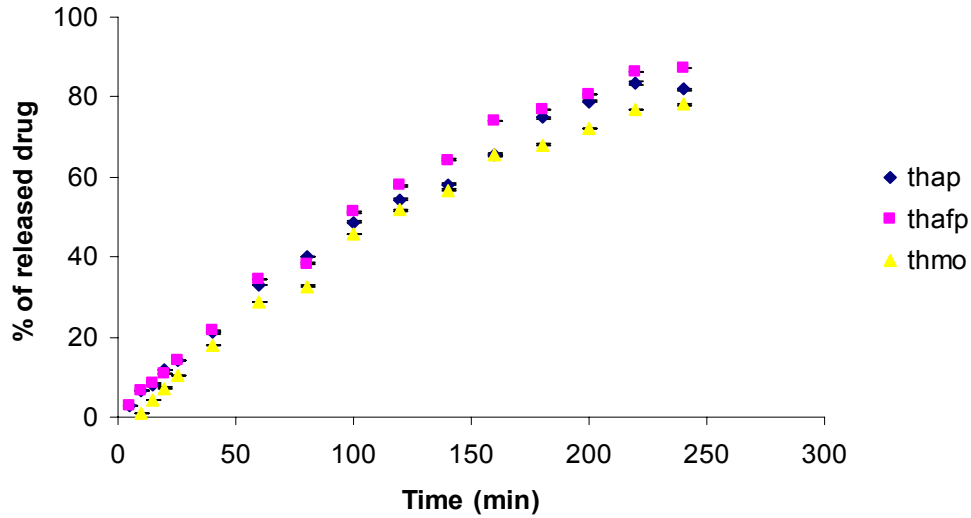


Figure 5.91.: Dissolution rate THAP, THAFP and THMO

THAP

Although, it was shown that THAP tablets had a very slow dissolution rate, adding a certain amount of MCC in the tablets extremely improved dissolution. Increasing content of MCC in the binary mixtures, dissolution rate became higher. This phenomenon can be explained by disintegration property of MCC. Tablets contained MCC disintegrated very fast (see table 5.23) allowing fast release of Theophylline from the tablets. In the case of tablets made from the pure Theophylline there is no any disintegration, they are gradually dissolved and dissolution rate was very slow - 200 min.

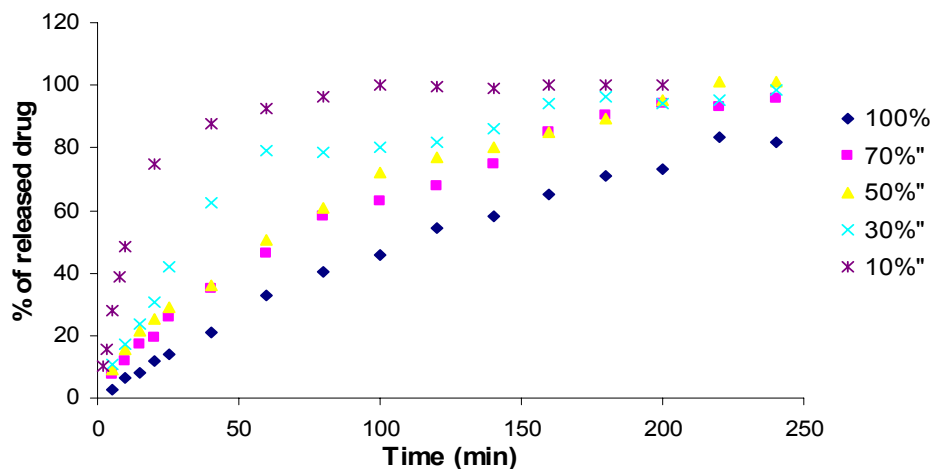


Figure 5.92.: Dissolution rate of the binary mixtures THAP/MCC

Figure 5.93 to figure 5.98 showed the effect of roll compaction on dissolution rate of THAP. The USP requirement for drug release from Theophylline tablets is: not less than 80% of drug has to be released in 45 minutes⁷⁰. The amount of the drug which complied with USP requirement was released from tablets produced by direct compaction in the binary mixtures in the range 100%, 70%, 50%, 0% and 10% of THAP and the rest of MCC at the following time points: 200 min, 160 min, 140 min, 100 min and 40 minutes, respectively. The tablets produced by roller compaction at pressure of 20 bars, from the same binary mixtures released the same amount of drug at the following time points: 200 min, 60 min, 40 min, 20 min and 5 min. It could be observed that, exception THAP 100% tablets, dissolution rate of tablets produced by roller compaction was significantly higher. Influence of roller compaction process parameters on dissolution rate of THAP was checked by increasing compaction pressure from 20 to 30 bars. The required amount of drug from the tablets produced at pressure of 30 bars was released at the following time points: 200 min, 40 min, 20 min, 10 min and 8 min. From these results it could be observed that differences in dissolution rate between tablets produced by direct compaction and roller compaction was significant, since difference between tablets produced by roller compaction at pressure of 20 and 30 bars was much less noticeable.

Although MCC improved dissolution rate of THAP, comparing to granules, powder mixtures had slow release of drug. This could be explained that tablets produced from the powder mixtures did not disintegrate to granules and it took some time that drug could be released from the tablets.

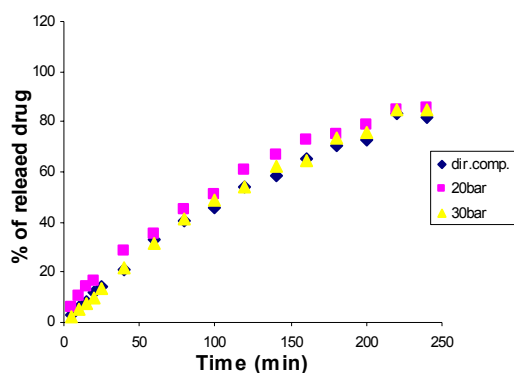


Figure 5.93.: Dissolution rate – THAP100%

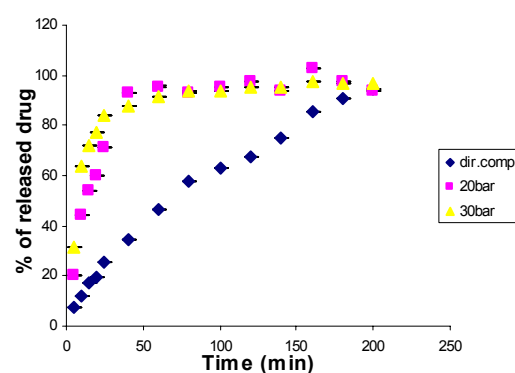


Figure 5.94.: Dissolution rate – binary mixture THAP70% + MCC 30%

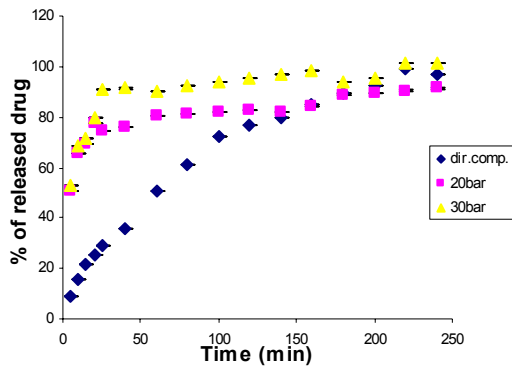


Figure 5.95.: Dissolution rate – binary mixture THAP50% + MCC 50%

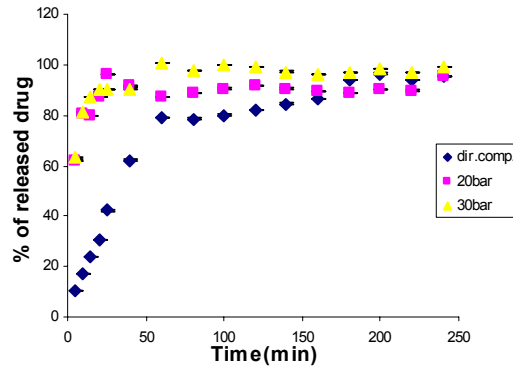


Figure 5.96.: Dissolution rate – binary mixture THAP30% + MCC 70%

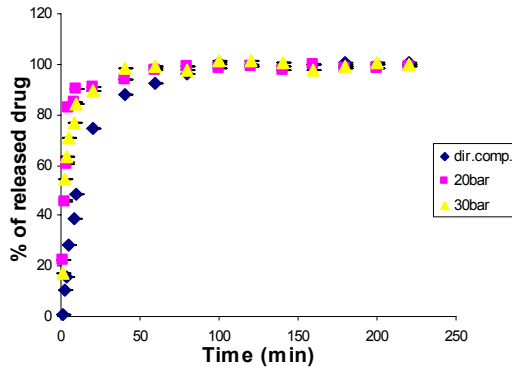


Figure 5.97.: .Dissolution rate – binary mixture THAP10% + MCC 90%

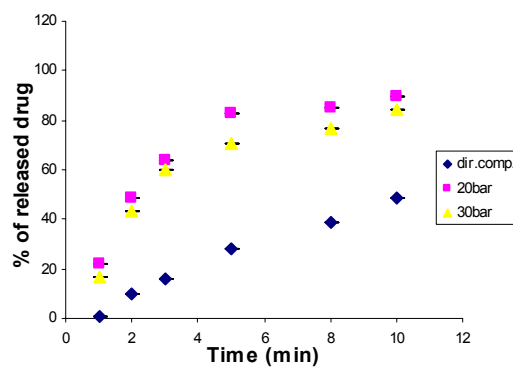


Figure 5.98.: Dissolution rate – binary mixture THAP10% + MCC90% - 10min

Figure 5.97 and figure 5.98 showed the same process, the dissolution rate of the binary mixture THAP10% + MCC 90%, at sampling point 240 and 10 minutes, respectively. This is shown because almost complete release of the drug was finished in first 10 minutes and in figure 5.97 it was not possible to observe real difference in dissolution rate of tablets produced by direct compaction and roller compaction.

THAFP

Even the particle size of THAFP was much smaller than the particle size of THAP, dissolution rate of these two materials were not significantly different (see figure 5.91). Due to the fact that original powder of THAFP contained agglomerated

particles, which decreased specific surface area and reduced drug release from the tablets, dissolution rate of THAFP tablets was slow. Analogous to THAP during the dissolution process THAFP was transformed to monohydrate and dissolution rate was influenced by this transformation.

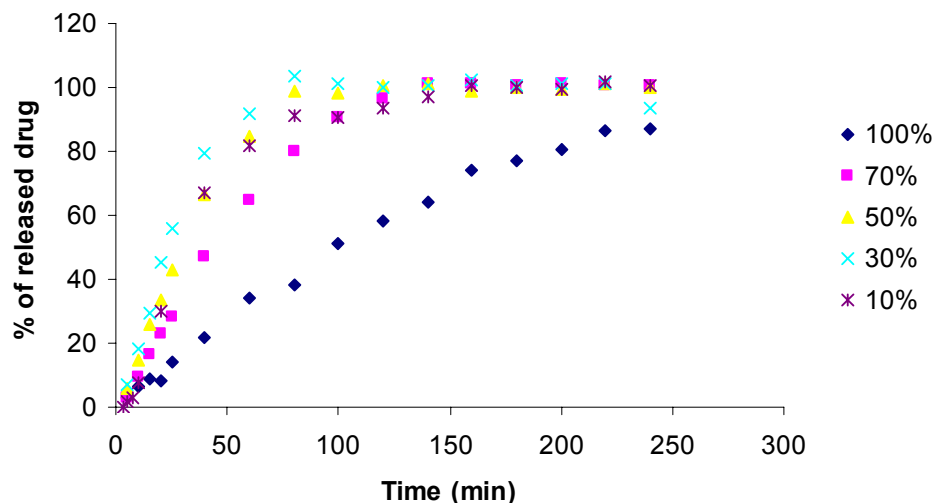


Figure 5.99.: Dissolution rate of the binary mixtures THAFP/MCC – direct compression

In an equivalent way as in the case of THAP, roller compaction improved dissolution rate of THAFP. Tablets produced from pure THAFP even after roller compaction had unaffected dissolution rate because disintegration rate was almost unchanged after roller compaction. Adding MCC in the mixture dissolution rate was extremely increased and increasing was proportional to amount of MCC, see figure 5.100 to figure 5.105.

Tablets contained 100%, 70%, 50%, 30% and 10% of THAFP, prepared by direct compaction USP requirement ⁷⁰ complied at the following time points : 200 min, 80 min, 60 min, 40 min, 20 min. The same amount of drug from the same binary mixtures produced by roller compaction at pressure of 20 bars was released at time points: 200 min, 25 min, 15 min, 10 min and 3 min.

In an equivalent way as tablets produced by direct compaction, the tablets prepared by roller compaction showed the same trend of behavior during dissolution

measurement, see figure 7.2, Appendix. Dissolution rate was increased by increasing the amount of MCC in the tablets.

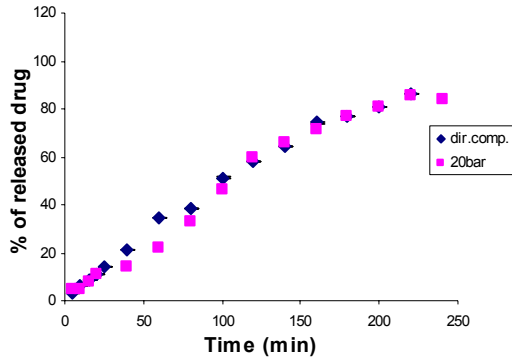


Figure 5.100.: Dissolution rate – THAFP100%

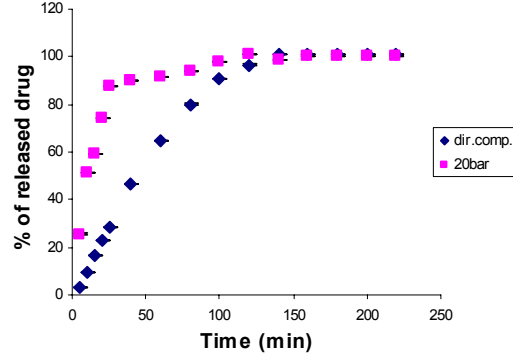


Figure 5.101.: Dissolution rate – binary mixture THAFP70% + MCC30%

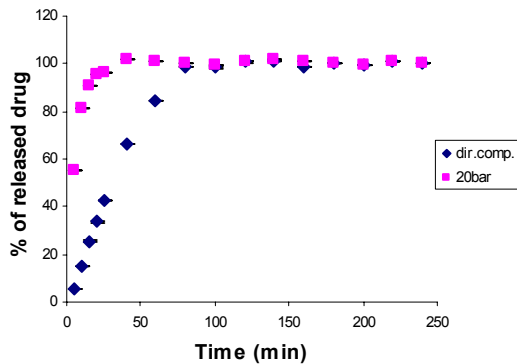


Figure 5.102.: Dissolution rate – binary mixture THAFP50% + MCC50%

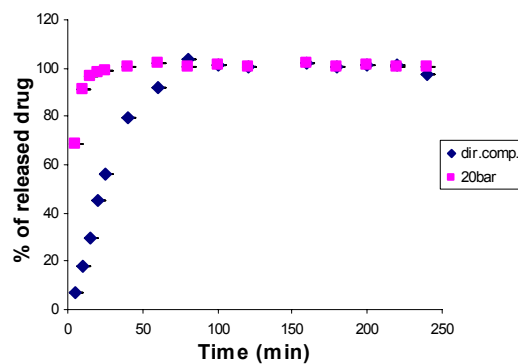


Figure 5.103.: Dissolution rate – binary mixture THAFP30% + MCC70%

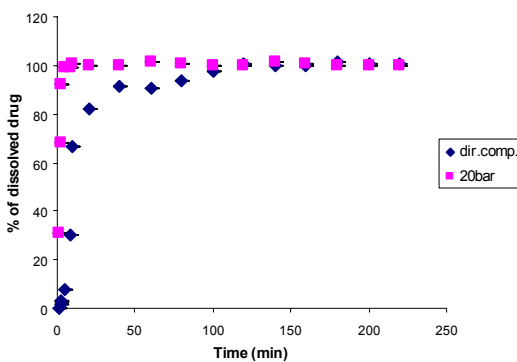


Figure 5.104.: Dissolution rate – binary mixture THAFP10% + MCC90%

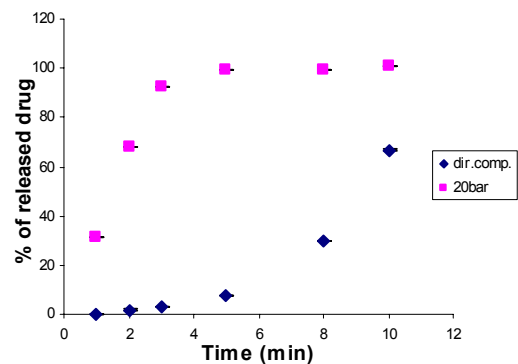


Figure 5.105.: Dissolution rate – binary mixture THAFP10% + MCC90%-10 min.

Figure 5.104 and figure 5.105 demonstrated dissolution rate of the binary mixture THAFP 10% + MCC 90% at sampling point 240 and 10 minutes respectively.

THMO

Although, it was shown that during dissolution process THAP and THAFP were transformed to THMO (see figure 5.89 and figure 5.90) dissolution rate of THMO was still lower than the two other grades of Theophylline, see figure 5.91.

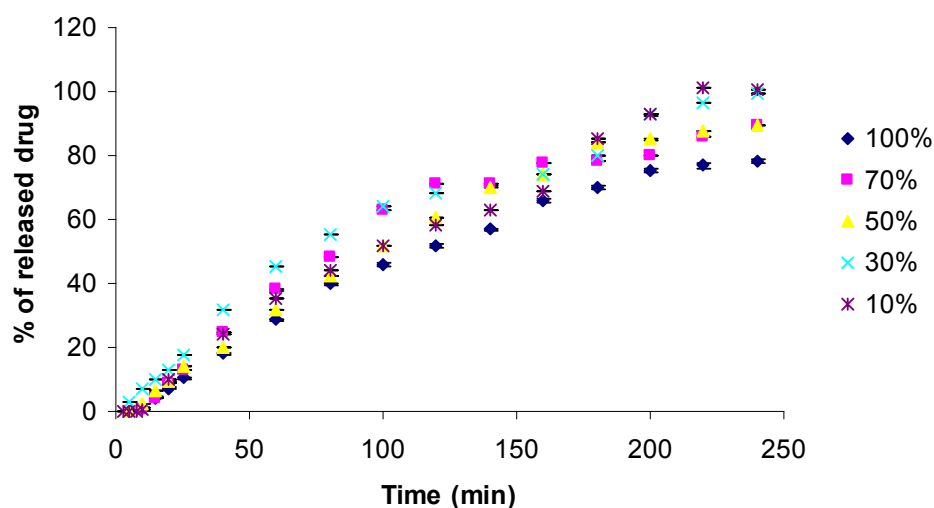


Figure 5.106.: Dissolution rate of the binary mixtures THMO/MCC – direct compression

Roller compaction extremely increased dissolution rate of the THMO tablets. Tablets produced by direct compression after adding of MCC still had a very low dissolution rate. Figure 5.106 showed that even after MCC was added, the difference in dissolution rate was much lower than in the case of THAP and THAFP. As it was previously mentioned that variation in specific surface area of THMO and monohydrate which resulted from initially anhydrate surface. To comply with USP requirement for drug dissolution rate for tablets produced by direct compression in the binary mixtures contained 100%, 70%, 50%, 30% and 10% it took 240 min, 220 min, 180 min, 160 min and 180 min. respectively. For the same tablets prepared by roller compaction at pressure of 20 bars to reach the same criteria it was necessarily: 180 min, 100 min, 20 min, 15 min and 8 min.

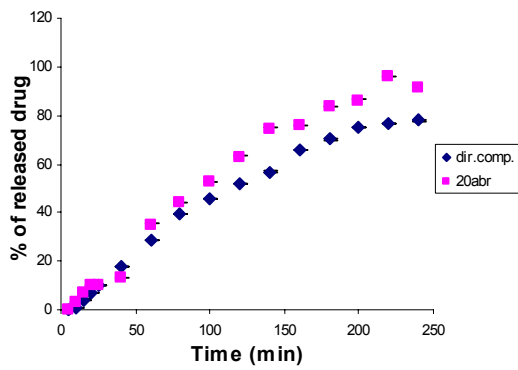


Figure 5.107.: Dissolution rate – THMO100%

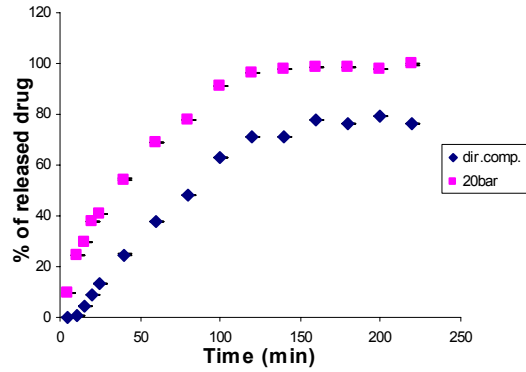


Figure 5.108.: Dissolution rate – binary mixture THMO70% + MCC30%

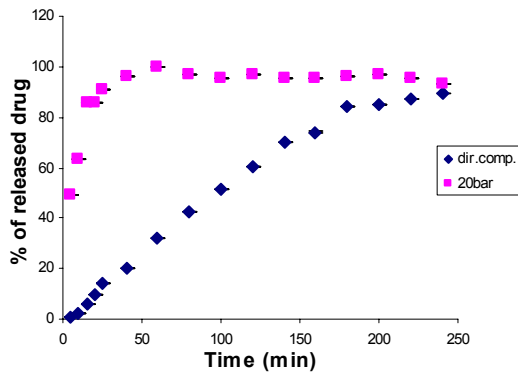


Figure 5.109.: Dissolution rate – binary mixture THMO50% + MCC50%

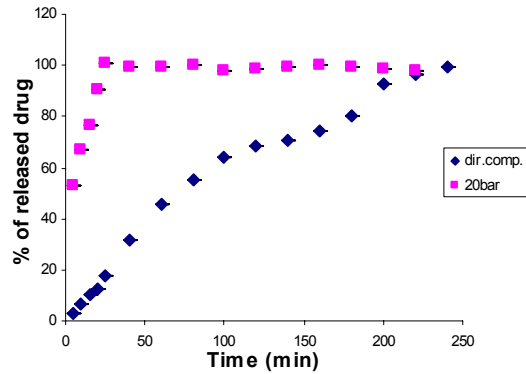


Figure 5.110.: Dissolution rate – binary mixture THMO30% + MCC70%

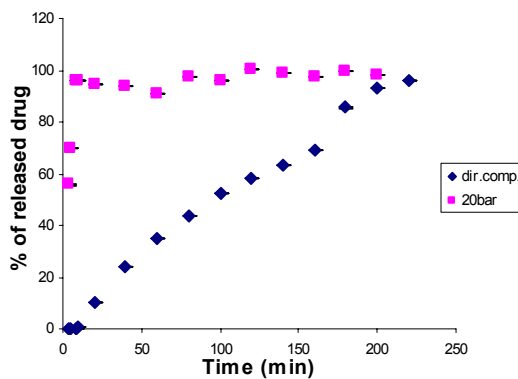


Figure 5.111.: Dissolution rate – binary mixture THMO10% +MCC 90%

6. Conclusions

Compaction in a roll press is more complicated than it looks at first sight. Many parameters (feeding rate, compaction pressure, rolls speed and roll gap) are involved and lack of understanding of compaction mechanisms often results in a product that not possesses the desirable characteristics. Therefore, physical-chemical properties of the active materials and excipients, that are normally determined in the preformulation study, should be very important for the setting of the process parameters.

Particle size distribution, specific surface area, particles shape and flowability are characteristics that are very important to know before process parameters are chosen. Due to the fact that application of high pressure during the process of roller compaction could induce transformation processes between two pseudo polymorphic forms or from one polymorph to another, Theophylline was chosen as model drug. It exists as anhydrate and monohydrate, and anhydrate has two polymorphic forms.

Characterization of the materials (THAP, THAFP, THMO and MCC) showed that they are different according to their physical-chemical properties. THAFP had a very small particle size followed by THMO and THAP with much bigger particles. This is one aspect influencing powder flowability, but due to particle shape all three materials had a very poor flowability. SEM images showed elongated shape of Theophylline particles and fibrous shape of MCC particles.

THAP, THAFP and THMO used in this study were in stable polymorphic form. DSC measurements of compacts (roller compaction), granules (milling) and tablets (tableting) showed that after processing of the materials melting point was not affected by roller compaction. The endothermic peak of THMO indicated that even after all mentioned processes dehydration of monohydrate did not occur.

As it is well accepted that X-Ray is a method of choice for determination of the material identity and polymorphic changes during the technological processes it was used in order to confirm results obtained by DSC.

Since it is obvious that DSC thermograms and X-Ray powder patterns of the original and processed materials were identical, it could be considered that roller compaction,

milling and tableting did not influence pseudopolymorphic/polymorphic form of Theophylline.

Different mathematical equations were applied to characterize different pseudopolymorphs and different particle size of the same polymorphs during roller compaction, and their effect on the final properties of the tablets produced by direct compaction and roller compaction was investigated.

The results obtained by Heckel and modified Heckel equation demonstrated that compressibility of THAP and THAFP was decreased after roller compaction and with further increasing compaction pressure compressibility of THAP was decreased.

In contrast to these two materials THMO granules produced by roller compaction showed a higher compressibility than THMO powder. Although, roller compaction affected compressibility of all three materials differences which occurred were not statistically significant. MCC, known as very compressible and compactable material combined with THAP, THAFP, and THMO significantly affected the properties of the used active substances. The whole range of the binary mixtures showed more plastic behavior under pressure than both individual materials either powder or granules were used.

Tensile strength values indicated that the most compactable material is MCC followed by THMO, THAP and THAFP. Regarding the particle size distribution, THAFP supposed to have higher tensile strength than THAP. This should be due to higher specific surface area available for compaction, but due to agglomeration which occurred in the original THAFP powder, tensile strength of THAP was higher. The highest value of THMO tensile strength could be explained with the highest moisture content that could improve compressibility and compactibility. After roller compaction tensile strength of THAP, THAFP and THMO tablets was not significantly decreased, but MCC tablets produced by roller compaction showed extremely lower tensile strength. As the amount of MCC in the binary mixtures was increased differences in tensile strength of tablets prepared by direct compaction and roller compaction was more prominent. Although, according to Heckel equation THAP, THAFP, THMO and MCC showed the same behavior under compression, they showed different trend of tensile strength changing after roller compaction. Reducing tensile strength after roller compaction is a typical property of the plastic material and since it was noticed

for MCC, it could be considered as more plastic material than THAP, THAFP and THMO. Increasing the pressure during roller compaction did not further reduce tensile strength even markedly plastic material.

The model proposed by Leuenberger 1982²⁸, connects the parameters compressibility and compactibility of the materials and according to this model compressibility of all four materials was similar to each other, while MCC was the most compactable material.

Regardless of the production method (direct compaction or roller compaction), tablets of pure THAP, THAFP and THMO had a very slow disintegration time. Adding MCC to tablets, disintegration time was increased. Already, rapid disintegration time of tablets which contained MCC, roller compaction further improved. Tablets produced by roller compaction fast disintegrated to granules, while tablets produced by direct compaction were more dissolvable.

Due to much smaller particle size of THAFP, its dissolution rate supposed to be much higher. Agglomeration of THAFP particles led to decreasing of specific surface area exposed to a solvent and in the same time decreasing of drug release. Even particles were agglomerated; THAFP still showed higher dissolution rate, but a difference was not highly expressed as it was expected.

During the dissolution process THAP and THAFP transformed to monohydrate. Due to the fact that transformation was very fast, almost during the whole process Theophylline was in form of monohydrate. Although, THAP, THAFP were transformed to monohydrate, they still had a bit higher dissolution rate than THMO. This could be explained by a different shape and specific surface area of transformed anhydrate particles and original monohydrate particles. Dissolution rate of tablets produced from pure THAP, THAFP and THMO was very slow, and adding of MCC significantly increased it. As it was mentioned before, MCC improved disintegration of tablets and in the same time faster release of the drug was achieved. After roller compaction dissolution rate of the tablets was extremely higher. Faster disintegration rate of the tablets produced by roller compaction to granules provided easier liberation of the drug.

In general, it could be considered that roller compaction did not significantly change compressibility of the materials, and for THAP, THAFP and THMO even compactibility was unchanged. Although, MCC as material with remarkably plastic behavior showed reduced compactibility, it still was exceeded by comparison to the other materials. Due to observation that materials with different properties under compression showed various results, it is essential to find an optimum composition in formulation. Well designed tablet formulation produced by roller compaction should maintain a good balance between plasticity and fragmentation. As it is shown in this study the binary mixtures of MCC as very plastic material was responsible for mechanical strength of the tablets. Observing the properties of the tablets produced from THAP, THAFP and THMO, they could be considered as materials partly fragmented during compaction. In the combination with MCC, their function was to minimize effect of particles enlargement occurred by roller compaction.

Measurement of disintegration time and dissolution rate of the tablets with constant porosity, prepared by direct compaction and roller compaction, showed that roller compaction is a method of choice for immediate release dosage forms.

The results impressively showed that the choice of right excipients in combination with the certain drug has a major role no matter how the physical properties of the drug were at the beginning.

7. Appendix

Table 7.1.: Tensile strength (N/cm²) of THAP, MCC and their binary mixture at different compression force (kN) – powder (n=3)

| % of THAP | 1 kN | 2 kN | 3 kN | 4 kN | 6 kN | 8 kN | 10 kN | 12 kN |
|-----------------------|--------|--------|--------|--------|--------|---------|---------|---------|
| In the binary mixture | | | | | | | | |
| 100% | 19.51 | 51.92 | 81.01 | 109.32 | 155.91 | 189.99 | 227.63 | 260.63 |
| (s.d.) | (1.69) | (3.28) | (4.77) | (3.77) | (3.32) | (3.63) | (7.38) | (14.42) |
| 70% | 16.69 | 49.59 | 90.41 | 128.39 | 195.28 | 252.01 | 304.22 | 367.17 |
| (s.d.) | (0.80) | (3.56) | (2.57) | (1.64) | (0.93) | (5.82) | (3.21) | (10.99) |
| 50% | 18.99 | 57.86 | 91.83 | 155.96 | 244.11 | 332.11 | 403.52 | 484.12 |
| (s.d.) | (0.69) | (3.92) | (1.60) | (6.57) | (8.53) | (9.96) | (9.52) | (11.75) |
| 30% | 25.93 | 61.25 | 127.15 | 159.86 | 270.88 | 360.81 | 428.94 | 551.75 |
| (s.d.) | (4.04) | (3.93) | (6.61) | (6.78) | (4.02) | (9.80) | (14.32) | (31.17) |
| 10% | 40.78 | 112.86 | 189.11 | 252.31 | 404.46 | 544.38 | 658.95 | 778.31 |
| (s.d.) | (1.09) | (9.98) | (9.61) | (0.53) | (2.43) | (18.41) | (6.35) | (31.71) |
| 0% | 29.89 | 82.85 | 142.38 | 201.88 | 300.25 | 453.68 | 576.09 | 665.98 |
| (s.d.) | (1.96) | (3.65) | (2.13) | (1.63) | (8.08) | (14.11) | (6.76) | (10.61) |

Table 7.2.: Tensile strength (N/cm²) of THAP, MCC and their binary mixture at different compression force (kN) – granule 20 bars (n=3)

| % of THAP in the binary mixture | 1 kN | 2 kN | 3 kN | 4 kN | 6 kN | 8 kN | 10 kN | 12 kN |
|---------------------------------------|--------|--------|---------|---------|--------|---------|---------|---------|
| 100% | 17.98 | 43.52 | 70.63 | 98.66 | 138.78 | 161.21 | 194.87 | 237.86 |
| (s.d.) | (1.45) | (5.85) | (15.33) | (2.44) | (8.01) | (11.72) | (5.41) | (7.26) |
| 70% | 9.79 | 35.46 | 63.89 | 93.16 | 147.86 | 205.08 | 259.49 | 302.95 |
| (s.d.) | (1.39) | (1.78) | (4.19) | (4.73) | (8.93) | (9.72) | (9.56) | (18.55) |
| 50% | 11.76 | 38.26 | 64.27 | 100.04 | 143.23 | 226.11 | 315.82 | 364.96 |
| (s.d.) | (0.69) | (3.92) | (1.60) | (6.57) | (8.53) | (9.96) | (9.52) | (11.75) |
| 30% | 7.93 | 31.83 | 59.56 | 81.93 | 163.71 | 216.81 | 281.61 | 352.52 |
| (s.d.) | (0.68) | (2.97) | (6.65) | (12.17) | (6.33) | (9.23) | (11.89) | (23.41) |
| 10% | 11.72 | 38.18 | 76.34 | 118.31 | 189.13 | 303.04 | 364.68 | 469.41 |
| (s.d.) | (0.72) | (4.56) | (3.28) | (4.91) | (7.33) | (15.28) | (15.61) | (19.53) |
| 0% | 17.11 | 52.37 | 90.41 | 128.39 | 195.28 | 252.01 | 304.22 | 367.17 |
| (s.d.) | (1.73) | (2.07) | (2.57) | (1.64) | (0.93) | (5.82) | (10.99) | (3.22) |

Table 7.3.: Tensile strength (N/cm²) of THAP, MCC and their binary mixture at different compression force (kN) – granule 30 bars (n=3)

| % of THAP in the binary mixture | 1 kN | 2 kN | 3 kN | 4 kN | 6 kN | 8 kN | 10 kN | 12 kN |
|---------------------------------------|--------|--------|--------|--------|--------|---------|---------|---------|
| 100% | 12.91 | 33.81 | 58.51 | 80.63 | 115.70 | 148.39 | 182.51 | 227.97 |
| (s.d.) | (0.84) | (5.08) | (1.93) | (2.44) | (5.86) | (14.42) | (7.81) | (14.74) |
| 70% | 11.84 | 31.69 | 54.47 | 79.58 | 129.46 | 171.68 | 228.95 | 258.25 |
| (s.d.) | (0.78) | (4.87) | (4.01) | (3.44) | (5.11) | (4.71) | (7.79) | (15.62) |
| 50% | 9.59 | 29.66 | 52.15 | 80.11 | 134.66 | 188.77 | 249.55 | 313.51 |
| (s.d.) | (0.06) | (1.49) | (3.59) | (3.25) | (3.06) | (5.27) | (4.82) | (10.17) |
| 30% | 7.93 | 31.83 | 59.56 | 81.93 | 163.71 | 216.81 | 281.61 | 352.52 |
| (s.d.) | (1.38) | (2.96) | (4.91) | (2.88) | (5.11) | (4.71) | (7.79) | (13.62) |
| 10% | 7.24 | 18.93 | 41.17 | 70.27 | 131.33 | 187.25 | 228.44 | 297.92 |
| (s.d.) | (2.64) | (2.24) | (3.23) | (9.31) | (5.96) | (3.98) | (13.66) | (2.93) |
| 0% | 8.00 | 28.17 | 49.94 | 77.83 | 132.24 | 196.71 | 275.99 | 331.75 |
| (s.d.) | (0.73) | (3.78) | (2.79) | (3.05) | (1.55) | (5.82) | (11.7) | (10.84) |

Table 7.4.: Tensile strength (N/cm²) of THAFP, MCC and their binary mixture at different compression force (kN) – powder (n=3)

| % of THAFP in the binary mixture | 1 kN | 2 kN | 3 kN | 4 kN | 6 kN | 8 kN | 10 kN | 12 kN |
|--|--------|---------|--------|---------|---------|---------|---------|---------|
| 100% | 34.18 | 59.05 | 83.97 | 101.72 | 140.62 | 165.89 | 218.11 | 233.49 |
| (s.d.) | (6.78) | (2.36) | (6.56) | (1.64) | (9.76) | (21.19) | (24.72) | (4.52) |
| 70% | 22.43 | 59.94 | 99.51 | 141.61 | 199.67 | 257.55 | 311.34 | 378.91 |
| (s.d.) | (2.62) | (3.39) | (1.76) | (12.49) | (1.63) | (9.61) | (17.43) | (17.23) |
| 50% | 20.64 | 61.42 | 111.34 | 148.41 | 233.21 | 313.97 | 400.48 | 480.31 |
| (s.d.) | (3.18) | (3.04) | (9.12) | (9.66) | (7.36) | (14.64) | (27.72) | (19.37) |
| 30% | 22.96 | 59.66 | 106.54 | 169.52 | 308.06 | 385.71 | 462.19 | 628.49 |
| (s.d.) | (1.91) | (0.73) | (3.79) | (9.96) | (20.52) | (8.77) | (7.92) | (10.62) |
| 10% | 29.13 | 93.08 | 138.22 | 271.72 | 351.37 | 466.17 | 624.32 | 742.02 |
| (s.d.) | (0.03) | (16.05) | (6.76) | (12.03) | (5.58) | (14.24) | (23.91) | (25.47) |
| 0% | 29.89 | 82.85 | 142.38 | 201.88 | 300.25 | 453.68 | 576.09 | 665.98 |
| (s.d.) | (1.96) | (3.65) | (2.13) | (1.63) | (8.08) | (14.11) | (6.76) | (10.61) |

Table 7.5.: Tensile strength (N/cm²) of THAFP, MCC and their binary mixture at different compression force (kN) – granule 20 bars (n=3)

| % of THAFP in the binary mixture | 1 kN | 2 kN | 3 kN | 4 kN | 6 kN | 8 kN | 10 kN | 12 kN |
|--|--------|--------|--------|---------|---------|---------|---------|---------|
| 100% | 14.62 | 42.69 | 60.66 | 80.32 | 118.04 | 159.82 | 178.38 | 208.45 |
| (s.d.) | (0.03) | (4.23) | (7.16) | (2.77) | (5.04) | (12.42) | (6.68) | (10.69) |
| 70% | 12.92 | 36.84 | 70.37 | 99.09 | 156.74 | 224.93 | 298.31 | 353.89 |
| (s.d.) | (0.02) | (4.01) | (3.48) | (6.11) | (22.25) | (13.17) | (20.39) | (28.61) |
| 50% | 11.54 | 37.37 | 57.35 | 89.89 | 162.02 | 222.00 | 309.31 | 363.04 |
| (s.d.) | (0.78) | (2.42) | (3.27) | (10.55) | (14.11) | (21.94) | (28.97) | (24.82) |
| 30% | 10.07 | 28.44 | 59.65 | 100.15 | 179.98 | 233.18 | 308.85 | 424.23 |
| (s.d.) | (0.77) | (5.74) | (0.75) | (5.16) | (7.49) | (12.51) | (16.64) | (25.69) |
| 10% | 9.88 | 31.41 | 64.08 | 99.69 | 192.69 | 276.15 | 348.05 | 419.67 |
| (s.d.) | (2.12) | (1.63) | (9.88) | (2.63) | (11.12) | (21.27) | (19.72) | (25.07) |
| 0% | 17.11 | 52.37 | 90.41 | 128.39 | 195.28 | 252.01 | 304.22 | 367.17 |
| (s.d.) | (1.73) | (2.07) | (2.57) | (1.64) | (0.93) | (5.82) | (10.99) | (3.22) |

Table 7.6.: Tensile strength (N/cm²) of THMO, MCC and their binary mixture at different compression force (kN) – powder (n=3)

| % of THAP in the binary mixture | 1 kN | 2 kN | 3 kN | 4 kN | 6 kN | 8 kN | 10 kN | 12 kN |
|---------------------------------------|--------|--------|--------|--------|--------|---------|---------|---------|
| 100% | 23.91 | 57.58 | 97.02 | 124.07 | 164.58 | 200.09 | 231.22 | 254.25 |
| (s.d.) | (2.54) | (1.72) | (1.09) | (2.92) | (7.84) | (3.07) | (1.34) | (4.02) |
| 70% | 17.62 | 52.65 | 92.47 | 132.96 | 210.53 | 272.07 | 326.24 | 370.39 |
| (s.d.) | (1.93) | (1.58) | (2.81) | (5.71) | (4.84) | (1.22) | (2.47) | (5.08) |
| 50% | 19.33 | 61.82 | 111.99 | 164.29 | 261.35 | 359.03 | 431.97 | 500.17 |
| (s.d.) | (1.25) | (2.29) | (1.06) | (1.15) | (5.11) | (14.62) | (6.94) | (9.06) |
| 30% | 27.66 | 76.91 | 133.07 | 193.39 | 299.43 | 441.37 | 523.48 | 611.07 |
| (s.d.) | (0.09) | (1.57) | (2.78) | (4.71) | (5.37) | (8.88) | (1.01) | (19.95) |
| 10% | 37.56 | 104.04 | 168.37 | 243.64 | 397.18 | 525.33 | 646.38 | 754.61 |
| (s.d.) | (1.27) | (0.58) | (2.39) | (2.54) | (1.03) | (4.03) | (20.32) | (7.87) |
| 0% | 29.89 | 82.85 | 142.38 | 201.88 | 300.25 | 453.68 | 576.09 | 665.98 |
| (s.d.) | (1.96) | (3.65) | (2.13) | (1.63) | (8.08) | (14.11) | (6.76) | (10.61) |

Table 7.7.: Tensile strength (N/cm²) of THMO, MCC and their binary mixture at different compression force (kN) – granules 20 bars (n=3)

| % of THAP in the binary mixture | 1 kN | 2 kN | 3 kN | 4 kN | 6 kN | 8 kN | 10 kN | 12 kN |
|---------------------------------------|--------|--------|--------|--------|---------|---------|---------|---------|
| 100% | 10.51 | 29.02 | 46.28 | 73.35 | 142.66 | 174.87 | 206.96 | 242.55 |
| (s.d.) | (0.04) | (4.23) | (6.47) | (4.49) | (10.99) | (28.62) | (25.27) | (10.47) |
| 70% | 10.01 | 36.53 | 64.53 | 100.79 | 155.29 | 239.61 | 281.63 | 350.71 |
| (s.d.) | (0.77) | (4.28) | (4.09) | (8.76) | (8.15) | (13.44) | (8.45) | (6.77) |
| 50% | 11.02 | 33.84 | 61.29 | 99.44 | 181.14 | 239.18 | 314.28 | 381.54 |
| (s.d.) | (2.47) | (2.92) | (3.33) | (0.93) | (7.57) | (9.68) | (10.52) | (8.41) |
| 30% | 12.26 | 37.57 | 70.85 | 111.11 | 194.56 | 270.03 | 347.86 | 406.42 |
| (s.d.) | (0.75) | (3.16) | (1.36) | (9.08) | (8.33) | (11.05) | (6.51) | (21.25) |
| 10% | 13.66 | 45.64 | 80.94 | 124.85 | 231.98 | 305.62 | 410.48 | 472.48 |
| (s.d.) | (0.65) | (3.04) | (4.92) | (7.98) | (2.08) | (14.14) | (18.34) | (16.16) |
| 0% | 17.11 | 52.37 | 90.41 | 128.39 | 195.28 | 252.01 | 304.22 | 367.17 |
| (s.d.) | (1.73) | (2.07) | (2.57) | (1.64) | (0.93) | (5.82) | (10.99) | (3.22) |

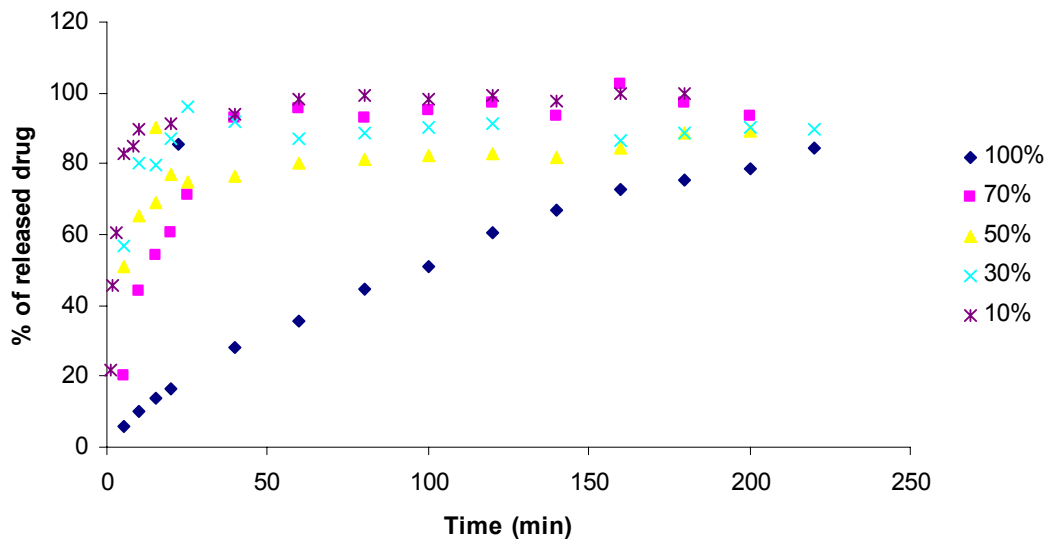


Figure 7.1.: Dissolution rate of the binary mixtures THAP/MCC - 20bar

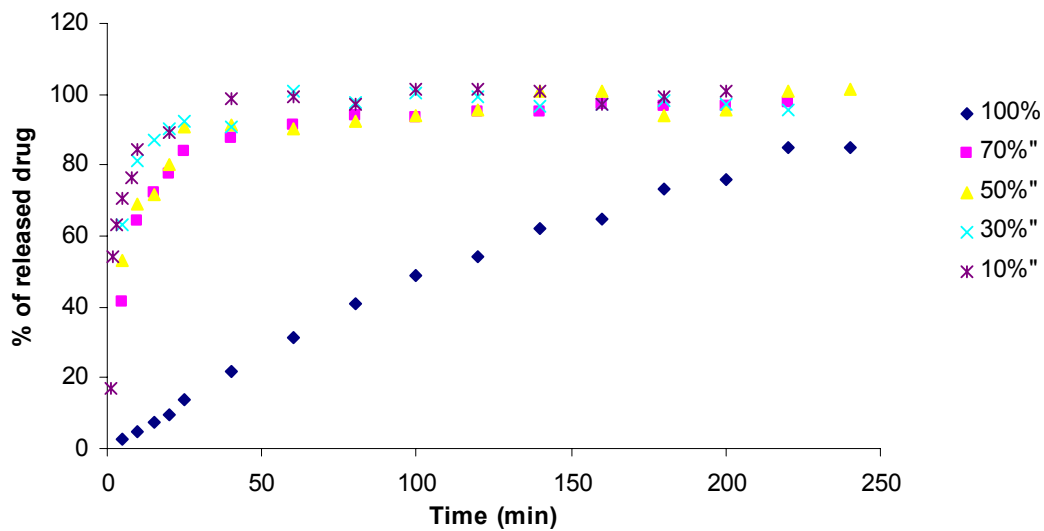


Figure 7.2.: Dissolution rate of the binary mixtures THAP/MCC - 30bar

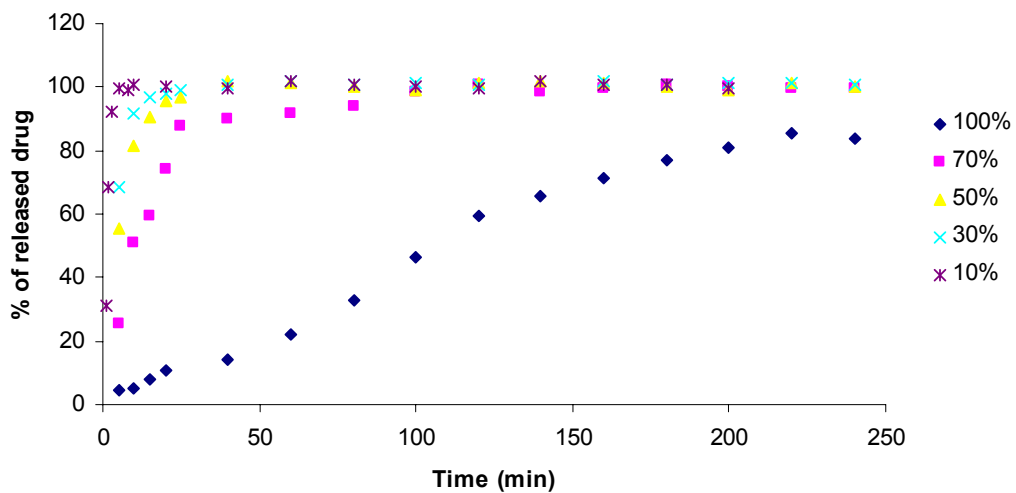


Figure 7.3.: Dissolution rate of the binary mixtures THAFP/MCC - 20bar

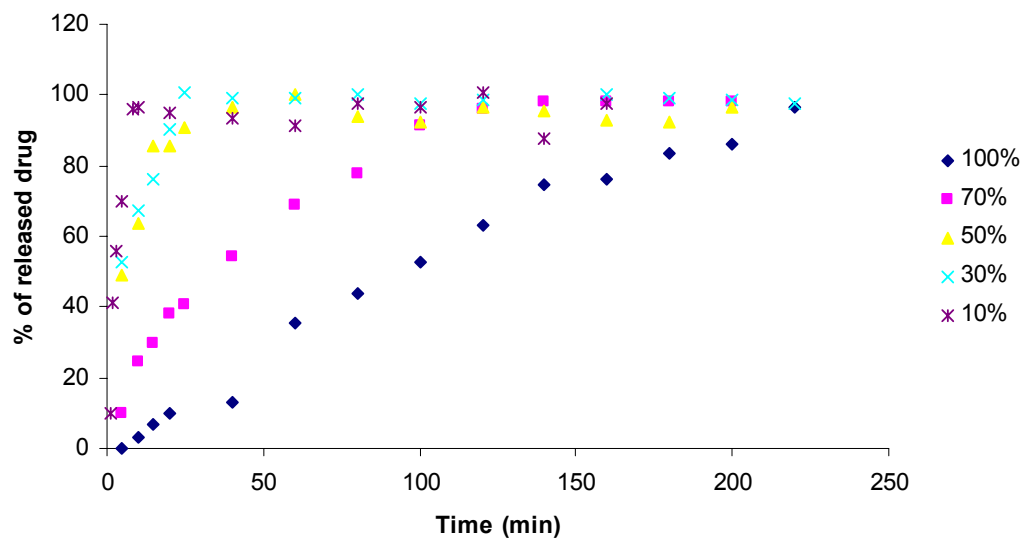


Figure 7.4.: Dissolution rate of the binary mixtures THMO/MCC - 20bar

- 1 Gereg, G.W., Cappola, M.L. (2002) Roller Compaction Feasibility for New Drug Candidates. *Pharmaceutical Technology Yearbook 2002*, 14-23
- 2 Guigon, P., Simon, O. (2003) Roll Press Design - Influence of Force Feed Systems on Compaction. *Powder Technology* 130 (1), 41-48
- 3 Berggren, J. (2003) Engineering of Pharmaceutical Particles: Modulation of Particle Structural Properties, Solid State, Stability and Tableting Behavior by the Drying Process. In *Department of Pharmacy*, pp. 58, Uppsala University
- 4 Summers M., Aulton M. (2002) Granulation. In *Pharmaceutics: The science of dosage Forms Design* (M.E.Aulton, ed.), Elsevier Science
- 5 Augsburger L. L., Vuppala M. K. (1997) Theory of Granulation. In *Handbook of Pharmaceutical Granulation technology* (Vol. 81) (Parikh, Dilip M., ed.), pp. 7-24, Marcel Dekker Inc
- 6 Orelli, J. C. (2005) Search for Technological Reasons to Develop a Capsule or a Tablet Formulation. In *Philosophisch-Naturwissenschaftlichen Fakultet*, University of Basel
- 7 Carstensen, J. T. (2001) Wet Granulation. In *Advanced Pharmaceutical Solids* (Vol. 110) (Carstensen, J. T., ed.), pp. 353-374, Marcel Deckker, Inc
- 8 Miller, R. W. (2005) Roller Compaction Technology. In *Handbook of Pharmaceutical Technology* (Vol. 154) (Parikh, D.M., ed.), Synthron Pharmaceutical Inc
- 9 Fitzpatrick, Company. Introduction to Roll Compaction and the Fitzpatrick Chilsonator.
- 10 Bindhumadhavan, G., Adams, M.J., Greenwood, R.W. ,Fitzpatrick, S. (2005) Roll Compaction of a Pharmaceutical Excipients: Experimental Validation of Rolling Theory for Granular Solids. *Chemical Engineering Science* 60 (14), 3891-3897
- 11 Kleinebudde, P. (2004) Roll Compaction/Dry granulation: Pharmaceutical Application. *European Journal of Pharmaceutics and Biopharmaceutics* 58 (2), 317-326
- 12 Johanson, J. R. (1965) A Rolling Theory for Granular Solids. *ASME, Journal of Applied Mechanisms* 32 (4), 842-848
- 13 Bourseu, F.R.G. L. (2001) Investigation on Roll Pressing as a Forming Operation. University of Birmingham

- 14 Dec, R. T., Zavaliangos, A.,Cunningham, J. C. (2003) Comparison of Various Modeling Methodes for Analysis of Powder Compaction in Roller Press. *Powder Technology* 130 (1-3), 265-271
- 15 Bultman, M. (2003) The Compactor.
- 16 Guigon, P. , Simon, O. , Saleh, K., Bindhumadhavan, G. , Adams, M. J.,Seville, J. P.K. (2007) Roll Pressing. In *Handbook of Powder Technology - Granulation* (Vol. 11) (Seville, J.P.K, ed.), pp. 255-288, Maercel Dekker, Inc.
- 17 Zhang, G.Z., Devalina, L., Schmitt, E.A.,Qiu, Y. (2004) Phase Transformation Considerations During Process Development and Manufacture of Solid Oral Dosage Forms. *Advanced Drug Delivery Reviews* 56 (3), 371-390
- 18 S. Wennerstrum, T. Kendrick, J. Tomaka, J. Cain. (2002) Size Reduction solutions for hard-to-reduce materials. *Powder and Bulk Engineering*
- 19 G. S. Rekhi, M. K. Vuppala. (1997) Sizing of Granulation. In *Hanbook of Phamaceutical Granulation Technology* (Vol. 81) (D.M., Parikh, ed.), pp. 389-418, Marcel Dakkar Inc.
- 20 Fitzpatrick, Company. *Introduction to Milling with a Fitzmill*
- 21 J. Russell, Jr. Lantz. (1990) Size Reduction. In *Pharmaceutical Dosage Forms: Tablets* (Vol. 2) (H. A. Lieberman, L. Lachman, J. B. Schwartz, ed.), pp. 107-199, Marcel Dakkar Inc.
- 22 Sheth, B. B., Bandelin, F. J.,Shangrow, R. F. (1980) Compressed Tablets. In *Pharmaceutical Dosage Forms: Tablets* (Vol. 1) (Lachman, L., ed.), pp. 109-185, Marcel Decker Inc
- 23 Martell, P. Particulate Study of Paracetamol Tablets During Compaction. In *Department of Chamical Engineering*, University of Queensland
- 24 Nyström, C.,Karehill, P.G. (1995) The Importance of Intermolecular Bonding Forces and the Concept of Bonding Surface Area. In *Pharmaceutical Powder Compaction Technology* (Vol. 71) (Nyström, C., ed.), Marcel Dekker Inc.
- 25 Parrott, E.L. (1990) Compression. In *Pharmaceutical Dosage Forms: Tablets* (Vol. 2) (Schwartz, J.B., ed.), pp. 201-243, Marcel Dakkar Inc.
- 26 Mattsson, S. (2000) Pharmaceutical Binders and Their Function in Directly Compressed Tablets. In *Faculty of Pharmacy, Acta Universitatis Upsaliensis*
- 27 Odeku, O.A. (2007) The Compaction Properties of Pharmaceutical Powders are Characterised by their Compressibility and Compactibility. *The Compaction of Pharmaceutical Powders*

-
- 28 Leuenberger, H. (1982) The Compressibility and Compactibility of Powder systems. *International Journal of Pharmaceutics* 12 (1), 41-55
- 29 Ilkka, J. ,Paronen, P. (1993) Prediction of the Compression Behavior of Powder Mixtures by the Heckel Equation. *International Journal of Pharmaceutics* 94 (1-3), 181-187
- 30 Denny, P. J. (2002) Compaction Equations: a Comparison of the Heckel and Kawakita Equation. *Powder Technology* 127 (2), 162-172
- 31 Zhang Y., Law Y., Chakrabarti S. (2003) Physical Properties and Compact Analysis of Commonly Used Direct Compression Binders. *AAPS PharmSciTech* 4 (4), 1-11
- 32 Medina, M. L. R. (2005) Preparation, Characterization and Tableting Properties of Cellulose II Powders. University of Iowa
- 33 Kuentz M. , Leuenberger H. (1998) Pressure Susceptibility of Polymer Tablets as a Critical Property: A Modified Heckel Equation. *Journal of Pharmaceutical Science* 88 (2), 174-179
- 34 Jetzer W. , Leuenberger H. , Sucker H. (1984) Compressibility and compactibility of powder systems. *Pharmaceutical Technology* 7 (11), 33-48
- 35 E.N.Hiestand. (1996) Rationale for and the Measurement of Tablet Indices. In *Pharmaceutical Powder Compaction Technology* (Vol. 71) (G.Alderborn, C.Nyström, ed.), pp. 219-282, Marcel Dekker Inc.
- 36 S.J.Wu, C.Sun. (2007) Intensivity of Compaction Properties of Brittle Granules to Size Enlargement by Roller Compaction. *Journal of Pharmaceutical Science* 96 (6), 1445-1450
- 37 Pitt K., Sinka C. (2007) Tableting. In *Handbook of Powder Technology - Granulation* (Vol. 11) (Salman A.D. , Hounslow M.J. , Seville J.P.K., ed.), pp. 736-778, Elsevier
- 38 Neuhaus, T. (2007) Investigation and Optimization of the Presster-A Linear Compaction Simulator for Rotary Tablet Presses. In *Institut für Pharmazeutische Technologie*, pp. 1-4, Der Rheinischen Friedrich-Wilhelms Universität Bonn
- 39 Ceballos A., Cirri M., Maestrelli F., Corti G., Mura P. (2005) Influence of Formulation and Process Variables on In Vitro Release of Theophylline from Directly-Compressed Eudragit Matrix Tablets. *Il Farmaco* 60, 913-918

- 40 Ly, J.P.H. (1997) Development of an Oral Microspherical Formulation for Bimodal In Vitro release of Theophylline. In *Department of Pharmaceutical Sciences*, University of Toronto
- 41 Salameh, A. K. ,Taylor, L.S. (2006) Physical Stability of Crystal Hydrates and their Anhydrates in the Presence of Excipients. *Journal of Pharmaceutical Science* 95 (2), 446-461
- 42 Sakata Y., Shiraishi S., Otsuka M. (2005) Effect of Tablet geometrical Structure on the Dehydration of Creatine Monohydrate Tablets, and Their Pharmaceutical Properties. *AAPS PharmSciTech* 6 (3), 527-535
- 43 Suzuki, E., Shimomura, K.,Sekiguchi, K. (1989) Thermochemical Study of Theophylline and Its Hydrate. *Chem.Pharm.Bull.* 37 (2), 493-497
- 44 Debnath S., Suryanarayanan R. (2004) Influence of Processing - Induced Phase Transformations on the Dissolution of Theophylline Tablets. *AAPS PharmSciTech* 5 (1)
- 45 Phadnis, N. V.,Suryanarayanan, R. (1997) Polymorphism in Anhydrous Theophylline - Implications on the Dissolution Rate of Theophylline Tablets. *Journal of pharmaceutical science* 86 (11), 1256-1263
- 46 Airaksinen S., Karjalainen M., Räsänen E., Rantanen J., Yliruusi J. (2004) Comparison of the Effect of two Drying Methods on Polymorphism of Theophylline. *International Journal of Pharmaceutics* 276 (1-2), 129-141
- 47 Brittain H.G., Bogdanowich S.J., Bugay D.E., Devinentis J., Lewen G., Newman A.W. (1991) Physical Characterization of Pharmaceutical Solids. *Pharmaceutical Research* 8 (8), 963-973
- 48 Teipel U., Mikonsaari I. (2004) Determining Contact Angle of Powders by Liquid Penetration. *Partical&Partical Systems Characterization* 21, 255-260
- 49 Airaksinen, S. , Karjalainen, M. , Räsänen, E. , Rantanen, J. ,Yliruusi, J. (2004) Comparison of the Effect of Two Drying Methods on Polymorphism of Theophylline. *International Journal of Pharmaceutics* 276 (1-2), 129-141
- 50 Rootare, H.M.,Prenzlow, C.F. (1967) Surface Area from Mercury Porosimeter Measurements. *Journal of Physical Chemistry* 71 (8), 2733-2736
- 51 Dees, P. J.,Polderman, J. (1981) Mercury Porosimeter in Pharmaceutical Technology. *Powder Technology* 29 (1), 187-197
- 52 Freitag F., Kleinebudde P. (2002) How Do Roll Compaction/Dry Granulation Affect the Tableting Behavior of Inorganic Materials? Comparison of Four

- Magensium Carbonates. *European Journal of Pharmaceutical Sciences* 19 (4), 281-289
- 53** Tye C.K., C.Sun, G.E.Amidon. (2004) Evaluation of Effects of Tableting Speed on the Relationships between Compaction pressure, Tablet Tensile Strength and Tablet Solid Fraction. *Journal of Pharmaceutical Science* 94 (3), 465-472
- 54** Kuentz M. , Leuenberger H. (2000) A New Theoretical Approach to Tablet Strength of a Binary Mixture Consisting of a Well and a Poorly Compactable Substances. *European Journal of Pharmaceutics and Biopharmaceutics* 49 (2), 151-159
- 55** Suihko, E., Lehto, V.P., Ketolainen, J., Laine, E.,Paronen, P. (2001) Dynamic Solid-State and Tableting Properties of Four Theophylline Forms. *International Journal of Pharmaceutics* 217 (1-2), 225-236
- 56** Gereg G.W., Cappola M.L. (2002) Roller Compaction Feasibility for New Drug Candidates. *Pharmaceutical Technology Yearbook 2002*, 14-23
- 57** Li, Q., Rudolph, V., Weigl, B.,Earl, A. (2004) Interparticle Van der Waals Force in Powder Flowability and Compactibility. *International Journal of Pharmaceutics* 280 (1), 77-93
- 58** Wells, J.I. (1988) *Pharmaceutical Preformulation: the Physicochemical Properties of Drug Substances*, Ellis Horwood Limited
- 59** Nagel, M.K,Peck, G.E. (2003) Investigating the Effects of Excipients on the Powder Flow Characteristics of Theophylline Anhydrous Powder Formulations. *Drug Development and Industrial Pharmacy* 29 (3), 227-287
- 60** Brittain, H. G.,Grant , D.J.W. (1999) Effects of Polymorphs and Solids State Solvation on Solubility and Dissolution Rate. In *Polymorphism in Pharmaceutical Solids* (Vol. 95) (Brittain, H.G., ed.), pp. 279-325, Marcel Dekker Inc.
- 61** Muster, T.H.,Prestidge, C.A. (2005) Water Adsorption Kinetics and Contact Angles of Pharmaceutical Powders. *Journal of Pharmaceutical Science* 94 (4), 861-870
- 62** Hertig, M. G. ,Kleinebudde, P. (2007) Roll Compaction/Dry Granulation: Effect of Raw Material Particle Size on Granule and Tablet Properties. *International Journal of Pharmaceutics* 338 (1-2), 110-118

-
- 63** Jain, S. (1999) Mechanical Properties of Powders for Compaction and Tableting: An Overview. *Pharmaceutical Science & Technology Today* 2 (1), 20-31
- 64** Xiarong, H., Seccrest, P.J., Amidon, G.E. (2006) Mechanistic Study of the Effect of Roller Compaction and Lubricant on Tablet Mechanical Strength. *Journal of Pharmaceutical Science* 96 (5), 1342-1355
- 65** B.Van Veen, K.Van Der Voort Maarschalk, G.K.Bolhuis, K.Zuurman, H.W.Frijlink. (2000) Tensile Strength of Tablets Containing Two Materials with a Different Compaction Behavior. *International Journal of Pharmaceutics* 203 (1-2), 71-79
- 66** S.Malkowska, K.A.Khan (1983) Effect of Re-compression on the Properties of Tablets Prepared by Dry Granulation. *Drug Development and Industrial Pharmacy* 9 (3), 331-347
- 67** J.S.M. Garr, M.H.Rubinstein. (1991) The Effect of Rate of Force Application on the Properties of Microcrystalline Cellulose and Dibasic Calcium Phosphate Mixtures. *international journal of pharmaceutics* 73 (1), 75-80
- 68** Randall, C.S. (1995) Particle Size Distribution. In *Physical Characterization of Pharmaceutical Solids* (Vol. 70) (H.G., Brittain, ed.), pp. 157-183, Marcel Dekker Inc.
- 69** Aaltonen, J. (2007) From Polymorph Screening to Dissolution Testing. In *Division of Pharmaceutical Technology*, pp. 27-28, University of Helsinki
- 70** Usp. (2005) Official Monograph /Theophylline. In *United States Pharmacopeia* 28, *National Formulary* 23

Curriculum Vitae

Name Ervina Hadzovic
Date of Birth 21st June 1977
Place of Birth Dobojski, Bosnia and Herzegovina

Education

1992 - 1996 Gymnasium, Tesanj, Bosnia and Herzegovina
1996 - 2003 Study in Pharmacy at the University of Pharmacy in Sarajevo, Bosnia and Herzegovina
2005-2008 PhD study under supervision of Prof. Dr. H. Leuenberger at the Institute of Pharmaceutical technology, University of Basel, Switzerland
Assistant in practical courses in semi-solid dosage form at the Institute of Pharmaceutical technology, University of Basel, Switzerland

Work experience

2003 6 months of practical work in the pharmacy "Apoteke Sarajevo", Sarajevo, Bosnia and Herzegovina
Since March 2003 Development Department in the pharmaceutical company "Bosnalijek dd", Sarajevo, Bosnia and Herzegovina
1 year of the practical trainee in pharmaceutical technology at the Production Department in "Bosnalijek"